SMART SENSING SYSTEM FOR A LATERAL MICRO DRILLING ROBOT

by

Jose Alejandro Solorio Cervantes

A Thesis

Submitted to the Faculty of Purdue University

In Partial Fulfillment of the Requirements for the degree of

Master of Science

Department of Engineering Technology

West Lafayette, Indiana

August 2021

THE PURDUE UNIVERSITY GRADUATE SCHOOL
STATEMENT OF COMMITTEE APPROVAL

Dr. Jose Garcia, Chair
School of Engineering Technology

Dr. Brittany Newell, Co-Chair
School of Engineering Technology

Dr. Mark French
School of Engineering Technology

Dr. Nathan Schultheiss
School of Chemical Engineering

Approved by:
Dr. Duane D. Dunlap

This work is dedicated to my family. A special feeling of gratitude to my loving parents, Mayolo and Claudia, whose support and example have encouraged me always to look further and give my best. To my sister, Arianna, who has a special place in my life.

I also dedicate this work to my friends, who have supported me throughout the process.

I give special thanks to my mentors and advisors, Dr. Jose Garcia and Dr. Brittany Newell. Without their support and motivation, this work could not have been possible.

Finally, I want to dedicate this work in memory of my grandmother Celia, whose love for me knew no bounds. You will accompany me forever.

ACKNOWLEDGMENTS

Throughout the writing of this thesis, I have received a great deal of support and assistance.

I want to thank my committee members who have been sharing their knowledge and advising me these two years. Thank you, Dr. Nathan Schultheiss and Dr. Mark French, for their insightful comments and suggestions. Additionally, I am deeply grateful to Dr. Brittany Newell and Dr. Jose Garcia for their assistance at every stage of this research project and their unwavering support and belief in me.

I would like to acknowledge and extend my sincere thanks to my colleague Santiago Guevara, who has accompanied and supported me on this project since day one.

My gratitude extends to the sponsors of this project for the funding opportunity to undertake my studies and do research at Purdue University.

TABLE OF CONTENTS

LIST OF FIGURES 8
LIST OF TABLES 11
GLOSSARY 12
ABSTRACT 14
CHAPTER 1. INTRODUCTION 15
1.1. The Problem 17
1.1.1. Significance 17
1.2. The Purpose 18
1.2.1. Research Questions 18
1.2.2. Significance 19
1.3. The Impact 19
1.4. Assumptions 21
1.5. Delimitations 22
1.6. Limitations 22
1.7. Micro Drilling Robot Implementation 23
CHAPTER 2. REVIEW OF LITERATURE 26
2.1. Rotary Drilling 27
2.2. Basin Conditions 29
2.3. Wellbore Conditions and Geometric Constraints 34
2.4. Weight on Bit (WOB) and Torque Calculations 37
2.5. Statistical Modeling Techniques in Drilling Applications 39
2.6. Smart Sensors 40
2.7. Telemetry Technologies 42
2.7.1. Electromagnetic 42
2.7.2. Mud Pulse 43
2.7.3. Acoustic 43
2.7.4. Wired 44

2.8. Data Security and Privacy 45
2.9. Summary 46
CHAPTER 3. RESEARCH METHODOLOGY 47
3.1. Introduction 47
3.2. Measuring variables 47
3.3. Treatment and Instrumentation 49
3.4. Test Bench 49
3.5. Model and Architecture 53
3.5.1. Sensors 54
3.5.1.1. Pressure Transducer 54
3.5.1.2. Flow Meter 57
3.5.1.3. Position Transducer 58
3.5.2. Sensor Communication Protocols 63
3.5.3. Signal Processing 64
3.5.3.1. Data Acquisition 66
3.5.3.2. Telemetry 69
3.6. Cloud-based Dashboard 71
CHAPTER 4. RESULTS 72
4.1. Dashboard 72
4.2. Printed Circuit Board (PCB) 74
4.3. Experimental Tests 76
4.4. Analysis of Results 77
4.4.1. ANOVA 83
4.4.1.1. Model 83
4.4.1.2. Results 84
4.4.1.3. Conclusions 87
CHAPTER 5. SUMMARY, CONCLUSIONS, AND RECOMMENDATIONS 90
5.1. Future Work and Conclusions 90
5.1.1. Conclusions 90

5.1.2. Micro Drilling Robot Implementation 91
LIST OF REFERENCES 96
APPENDIX A. NODE-RED OPERATIONAL BLOCK FLOWS 107
APPENDIX B. ELECTRONIC SCHEMATIC 109
APPENDIX C. ANOVA TABLES 110
APPENDIX D. PCB 112

LIST OF FIGURES

Figure 1.1. Principal types of petroleum types (Britannica, 2017). 15

Figure 1.2. Flow diagram of the research project phases. 24

Figure 2.1. Sensing and fluid power systems connection diagram. 26

Figure 2.2. Industrial robotics and sensing and communication systems connection diagram. ... 27

Figure 2.3. Rotary drilling schematic with its main components (left). Directional drilling techniques (center and right) (Azar & Samuel, 2007). 28

Figure 2.4. The Illinois Basin (Panno, 2018). 30

Figure 2.5. Schematic of induced stresses and typical stress-strain curves for rock failure (Azar & Samuel, 2007). 31

Figure 2.6. Stresses in compressive strength test and tooth penetration (Azar & Samuel, 2007). 32

Figure 2.7. Core (black dots) and wire-line log derived matrix density, porosity, intrinsic permeability, matrix thermal conductivity, and specific heat capacity (Rockhold et al., 2014). . 33

Figure 2.8. Core (black dots) and wire-line log derived bulk density, compressional slowness (DTCO), shear slowness (DTSM), Poisson's ratio, and isotropic Young's modulus (Rockhold et al., 2014). 33

Figure 2.9. Well casing diagram (Industrimigas, 2013). 35

Figure 2.10. Oil rig diagram with main components (Freudenrich & Strickland, 2018). 36

Figure 2.11. Wellhead or “Christmas tree” (Lee, 2017). 36

Figure 2.12. Completed well (McDowell, 2006). 37

Figure 3.1. Hydraulic test bench. 50

Figure 3.2. Cylinder and position transducers arrangement. 51

Figure 3.3. Test bench hydraulic circuit. 52

Figure 3.4. Pressure transducer PX309-5KG5V (Omega Engineering, n.d.). 55

Figure 3.5. Pressure transducer LM/2345-11 (Honeywell, n.d.). 55

Figure 3.6. Pressure Sensor Architecture LM/2345-11. 56

Figure 3.7. Pressure Sensor Architecture PX309-5KG5V 56

Figure 3.8. Flow transducer FSC-375 (Flo-Tech, 2019). 57

Figure 3.9. Flow Transducer Architecture FSC-375. 57
Figure 3.10. String pot sensor internal mechanism (TE Connectivity, 2020). 58
Figure 3.11. A magnetic sensor positioned in a pneumatic cylinder (SICK Sensor Intelligence, n.d.). 59
Figure 3.12. VSM-2 miniature self-contained sensor (Banner, n.d.)... 59
Figure 3.13. Model IX image-based laser sensor (Keyence, n.d.). 60
Figure 3.14. MPA magnetic sensor (SICK Sensor Intelligence, n.d.). 61
Figure 3.15. Position transducer architecture for MPA-107THTP0B01. 62
Figure 3.16. Position transducer model SP2 (TE connectivity, n.d.)... 62
Figure 3.17. Position transducer architecture for SP2-4. 63
Figure 3.18. Raspberry Pi 4 Model B (Upton, 2019)... 65
Figure 3.19. Analog to Digital Converter ADS1115 (Earl, n.d.). 66
Figure 3.20. XY-IT0V 4-20 mA to 0-5 V converter module (Amazon, n.d.). 67
Figure 3.21. Voltage divider circuit. 68
Figure 3.22. Sine wave to PWM converter circuit.. 68
Figure 3.23. FV-5K10 PWM to voltage module (Amazon, n.d.). 69
Figure 4.1. Raspberry Pi monitoring and control. 72
Figure 4.2. Test bench monitoring and control.. 73
Figure 4.3. Example of plots generated for the ADC readings (time vs. voltage)........................ 74
Figure 4.4. Top and bottom view of the PCB for the test bench (57x72 mm). 75
Figure 4.5. 3-D view of the PCB for the test bench (57x72 mm)... 76
Figure 4.6. Normality plot for Experiment 1. 79
Figure 4.7. Normality plot for Experiment 2. 80
Figure 4.8. Normality plot for Experiment 3. 80
Figure 4.9. Residuals plots for Experiment 1. 82
Figure 4.10. Residuals plots for Experiment 2. 82
Figure 4.11. Residuals plots for Experiment 3. 83
Figure 4.12. Box plots for Experiment 1. 85

Figure 4.13. Box plots for Experiment 2. 86
Figure 4.14. Box plots for Experiment 3. 86
Figure 4.15. Piston rod extension for Experiment 1. 88
Figure 4.16. Piston rod extension for Experiment 2. 88
Figure 4.17. Piston rod extension and retraction cycles for Experiment 3. 89
Figure 5.1. Inertial Measurement Unit (IMU) BNO055 (Townsend, n.d.). 93
Figure 5.2. Inertial Measurement Unit Architecture. 93
Figure 5.3. Module INA169 (Adafruit Industries, n.d.). 94
Figure 5.4. Voltage and Current Transducer Architecture. 94
Figure 5.5. Hydraulic cylinder HZ16 (Bansbach Easy Lift, 2020). 95
Figure 5.6. Proposed control for the rotation of a motor. 95

LIST OF TABLES

Table 1.1. Micro-Drilling Robotic Device Specifications. 20
Table 2.1. Comparison Between Consumer IoT and IIoT (Sisinni et al., 2018) 45
Table 3.1. Variables Relevant for the Research. 49
Table 3.2. Test bench elements. 53
Table 3.3. Sensors required for the sensing system. 54
Table 3.4. Position sensor technologies summary. 60
Table 3.5. Ranking Parameters Table. 70
Table 4.1. Set of experiments. 77
Table 4.2. Anderson-Darling test results. 81
Table 5.1. Additional devices recommended to implement on the micro-drilling device. 92
Table C.1. ANOVA table for Experiment 1. 110
Table C.2. Multiple comparison test results for Experiment 1. 110
Table C.3. ANOVA table for Experiment 2. 110
Table C.4. Multiple comparison test results for Experiment 2. 110
Table C.5. ANOVA table for Experiment 3. 110
Table C.6. Multiple comparison test results for Experiment 3. 111
Table D.1. Description of PCB elements. 113

GLOSSARY

Casing - The tubular structure that is placed in the drilled well to maintain the well opening (Allaby, 2020).

Crude Oil - The mixture of liquid hydrocarbons in their natural state or obtained by condensation or extraction of natural gas (Office of Oil & Gas, 1997).

Deposit – One or more reservoirs grouped or related to each other within the same geological, structural, or stratigraphic characteristics (Allaby, 2020). There may be two or more reservoirs in the same reservoir, separated vertically or laterally by impermeable rocks or local geological barriers.

Downstream - The sector in charge of all those activities that go from refining crude oil to its commercialization and distribution (Kurdi, 2010). Gasoline and diesel are some of the downstream products.

Exploration & Production (E&P) - A specific sector within the oil and gas industry that researches new methods, techniques, and technologies to extract hydrocarbons (Kurdi, 2010).

Geological Formation – A rock unit that is distinctive enough to separate it from surrounding rock layers. The rock unit is formed of sediments and rock with similar lithology and sedimentary facies (Allaby, 2020).

Horizontal Directional Drilling (HDD) - A trenchless construction method used to install pipelines of various sizes and materials below the ground surface (Lowson, & Beckman, 1997).

Improved Oil Recovery (IOR) - Also known as tertiary recovery, and it is the extraction of hydrocarbons from an oil field that cannot be extracted otherwise (Zhang et al., 2018).

Midstream - The link in the oil chain that is in charge of all the tasks related to the transportation of crude oil and oil derivatives, whether by pipe, truck, or ship (Kurdi, 2010).

Natural Gas – The mixture of gaseous hydrocarbons at atmospheric pressure and 15°C as it arises from a deposit in its natural state (Allaby, 2020).

Oil Exploration – The term used in the oil industry to search for oil or gas (Sheehan, 2014).

Oil Reservoir – A rock formation in which oil and gas have accumulated (Ma et al., 2016).

Rate of Penetration (ROP) - The speed at which a drill bit breaks the rock (Allaby, 2020).

Reservoir – The stratum or subsoil sector that contains, or is thought to contain, an accumulation of hydrocarbons, which can be produced or extracted (Allaby, 2020).

Upstream - The exploration and production activities of the hydrocarbon industry. This link in the chain is in charge of searching for potential deposits and exploiting wells (Kurdi, 2010).

Weight on Bit (WOB) - The amount of downward force exerted on the drill bit (Allaby, 2020).

Well – The hole drilled in the rock from the surface of the earth of a deposit to explore or exploit the crude oil of the subsurface. Wildcat wells are those that are carried out without full knowledge of the rock structure (Allaby, 2020).

ABSTRACT

The oil and gas industry faces a lack of compact drilling devices capable of performing horizontal drilling maneuvers in depleted or abandoned wells in order to enhance oil recovery. The purpose of this project was to design and develop a smart sensing system that can be later implemented in compact drilling devices used to perform horizontal drilling to enhance oil recovery in wells. A smart sensor is the combination of a sensing element (sensor) and a microprocessor. Hence, a smart sensing system is an arrangement that consists of different sensors, where one or more have smart capabilities. The sensing system was built and tested in a laboratory setting. For this, a test bench was used as a case study to simulate the operation from a micro-drilling device. The smart sensing system integrated the sensors essential for the direct operational measurements required for the robot. The focus was on selecting reliable and sturdy components that can handle the operation Down the Hole (DTH) on the final lateral micro-drilling robot. The sensing system's recorded data was sent to a microcontroller, where it was processed and then presented visually to the operator through a User Interface (UI) developed in a cloud-based framework. The information was filtered, processed, and sent to a controller that executed commands and sent signals to the test bench's actuators. The smart sensing system included novel modules and sensors suitable for the operation in a harsh environment such as the one faced in the drilling process. Furthermore, it was designed as an independent, flexible module that can be implemented in test benches with different settings and early robotic prototypes. The outcome of this project was a sensing system able to provide robotic drilling devices with flexibility while providing accurate and reliable measurements during their operation.

CHAPTER 1. INTRODUCTION

Oil is a non-renewable resource formed over millions of years, as organic materials from dead organisms are exposed to intense heat and pressure (Allaby, 2020). Beneath the earth's crust, it is possible to find many different geological formations where oil can be stored.

Geologists classify reservoir shapes, or traps, into two types: structural and stratigraphic traps. Stratigraphic traps are formed when other beds seal a reservoir bed or when the permeability changes within the reservoir bed (Boomer, 2008). The principal types of stratigraphic traps can be seen in Figure 1.1. Lateral drilling or “horizontal drilling” is important in the oil and gas industry to improve the existing oil well’s productivity, creating access to different deposits across the section, and providing connectedness to the porous network where hydrocarbons reside.

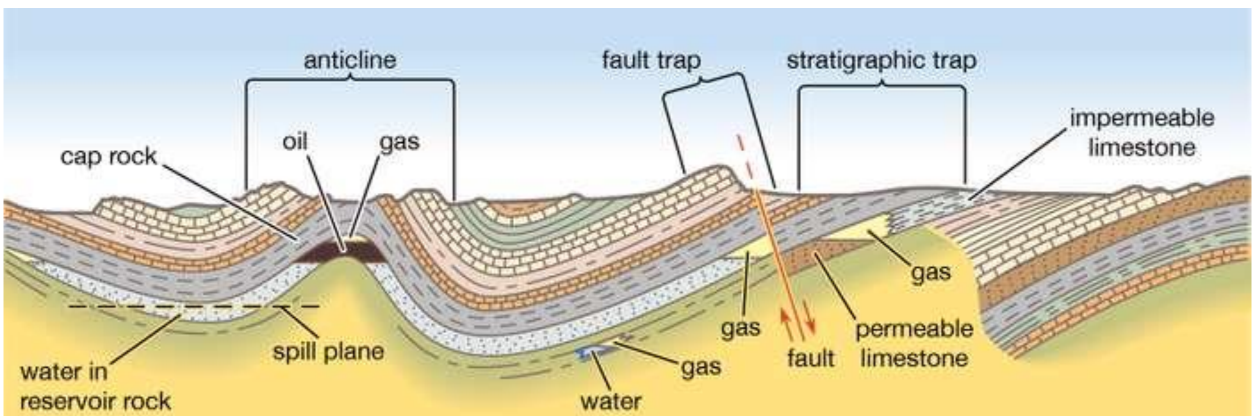

Figure 1.1. Principal types of petroleum types (Britannica, 2017).

The oil chambers are zones filled with petroleum that often must be accessed horizontally due to the geological properties of the ground surrounding them. This is because different formations enclose the chamber, and reaching it with typical drilling methods is not possible. The problem is that only 62% of oil can be extracted with vertical drilling techniques, and horizontal drilling technologies are required to enhance oil extraction in some stratigraphic traps (Office of Oil & Gas, 1997). Therefore, such a type of technique must be implemented as a way to increase the payout and profitability of depleted and abandoned wells (Sheehan, 2014).

Nowadays, vertical drilling techniques are widely used both for off-shore and on-shore oil deposits, and compact fluid power robots that integrate Down-the-Hole (DTH) and Rotary Steerable Drilling (RSD) technologies have been proven to be successful both in experimental settings and fields (Du et al., 2008; Wang et al., 2014). However, the oil and gas industry requires novel approaches to enhance the recovery and, as a consequence, increase their profits (Sheehan, 2014). Over the last three decades, step-change innovations have been developed and optimized, namely, Horizontal Directional Drilling (HDD) and hydraulic fracturing (Jongheon & Hyun, 2017).

Current HDD techniques have some drawbacks related to their operation and capabilities (Zhang et al., 2018). Commonly, HDD devices can steer in a range between 3-4 degrees/100 ft for long-radius applications and from 8-19 degrees/100 ft for medium radius applications. Short-radius applications require up to 100 degrees/100 ft of steering. Currently, short-radius drilling technologies are one of the most researched fields (Wang et al., 2019). On the other hand, hydraulic fracturing has been a widely used method to extract oil from structural and stratigraphic traps. Still, it has its limitations and drawbacks for oil extraction (Stephenson, 2015). A robot capable of reaching the structural and stratigraphic traps without the necessity of injecting, recirculating a high-pressure fluid, and cracking the rocks, would make a difference in the industry (Sheehan, 2014).

Horizontal drilling techniques have been implemented as a way to increase the payout and profitability by extracting oil from depleted and abandoned wells (Ma et al., 2016). Fluid power is widely used for a range of applications because it is very adaptable and reliable. Currently, it can be found in a variety of industries such as transportation, construction, aerospace, and manufacturing (Vacca, 2018). Researchers have found a solution to some of the challenges faced not only with the horizontal drilling process but in general within the oil and gas industry by using fluid-powered devices.

However, one disadvantage of fluid power systems is the low power efficiency derived from the several sources of power losses in the systems. Thus, hydraulic energy harvesting is a technology of current research that has the capacity to improve the energy efficiency of fluid power systems (Çιkιm et al., 2014). In addition, drilling processes have proven to be very energy inefficient due to the many factors involved in the operation, such as temperature, circulating pressure losses, and mechanical frictions (Chang et al., 2018). The average energy efficiency was estimated at 21%; thus, there is an enormous opportunity for research to address this problem (Oak Ridge National Laboratory, 2012). There are tools designed for horizontal drilling in the market, but they are not capable of performing drilling operations at a smaller scale, particularly in smaller well bores. Also, they require additional tools and significant, capital-intensive equipment on the surface to operate them.

1.1. The Problem

The oil and gas industry lacks compact drilling devices capable of performing horizontal drilling maneuvers in depleted or abandoned wells in order to enhance oil recovery in geological formations with hard-to-reach structural and stratigraphic traps. Developing such devices and integrating several systems to ensure a consistent and continuous drilling operation is challenging. This study focuses on the development of sensing systems that can be implemented in compact drilling devices, offering reliable measurements for guidance and control.

1.1.1. Significance

Only 62% of oil can be extracted through vertical drilling techniques (Office of Oil Gas, 1997); therefore, horizontal drilling technologies need to be investigated to maximize oil extraction in geological formations where hydrocarbons are trapped (Ma et al., 2016). Companies are continually looking for new methods and technologies to increase hydrocarbon extraction, and those who can implement horizontal drilling techniques can improve oil extraction by up to 42% (Sheehan, 2014).

Advancements in fluid power systems can improve efficiency, and therefore more powerful and compact machines can be developed for current applications.

During the drilling process, improvements such as enhanced operating efficiency of fluid-powered tools, precision during the operation, and reliable path-planning are only achievable with feedback from sensors and transducers. A transducer is a sensor or system element that converts a physical variable into an electric signal that can be read and interpreted by another system. The electric signal is a representation of the variable measured, and nowadays, intelligent sensors use machine learning and redundant measurements to improve data acquisition (Hu & Hao, 2013).

Therefore, a sensing system is one critical element of any drilling device since it allows the user to control and operate machinery. Additionally, the sensing system can provide information regarding the operation process, the environment, the device's health, and it can be used to feed data to other systems such as the control system that will coordinate the operation of the device.

1.2.The Purpose

The purpose of this project was to design and develop a smart sensing system that can be later implemented in compact drilling devices used to perform horizontal drilling to enhance oil recovery in wells. The sensing system is based on the advantages of both Measurement while Drilling (MWD) and Logging while Drilling (LWD) technologies. The developed system and cloud-based architecture are based on a modular design that can be easily implemented on drilling devices of different diameters while ensuring reliable measurements.

1.2.1. Research Questions

The research questions that had to be answered in order to realize the outcomes associated with the purpose are listed as follows:

a) What are the existing mechanisms used for drilling horizontal laterals for oil extraction in depleted and abandoned wells?
b) What type of telemetry system is required to ensure a reliable connection between the Bottom Hole Assembly (BHA) sensors and the surface?
c) What type of sensing and communication capabilities are required to gather real-time data while performing down-the-hole (DTH) drilling operations?
d) How will the information gathered from the sensors be interpreted and processed for the use of a lateral micro drilling device?

1.2.2. Significance

The research project's deliverable was a working prototype of a smart sensing system based on a modular design that can be implemented in robots capable of performing horizontal drilling operations. The system includes a cloud-based dashboard that provides a visual representation of the operational variables. Even though the research project was a part of a larger project with a broader goal, this thesis's scope focuses on designing and developing the sensing system and its communication components. The smart sensing system includes novel modules and sensors that provide output signals similar to those suitable for the operation in a harsh environment, such as those faced in the drilling process. The sensing system was designed considering it as a module that will be integrated into a prototype. Thus, it was designed to be flexible and to have the ability to be easily implemented in different testing settings.

The final goal and part of future work (refer to section 5.1.2) was to implement the sensing system in a compact robot that must be able to perform drilling operations in wellbores of between three and five inches in diameter. Such a robot will also be capable of creating horizontal laterals within the range of short-radius applications. The sensing system is a critical component that will enable the device mentioned above to achieve its goals by providing reliable measurements and real-time feedback to the operator. A thorough analysis of the sensors that a drilling device requires to operate was performed in order to ensure that the sensing system meets all the expected operational requirements, and its performance can be evaluated based on predefined criteria.

1.3. The Impact

Vertical drilling techniques cannot be used for all drilling operations. Frequently, the interbedded zones (geological formations where oil and gas are trapped) are inaccessible, and other techniques such as HDD are required (Ma et al., 2016). Sheehan (2014) estimated that companies able to implement HDD technologies could increase their hydrocarbon extraction by up to 42%, representing an increase in the well's payoff and the company's profits.

Nowadays, there have been developments in compact solutions for drilling operations. Jian et al. (2012) designed and implemented a steering mechanism for a drilling robot used for geological exploration. This robot can drill between 20-100 m and is composed of a drilling and a steering section. One key feature of their design is the use of electrical components that allows them to have a smaller design footprint, but their prototype has less drilling power. Therefore, a solution like this cannot be implemented in the oil and gas industry since a balance between power and size is required, which can be achieved using fluid and robust control systems. The table below shows the expected specifications that the micro-drilling robotic device will have. As can be seen, the robot's general specifications (e.g., dry weight, length) change according to the assembly type. However, the drilling and fluid power parameters are the same since the drilling operation is expected to be performed in the same basin. Thus, the power requirements have to be met independently of the type of assembly chosen.

Table 1.1. Micro-Drilling Robotic Device Specifications.

Category	**Parameter**	**Assembly type**
General		**Worm robot device**
	Dry weight	88 lb. (~40 kg)
	Diameter	3.3 in (0.084 m)
	Length	5.6 ft (1.71 m) (fixed)
Drilling		
	Bit type	Ø 3.75 in (0.095 m) PDC bit
	ROP	15 ft/hr (4.6 m/hr)
	WOB	450 pounds (2 kN)
	Turning radius/steering angle	100 ft / 16°
	Torque	100 Nm
	Rotational speed	[100;200] rev/min
Fluid Power		
	Pressure	1800 PSI (140 bar)
	Flow rate	5.9 GPM (22.3 liters/min)
	Hydraulic Horsepower	7.5 HP

Liu et al. (2019) provided a review and classification of downhole robots. They proposed two categories according to the type of structure and application. The first category is downhole traction robots, and the second is downhole drilling robots. The authors outlined that the critical component that differentiates these two categories is the presence of a circulation channel for the drilling mud across the robot. The drilling mud is an element required in the drilling operation for lubrication, temperature control, and to decrease the wear of the drill bit. In addition, it helps to remove the reservoir cuttings created caused by the drilling operation.

The significance of this project is summarized by two main aspects: time and costs. The drilling operation is continuous, highly sensitive to external factors, and an expensive process. According to Beattie (2020), the average cost-per-barrel of oil can go from 30-40 USD using conventional drilling methods and up to 40-90 USD when horizontal drilling techniques are implemented.

Therefore, a horizontal drilling device capable of enhancing the oil extraction in depleted wells can bring both a reduced time and an accelerated return on investment. However, such a device cannot be developed without a reliable and robust sensing system that allows it to maximize efficiency by improving its operational control.

1.4. Assumptions

For the project's purposes, the researcher made the following assumptions related to the smart sensing system's design considering its future implementation in a micro drilling robotic device. The smart sensing system is integrated into a test bench which will be used as an architecture to validate the system's reliability. The details of the test bench, operational characteristics, capabilities, and elements will be discussed in detail in Chapter 4.

The assumptions for this research work are listed below:

1. It is assumed that the test bench provides an environment with conditions similar to the ones expected during the drilling operation.
2. The currently selected sensors might not be the definitive ones that will be used in the micro drilling device. Still, they are similar in operation principle and provide a comparable output.
3. It is assumed that the laboratory tests' measurements are an accurate representation of the conditions and response of the sensing system DTH.

1.5. Delimitations

The delimitations for this research work are listed below:

1. The smart sensing system was designed to be easily implementable and adaptable to different compact drilling devices.
2. The opportunity exists to scale the system by adding more sensors. Still, the additional sensors must also be suitable for the harsh environment faced during a drilling operation and must provide an output readable by the Analog to Digital Converter (ADC). Otherwise, an additional signal conditioning component such as the ones in section 3.5.3 must be added.
3. The extent of the number and characteristics of the sensors that can be added will be limited by the microprocessor's capabilities to receive, process, and transmit the signals.
4. For future work, the sensing system will be implemented in a robotic drilling device of three to four inches in diameter and will fall into the category of "short-radius" horizontal drilling applications, that is, to steer and drill at a rate of ~100 degrees/100 ft.
5. The construction of a special enclosure for the electronics will be considered for the Printed Circuit Board (PCB) design, but it will not be part of this project's scope.
6. The research project's scope only considers the smart sensing system's development and testing of its sensors, communications, and user interface required for its functioning and operation.

1.6. Limitations

The researcher's fields of expertise are not oil extraction nor geology but rather are focused on industrial robotics, instrumentation, and fluid power systems. Therefore, a thorough review of the literature was performed, and continuous feedback from experts in the field was provided to fill any gaps in fundamental knowledge. To aid in replicability for a future industrial product, the researcher selected commercially available components to create a fully functional prototype of a smart sensing system when possible. For non-available and special elements, custom machined components were made. In the case of sensors that required additional electronics to protect from electrical overcharge, overcurrent, noise, and temperature, the researcher designed the necessary mechanisms to mitigate these factors that affected the system's reliability. There was also a limitation regarding the type of sensors that were used due to the harsh environment in which the system will be implemented in the future.

1.7. Micro Drilling Robot Implementation

The present work was part of a research project projected to be a three-year effort that is divided into three phases, as seen in Figure 1.2. The project's final expected outcome is to have a fully functional prototype of a micro drilling device that will be used in depleted wells for horizontal drilling.

Phase one of the project consisted of the initial proof of concept and a thorough literature review. This phase is intended to provide the researcher with the base knowledge required to understand the problem, the relevance, and the constraints. Phase one also included the prototype design, its different segments, frame, mechanism, and components. This phase's key deliverable was the virtual assembly and the first version of the bill of materials of the prototype.

Phase two of the project involved the construction and controlled testing of some of the prototype's mechanisms and components. For this phase, a test bench was created as well as the criteria for the Design of Experiments (DOE), and the researcher developed a smart sensing system that was implemented in a controlled environment. This phase required a high level of hardware and software development since this phase's deliverable was a physical working prototype. A set of systems and interfaces allowed an operator to perform activities in a controlled environment. A DOE was implemented to define the experiments to be performed on the test bench that will be developed. Data gathering and analysis were executed in each set of experiments to move forward to phase three.

Phase three consists of the optimization of the prototype. The data examined in Phase two will be utilized to perform design analysis and optimization that will lead to further improvements. The cycle of constant development, test, debugging, and implementation aims to have a working prototype that will be tested in a real environment. The design improvements will be focused on the manufacturability and reliability of the robot's frame and mechanisms and the experiments' replicability.

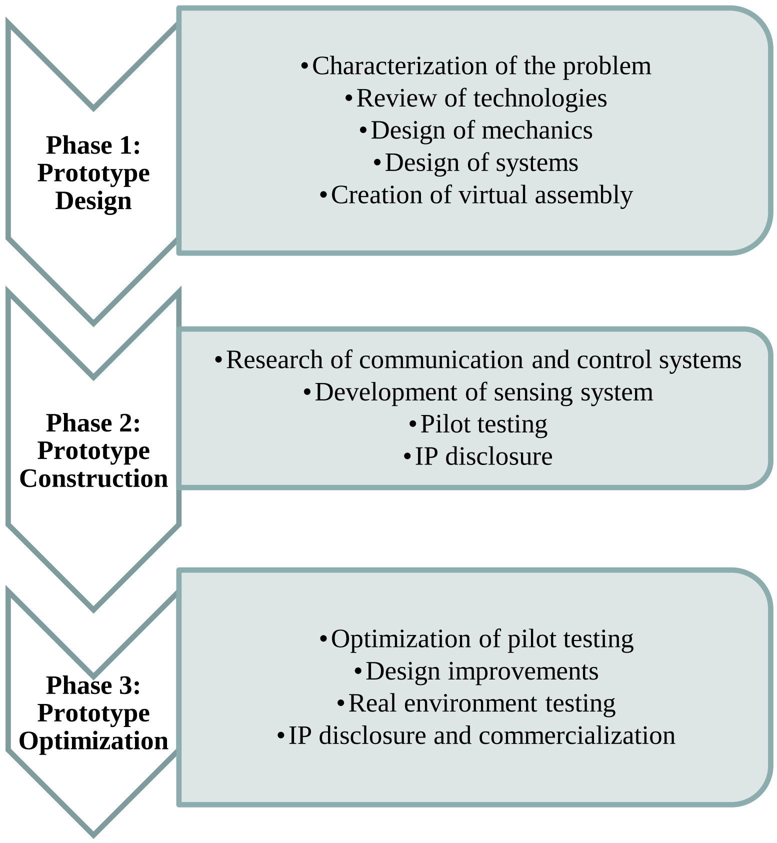

Figure 1.2. Flow diagram of the research project phases.

The project's scope focused on developing a smart sensing system that was designed for implementation in the drilling robot. The research project was divided into three pillars; the first one centered around the sensors and smart modules to be used, the second towards the communication, and the last one on the User Interface (UI).

The thesis focuses on Phase 2: Prototype Construction, specifically on the literature review of the communication and control systems used in the oil and gas industry. An in-depth analysis was done to identify such systems' characteristics and perform an evaluation to categorize each one's advantages and drawbacks. With qualitative and quantitative analysis, the researcher selected the most appropriate technologies to build such a sensing system.

A smart sensing system was developed, and it integrated the sensors required for the direct and indirect operational measurements as are necessary for the future's implementation on a drilling robot. The system was designed as an independent module that was implemented in a test bench but focusing on selecting reliable and sturdy components that will handle the operation DTH on the final micro drilling robot.

The system also integrated a User Interface (UI) that showed graphically the different variables being measured. The UI was deployed in a cloud-based dashboard. This will aid the user in making decisions regarding the operation of the robot. Finally, the integration of the sensing and communication systems was performed.

CHAPTER 2. REVIEW OF LITERATURE

The oil and gas industry is constantly evolving and searching for novel technologies and methods to increase the machinery's efficiency. The development of new devices and technologies to reach and enhance oil extraction is also continuously researched (Sampaio, 2017; Vestavik et al., 2011). Thus, the industry is very competitive, and the sponsors highly protect the findings and intellectual property generated by projects.

Figure 2.1 and Figure 2.2 show the connection diagrams generated to visualize and identify the connections between the sensing systems and other research project components, such as fluid power systems and industrial robotics within the oil and gas industry.

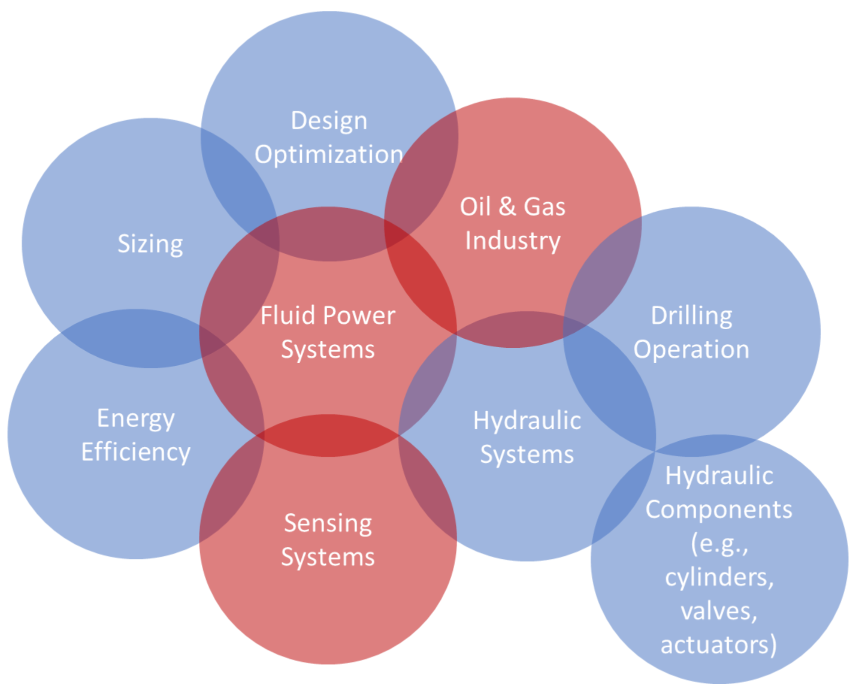

Figure 2.1. Sensing and fluid power systems connection diagram.

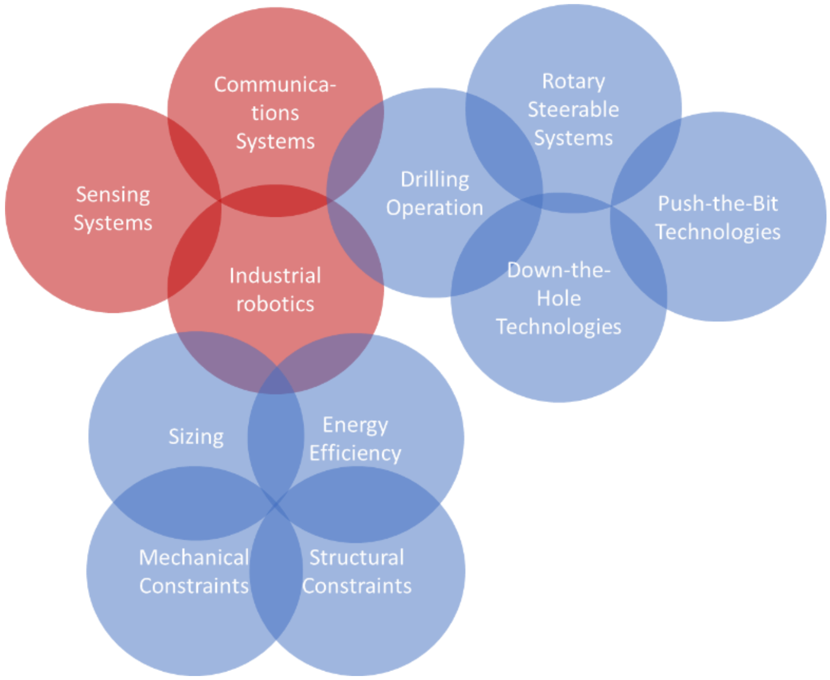

Figure 2.2. Industrial robotics and sensing and communication systems connection diagram.

2.1. Rotary Drilling

Rotary drilling systems were developed and are widely used for creating oil wells. They consist of a sharp rotating drill bit that applies force downwards and removes the cuttings with a circulating drilling fluid. However, when moving horizontally with this technique, more space is required, and more time is needed compared to other methods. The system must steer the drill bit using a cone angle of at least 6 degrees in any direction (in the case of using Rotary Steerable System – RSS). The use of a deflector shoe or using only part of the drill bit's nozzles allows for the creation of a new drilling path.

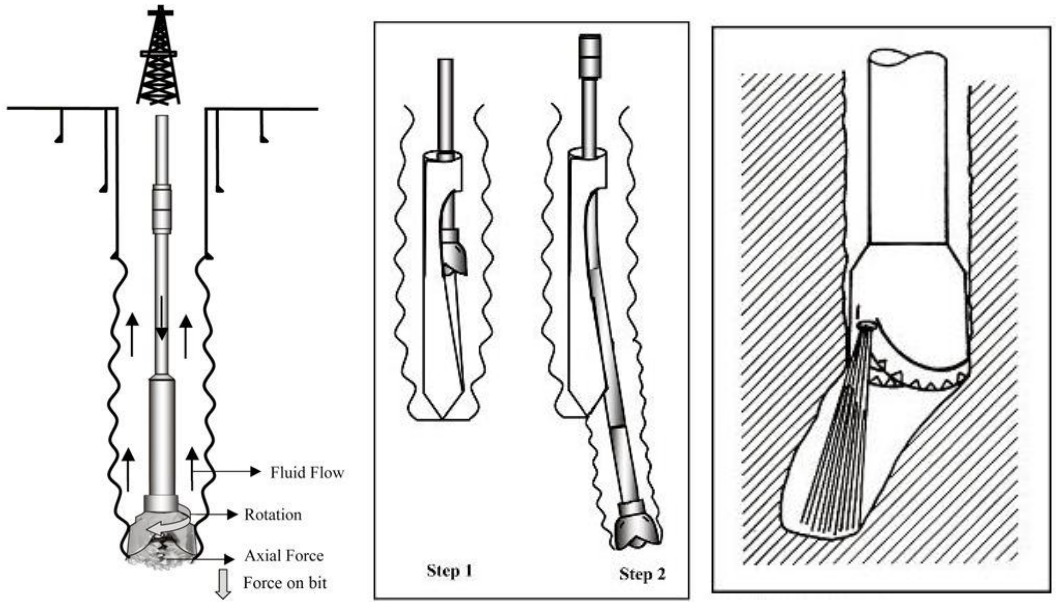

Figure 2.3. Rotary drilling schematic with its main components (left). Directional drilling techniques (center and right) (Azar & Samuel, 2007).

Directional drilling technologies demand has been growing in the last few decades as the oil and gas industry requires novel methods to access pay zones and enhance oil extraction (Park et al., 2013). The current research project presents a smart sensing system as one of the pillars to respond to the proposed research questions and achieve the expected outcomes, specifically thinking ahead to future applications and implementation in a drilling device with a Rotary Steerable System (RSS).

Park et al. (2013) identified Point-the-Bit and Push-the-Bit technologies as the most common types of RSS, and they introduced a new hybrid RSS. They found that more steerability can be achieved in small-diameter robots by having four axes of action instead of three (as most manufacturers currently have). Thus a mechanism similar to this one would be beneficial to perform more accurate drilling operations.

Kim et al. (2015) acknowledged directional RSS as the most advanced system for horizontal and unconventional drilling. In their article, the authors presented a model that aims to estimate and reduce RSS devices' friction. As they describe it, friction is one of the components of the drilling operation that reduces the tools' performance and increases the wear of the elements while adding to the "dog-leg" effect (creation of undesired conical trajectories).

One of the drawbacks of RSS is the precision and accuracy of the drilling operation. Devices that implement RSS tend to require stabilizers and centralizers to avoid the "dog-leg" effect and correctly create a path to the interbedded or pay zone (Fang et al., 2017). Researchers have design methods and technologies to increase the accuracy of RSS by adding torsional vibration analysis (Wang et al., 2014) or using the information gathered by sensors and algorithms to create 3D paths of the drilling device (Atashnezhad et al., 2014; Sampaio, 2017). Li et al. (2017) and Atashnezhad et al. (2014) have designed algorithms and prediction models to calculate the wellbore trajectories with a different approach.

Park et al. (2013) were not alone in the implementation of hybrid RSS. Kim et al. (2015) presented their version of an RSS using a three-axis steering mechanism and combining both push-the-bit and point-the-bit technologies. The implementation of these technologies, along with robust sensing and control systems, provided their robot with better steerability and increased overall length.

An RSS is complemented with control and sensing systems. Yang (2011) highlighted that in the past, such systems were only implemented in laboratory settings; however, nowadays, they can be found in Bottom Hole Assemblies (BHA). Yang implemented a Field Programmable Gate Arrays (FPGA)-based communication system with a closed-loop controller to increase the reliability of the drilling device. Similarly, Gooma (2016) designed a control system using a Gravitational Search Algorithm (GSA) and non-linear models to create a system that evaluates the drilling operation in real-time and adjusts it to preset settings in order to increase the performance. Similar models have been developed by Wilson (2017) and Baig (2015).

2.2. Basin Conditions

The optimal drilling method and the well cost prediction require a deep understanding of the location and well depth. A reservoir model, including the rock’s mechanical and thermal properties across the different basin areas, along with the operational measurements, is required to ensure a successful drilling process.

Knowing the geological composition of the basin where the robot will operate is important for the smart sensing system's design. Specifically, since the type of sensors that will be implemented and the enclosure into which they will be placed are related to the working environment.

In the geologic time scale, the Illinois Basin (Figure 2.4) contains formations from the Precambrian and Paleozoic up to the Mesozoic periods, with the Cambrian- through Pennsylvanian sections being the most relevant period for this work. The basin is filled with marine rocks ranging in this period (Panno et al., 2018). Most of the rock is sedimentary, having Limestone (Carbonate), Dolomite (Carbonate), Sandstone (Clastic), and Siltstone (Clastic).

Figure 2.4. The Illinois Basin (Panno, 2018).

Rocks have several properties that affect the drilling operation's performance, such as porosity, permeability, matrix composition, strength, and ductility. These properties are affected by in situ stresses. Field experience has demonstrated that the ROP decreases as the depth increases (Azar & Samuel, 2007). When a compressive load is applied at a controlled rate, rocks present two types of behavior. In the first case, the rock will deform (strain) almost linearly before it fails. This is called brittle failure. In the other case, the rock can strain a considerable amount before failure; this is called ductile failure.

In Figure 2.5, a schematic of the induced stresses under this type of loading on the rock is shown, and stresses are denoted by σ_1-principal maximum, σ_2-intermediate, and σ_3-minimum stresses. The typical stress-strain curves for rock failure can also be seen in the figure below. Curve 2 presents the scenario of increased confining pressure, which directly increases the minimum principal stress, generating higher values for both stress and strain for a brittle failure.

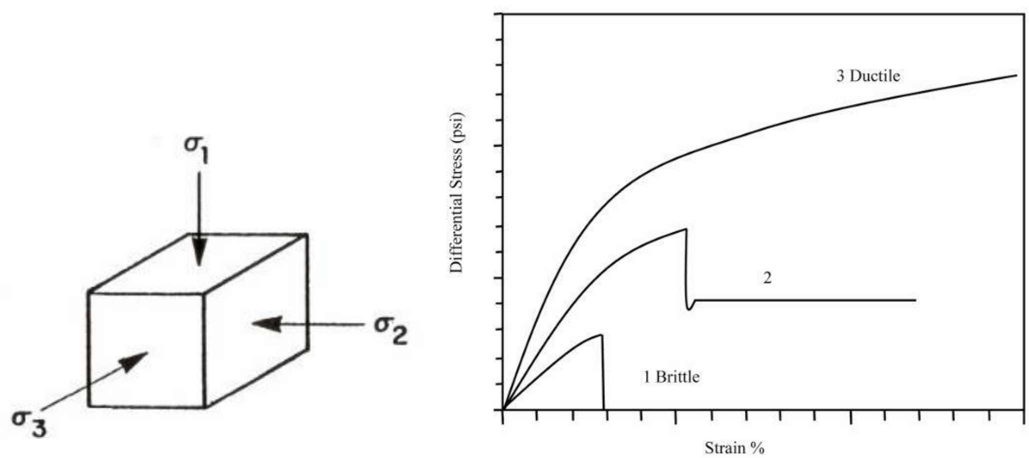

Figure 2.5. Schematic of induced stresses and typical stress-strain curves for rock failure (Azar & Samuel, 2007).

When drilling into the rock, the stresses at the drill bit are altered because the borehole fluid pressure is less than the overburden stress that initially acted on the rock. To predict a particular rock's strength, it is necessary to determine the local stresses and the pore pressures that are immediately adjacent to the drill bit teeth. From a general perspective, the minimum principal stress is perpendicular to the borehole bottom and is equal to the differential pressure, which is the difference between the borehole pressure (mud pressure) and the local pressure. Figure 2.6 shows how the ROP and stress are affected by the pore pressure increase.

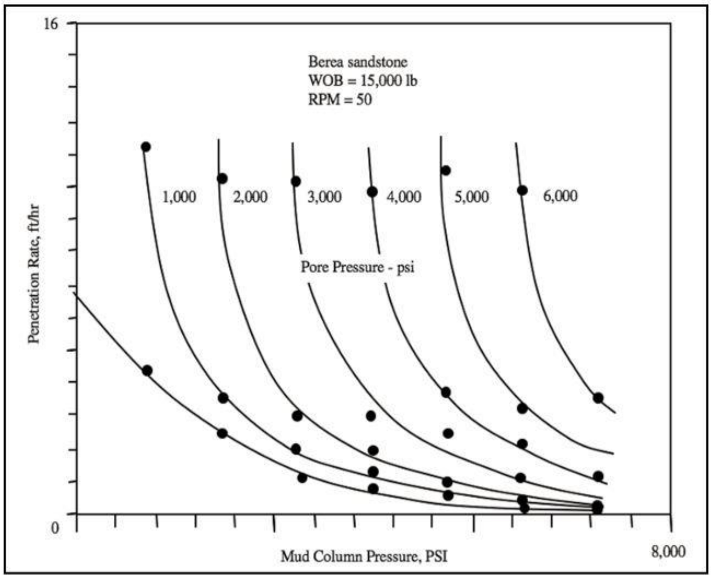

Figure 2.6. Stresses in compressive strength test and tooth penetration (Azar & Samuel, 2007).

The smart sensing system developed for this project is expected to be implemented into a prototype that will work predominantly with sandstone. As a sedimentary rock, it has a porosity value of around 0.15 ($\varphi = 0.15$) with a mineral composition of mostly quartz. The most relevant mechanical properties of the basin can be seen in Figure 2.7 and Figure 2.8. These properties were determined using mineral volume fractions and other log-derived and core data by (Rockhold et al., 2014) during the planning for the construction and operation of an underground CO_2 injection well in Morgan County, Illinois.

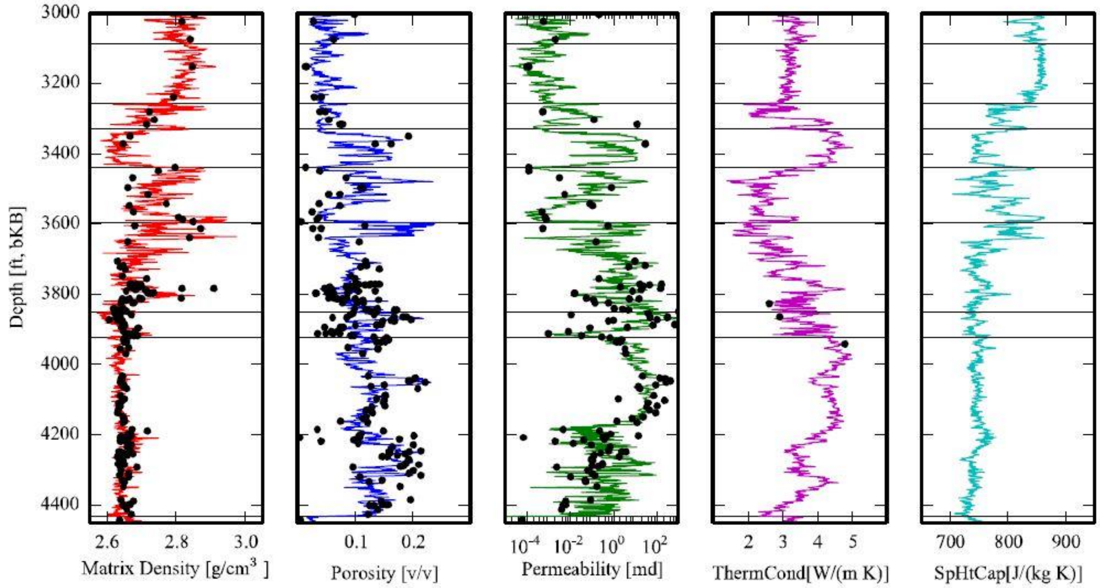

Figure 2.7. Core (black dots) and wire-line log derived matrix density, porosity, intrinsic permeability, matrix thermal conductivity, and specific heat capacity (Rockhold et al., 2014).

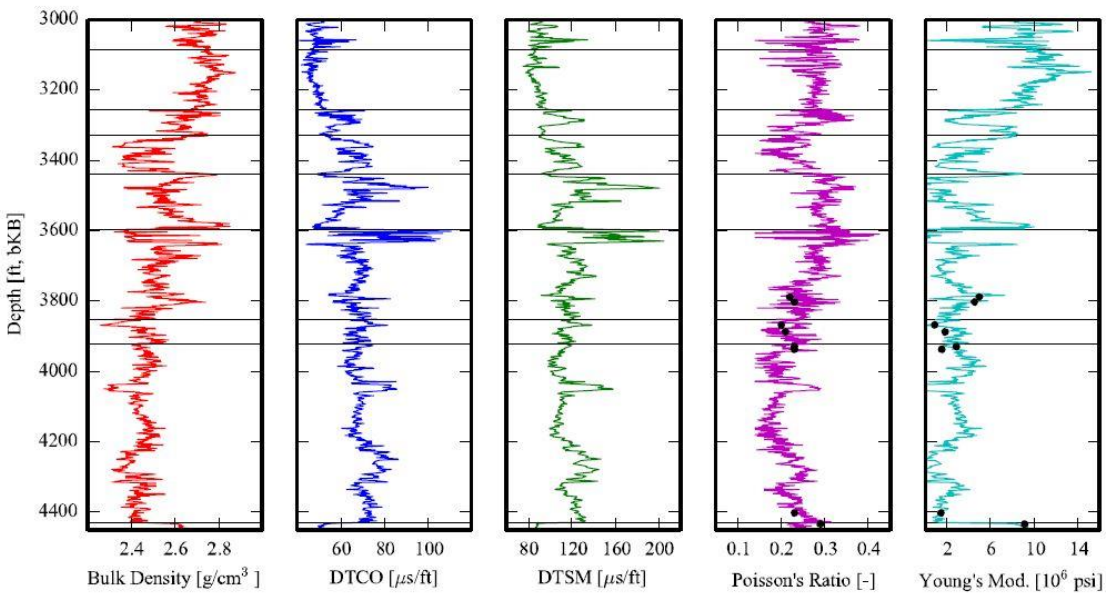

Figure 2.8. Core (black dots) and wire-line log derived bulk density, compressional slowness (DTCO), shear slowness (DTSM), Poisson's ratio, and isotropic Young's modulus (Rockhold et al., 2014).

2.3. Wellbore Conditions and Geometric Constraints

Depending on its purpose and/or function, there are different types of oil wells; exploration, appraisal, production, relief, and injection wells. For this project, the smart sensing system is expected to be implemented in a robot that will operate in production wells. According to Hossain and Al-Majed (2015), production wells are made to create a flow path from the reservoir to the surface, and after that, through pipelines to a storage facility or to a production or refinery facility.

The process of drilling a well for oil extraction is not an easy task. There are several steps involved that require specialized equipment, technical knowledge from experts, and weeks, or in some cases, months of preparation (Islam & Hossain, 2020).

a. Boring

The first step for creating the production well is laborious. This task is done with a drill bit and a set of pipes that are used to create a vertical hole in the ground. Depending on the geography and soil basin conditions, the well can be bored directly on top of the oil reserve. There are some cases where this cannot be done, and a directional drilling method must be used.

b. Circulation

Once the vertical drilling process starts, drilling fluid or “mud” is continuously injected into the hole and pumped back to the surface. This circulation helps to remove debris and rock cuttings from the hole. The drilling fluid also gives support and stability to the well, and it even acts as a cooling and lubricating element for the drill tool.

c. Casing

Once the desired depth is achieved, the casing is cemented in place to provide structural support to the well and prevent a possible collapse. The typical well casing diagram can be seen in the following figure.

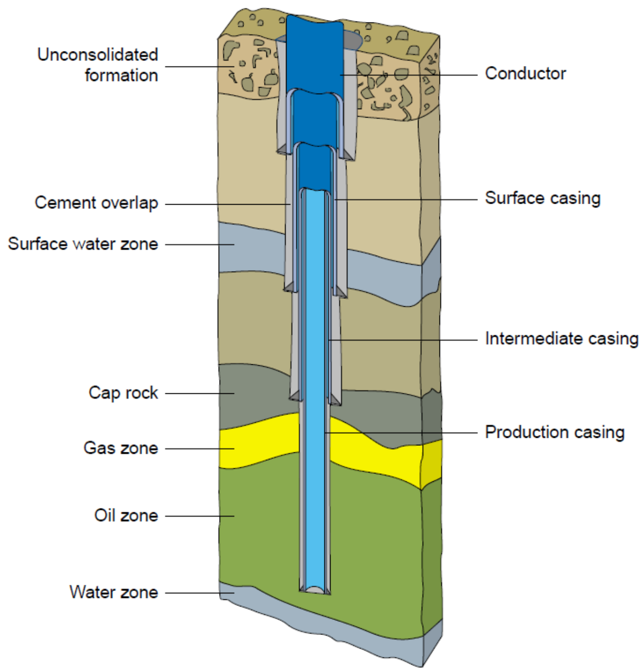

Figure 2.9. Well casing diagram (Industrimigas, 2013).

d. Completion

This process comes after drilling and casing the well, and it is the one in which the well is prepared to extract the oil. In this phase, small holes are made in the casing portion, which passed through the production zone. These holes are also called “perforations,” which provide a path for the oil to flow. When low pressures are present, a pump is installed to bring the oil to the surface (this occurs mainly in depleted zones).

e. Production

Production is the most critical phase in every well’s life cycle. In this phase, the oil rig (Figure 2.10) is placed along with the “Christmas tree” valve, which is a set of valves that regulate in and out pressures and flow, as well as the overall access to the wellbore. Through the Christmas tree (Figure 2.11), the oil is pumped into the surface using only the well’s pressure. Once the pressure decreases, a pump is connected to the Christmas tree so the oil can still be collected. The oil rig is removed once the well is drilled before production starts.

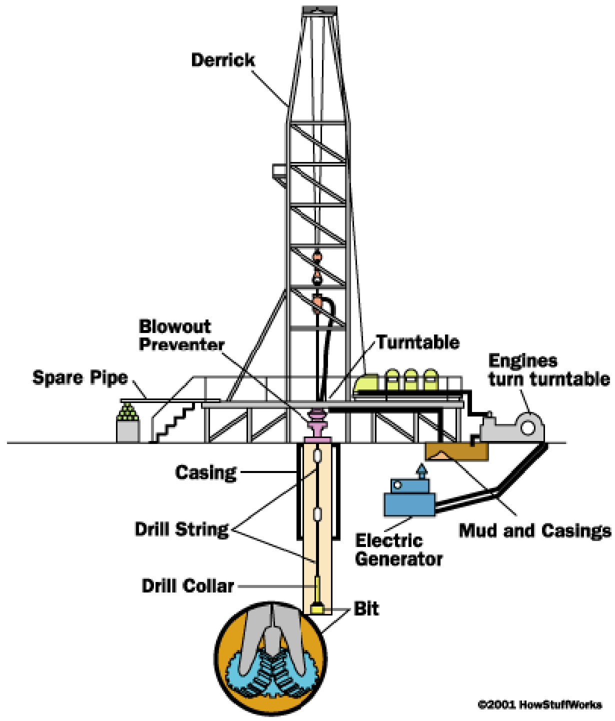

Figure 2.10. Oil rig diagram with main components (Freudenrich & Strickland, 2018).

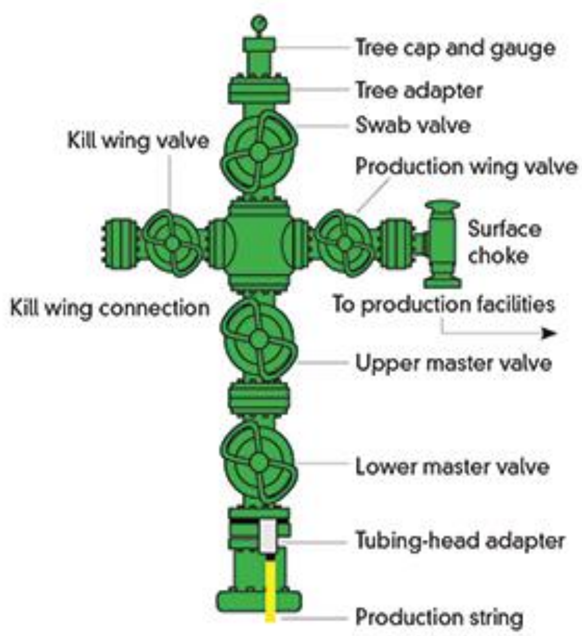

Figure 2.11. Wellhead or “Christmas tree” (Lee, 2017).

f. Abandonment

Once the well reaches the end of its useful life, it is plugged, closed, and abandoned to protect the surrounding environment. It is essential to mention that in most cases, the useful life is not determined by the amount of oil in the reserve, but by the economic impact of extracting from it. A well that is abandoned (Figure 2.12) still has some oil in interbedded zones, but to reach them would require alternate remedial methods such as horizontal drilling or another tertiary intervention technique.

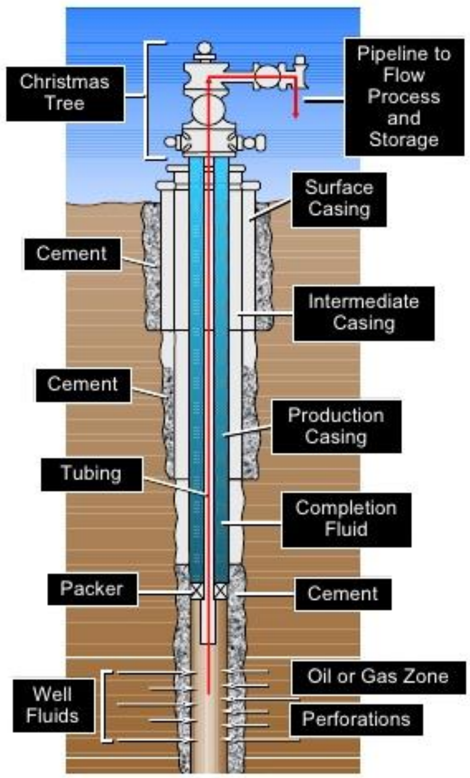

Figure 2.12. Completed well (McDowell, 2006).

2.4. Weight on Bit (WOB) and Torque Calculations

Researchers have worked and identified models for calculating variables related to drilling (indirect measurements). The work made by Soares et al. (2016) provides a summary and insight into the diverse and most used models available. The models evaluated have in common that they consider the rock's physical properties to estimate the Rate of Penetration (ROP). The three models presented by Soares consider the Revolutions per Minute (RPM) and the bit diameter.

The model developed by Bingham (1964), shown in Eq. 1, is the first evaluated and is the most general of the three presented. Such a model considers the WOB and two constants for rock formation: a and b.

$$ROP = a * RPM \left(\frac{WOB}{D_B}\right)^b \rightarrow (Eq. 1) \text{ (Bingham,1964)}$$

The second model evaluated is from Hareland and Rampersad (1994). Such a model was developed specifically for polycrystalline diamond compact (PDC) bits. The number of cutters and rock compressed area ahead of each cutter is considered to have an accurate estimation of the ROP required (Eq. 2).

$$ROP = \frac{14.14 * N_C * RPM * A_V}{D_B} \rightarrow (Eq. 2) \text{ (Hareland \& Rampersad,1994)}$$

The last model related to the penetration rate evaluated by Soares was developed by Motahhari et al. (2010). The model is shown in Eq. 3 and was designed not only to focus on PDC bits but also for drilling in sandstone formations. Motahhari's model integrates the rock's confined compressive strength, two empirical ROP exponents (α and γ), a bit-rock interaction and bit geometry coefficient, and the wear function on the bit.

$$ROP = W_f \left(\frac{G * RPM^{\gamma} * WOB^{\alpha}}{D_B * S}\right) \rightarrow (Eq. 3) \text{ (Motahhari et al., 2010)}$$

The researcher calculated other essential variables required to select components such as pressure, flow rate, and hydraulic horsepower based on the previous models. The torque calculation was based on the Illinois Basin's geological conditions, considering sandstone as the primary rock formation. The model proposed by (Wang et al. 2018) successfully relates the drilling parameters using a PDC bit with the rock mechanical parameters. The required torque to drill into sandstone using a 2.4” diameter PDC bit was calculated using Eq. 4.

$$M = \left[\frac{cV\cos\varphi\cos(\gamma+\psi)}{3N[1-\sin(\varphi+\gamma+\psi)]} + \frac{c\mu e\cos\varphi}{1-\sin\varphi}\right]\left[2R(L_1+L_2+L_3)-(L_1^2+L_2^2+L_3^2)\right] \rightarrow (Eq.4)$$ (Wang et al. 2018)

Where c is the rock cohesive resistance, V is the drilling rate, φ the angle of internal fraction, γ the cutting edge inclination angle (drill bit), ψ the angle between the cutting edge force on the rock fragment and the drill bit normal plane, μ is the friction coefficient between the drill bit and the rock, e is the drill bit thickness, N is the rotational speed, R is the drill bit radius, and L_i is the blade length.

The models presented by these authors will serve as an early approach for the indirect measurements that will be calculated in the future by the smart sensing system developed for the project, and that will be required once the system is implemented in the prototype.

2.5. Statistical Modeling Techniques in Drilling Applications

Statistical models use mathematical equations to encode information extracted from the data. In some cases, statistical modeling techniques can provide adequate models quickly and with less computer processing requirements, even in the case of problems where more flexible machine learning techniques (such as neural networks) may ultimately deliver better results. Statistical models can be used as a predictive baseline to judge the performance of more technologically advanced models.

Statistical models are widely used across several fields. In the oil and gas industry, for example, they are used to measure productivity in the oil extraction operation (Managi, 2012), the impact of oil price for manufacturers (Schwarz, 2013), or to develop models to estimate political impact caused by the industry (Mucci, 2015).

For this project, statistical models were used to allow for the implementation in the future of a control system using the sensing system's information. As mentioned before, the control and sensing systems feed each other with the required information to operate, and a measurement-while-drilling system is a solution that integrates both.

Some researchers like Sun (2010) and Jia (2011) decided to take a novel approach by creating systems specialized with specific variables (e.g., pressure or shear velocity). Still, the literature supports the theory that a broader approach allows for creating a device that can operate in a wider variety of settings.

ElGizawy (2009) developed a continuous MWD surveying system, which proved to be a simple yet cost-effective solution due to the use of Micro-Electro-Mechanical Systems (MEMS) sensors and an acquisition and processing system based on a Kalman filter. On the other hand, Luo (2010) defined the MWD systems as a critical component to increasing accuracy and control over the trajectory of the drilling devices. He proposed a methodology to create a MWD system that focuses on the progressive implementation of sensors into the drilling tool to debug and improve the measurements' reliability and accuracy.

Kimmes (2016) expanded the field by using MWD systems and incorporated vibration monitoring and ground-penetrating radar (GPR) to measure the drilling tool's operational variables and determine and find cracks on the wellbore. Simmilarly, Hadavand (2015) used MWD systems along with robust geomagnetic sensors to reduce positional uncertainty in DTH applications. The compensation model and the algorithm developed by Hadavand proved to be a solution to minimize inaccuracy in drilling operations.

In the last decade, researchers have focused their efforts on implementing new communications systems (e.g., wireless, fiber optic) (Wang, 2010) and continuously increase the reliability of the operation and path trajectory on drilling devices (Abughaban, 2017). As computational capacity in microcontrollers is increased, and sensors are developed, hybrid MWD systems continue to emerge.

2.6. Smart Sensors

One significant improvement implemented to sensors is the addition of smart capabilities. A smart sensor is the combination of a sensing element (sensor) and a microprocessor (Hunter et al., 2010). The processing capabilities transform the sensor from a passive component that simply converts a physical variable to an electrical signal into an element that can, for example, filter, process, store, and send data (Mahmood et al., 2021). A smart sensing system is a system that consists of various sensors, where one or more have smart capabilities. Nowadays, these systems are widely used across multiple fields for an extensive range of applications.

Afsarimanesh et al. (2016) developed a non-invasive, real-time smart sensing system used for the continuous monitoring of bone health and focusing on the detection of bone loss. Alavi et al. (2016) designed and implemented a continuous monitoring system to analyze pavement health using a series of piezoelectric self-powered sensors. The researchers could predict when the pavement was damaged or required maintenance with the information from the sensors and a statistical model's design.

Zaghari et al. (2020) developed a self-powered sensing system for a smart bearing in an aircraft jet engine. The developed system was designed to withstand high operating temperatures (above 125 °C) and provide real-time feedback to a control system through wired communication. Additionally, a wireless sensing system was implemented to collect environmental data as part of a data logger of the flight conditions.

Jagannathan & Priyatharshini (2015) developed a methodology for smart farming by integrating smart sensing and irrigation systems. The sensing system was used to acquire information on the soil's physical properties (e.g., pH, moisture, nutrient content), and the implementation was done using wireless communication. The sensing system fed the irrigation system the measurements and values required to perform actions based on the crop requirements. As a result, the authors successfully created an agricultural task automation system.

Smart sensing systems have also been effectively implemented to measure structures. Examples of these applications can be seen with the integration of sensing systems to analyze aerospace structures and ensure their safety and reliability (Zhang et al., 2007) or the monitoring of structural damage in civil infrastructures (i.e., bridges) by using piezoelectric and optical fiber sensors (Yun & Min, 2011).

As can be seen from the previous cases, smart sensing systems are used for both the control and the continuous monitoring of other systems; this pattern is consistent across the literature. Smart sensing systems are also highly adaptable, and their applications and capabilities can be easily changed according to the telemetry technology and the sensors used.

A type of smart module to be considered in the sensing system design is an Inertial Measurement Unit (IMU), which is an electronic device that measures and reports on the speed, orientation, and gravitational forces of a device, using a combination of accelerometers and gyroscopes (Wen, 2019). Inertial measurement units are typically used in consumer electronics and in systems employed to maneuver aircraft or vehicles. IMU's are also used in spacecraft, including shuttles, satellites, and landers (Dissanayake et al., 2001; Yi et al., 2009).

However, the applications of IMU's are not exclusive to maneuver other devices. Inertial Measurement Units can also be found in healthcare. For example, to use them to control artificial limbs (Moreno et al., 2006) and to measure motor fluctuations and dyskinesia tremor in patients with Parkinson's disease (Dai et al., 2015)

2.7. Telemetry Technologies

One challenge that has continuously been faced by the oil and gas industry is the transmission of data from the devices DTH to the surface reliably and consistently (Arps & Arps, 1964; Emmerich et al., 2015). There are four main types of telemetry used in drilling operations, but hybrids or combinations of them have also been implemented in recent years (Berro & Reich, 2019).

2.7.1. Electromagnetic

Electromagnetic telemetry is a technology in which a transmitter is placed near the end of the BHA, and a series of electromagnetic signals are sent to a receiver or antenna (Vong et al., 2005). The antenna can be either on the surface or drilled and placed into the ground. The electromagnetic signals carry the information from the sensors' DTH, which are then received, filtered, and processed (Franconi et al., 2014). One drawback of this technology is that the rock does not allow the signal to travel to the surface in some lithologies due to the geological properties. In such a case, some companies have developed systems that consist of running a wired antenna DTH to the shoe-case. Then the transmitter only sends the information to this point via electromagnetic waves. From this point to the surface, the data is sent through cables.

2.7.2. Mud Pulse

The mud pulse telemetry consists of sending a binary coding transmission using fluids. For this technology, a pulse generator is placed near the end of the BHA. The pulse generator is a valve that varies the pressure inside the drillstring; then, the pressure changes are measured by a pressure sensor that, with an ADC, will send a signal to a microcontroller (Jr et al., 2015). The signal can be either positive/negative or continuous and with a bandwidth that goes typically from 3 to 40 bits per second:

a. Positive pulse: A valve is closed and then opened to increase the system's pressure.
b. Negative pulse: A valve is opened and then closed to decrease the system's pressure.
c. Continuous-wave: A valve is gradually opened/closed, generating sinusoidal pressure fluctuations in the system.

The mud pulse telemetry usually integrates three phases: Analog data acquisition, data compression, and signal filtering, but in recent years two additional phases (signal modulation and signal filtering) have been added to improve the technology into what now is known as High-Speed Mud Pulse Telemetry (HSMPT) (Emmerich et al., 2015).

2.7.3. Acoustic

Acoustic telemetry works similarly compared to electromagnetic telemetry. In this case, an encoded sound wave is produced near the end of the BHA. The sound wave is propagated through the steel drillstring with the help of repeaters or "nodes" and received at the surface. Acoustic telemetry was identified as a potential technology to transmit information in the late 1940s, and it was analyzed and developed by pioneer researchers like Alarie & Petteruti (1968), Spinnler & Stone (1978), Squire & Whitehouse (1979), and Drumheller (1992).

Notable implementations of this type of telemetry can be found across the literature. Harper et al. (2003) successfully implemented an acoustic data-acquisition system that provided real-time BHA data wirelessly using acoustic signals sent through the production tubing (a tube used in the wellbore through which fluids are transported). This system reduced the time required for preparation before the drilling operation, hence, adding value and increasing time efficiency by reducing operational costs.

Nevertheless, the amount of data that can be sent with acoustic telemetry is one of its weaknesses. However, it has been demonstrated that this technology is more reliable and efficient for drilling operations in underbalanced conditions than other methods (Gardner et al., 2006). In recent years, developments have been made to address this challenge by increasing the amount of data that can be packed and sent (Hawthorn & Aguilar, 2017).

Data analysis algorithms and filters must be implemented for this technology to overcome noise, vibration, and acoustic impedance changes that often decrease the signal quality (Xie, 2017).

2.7.4. Wired

Wired telemetry is one of the most recently developed technologies for real-time DTH measurements. It consists of placing a high-resistance insulated coaxial cable and an induction coil embedded in the double-shouldered connection (location for the coils) inside each drillpipe joint. When the signal travels from the BHA to the surface, it modifies the current in the first induction coil, generating an electromagnetic field, which makes a current flow in the other coil, transmitting the current signal to the second junction and so on until reaching the surface (Franconi et al., 2014). This method offers faster data transmission and therefore is primarily used for LWD systems since lithology logs require more accurate sensors and, in some cases, video transmission (Gravdal et al., 2010; Wolfe et al., 2009).

Redundancy measurements and Data Validation and Reconciliation (DVR) algorithms are commonly used to decrease noise on signals and estimate unmeasured data on wired telemetry applications.

2.8. Data Security and Privacy

The Internet of Things (IoT) is a platform that has seen significant development and has become a reality. Projections show that by 2021, 28 billion devices across several applications in various fields will be connected to the Internet (Sisinni et al., 2018), and this will grow to 30.9 billion by 2025 (Liu, 2020). The IoT market is one of the most promising in the technology and electronics fields (Khanna & Kaur, 2020). The projected global IoT spending for 2023 was estimated to be approximately 1.1 trillion USD. Besides, in 2019, the IoT managed services market revenue worldwide was 34.8 billion USD (Liu, 2020)

Even though IoT is the central platform for connecting devices, authors have divided it into several categories according to their application, field, or final user (Ray, 2018; Sehrawat & Gill, 2019). The Industrial Internet of Things (IIoT) is one of the branches of IoT that is oriented to provide solutions to companies and manufacturers by optimizing their processes and providing them with solutions to overcome the challenges. This is generally termed as the Fourth Industrial Revolution or Industry 4.0 (Sisinni et al., 2018).

However, data security and privacy have always been concerns faced by researchers and supporters of IoT and its branches (Mahmood et al., 2021; Zhang et al., 2014). Table 2.1 shows the challenges faced by the branch of Consumer IoT and IIoT have clear differences.

Table 2.1. Comparison Between Consumer IoT and IIoT (Sisinni et al., 2018)

	Consumer IoT	**Industrial IoT**
Impact	Revolution	Evolution
Service Model	Human-centered	Machine-oriented
Current Status	New devices and standards	Existing devices and standards
Connectivity	Ad-Hoc (infrastructure is not tolerated; nodes can be mobile)	Structured (nodes are fixed; centralized network management)
Criticality	Not stringent (excluding medical applications)	Mission-critical (timing, reliability, security, privacy)
Data Volume	Medium to High	High to Very High

A demonstration of the relevance that companies and developers put into this topic is that Liu (2020) estimated that the IoT security market revenue was 11.5 billion USD in 2019.

For the development of the smart sensing system, information security was considered in order to preserve data integrity and privacy when sending information from end to end across the communication protocol selected.

2.9. Summary

Across the literature, Rotary Steerable Systems (RSS), specifically push-the-bit and point-the-bit types, implemented using fluid-powered devices, have proven to be a reliable solution for horizontal drilling. Inaccuracy, the major disadvantage of RSS, has been minimized by researchers with the implementation of robust sensing and control systems. Regarding this topic, Measurement while Drilling sensing systems are the most reliable due to their construction and industrial communication capacities. For the control system, closed-loop controllers implemented with microcontrollers are the most widely accepted solution due to the size of components and low-power electronics.

From the literature review presented in this chapter, it can be determined that the proposed project is relevant to the oil and gas industry due to the importance of sensing systems while drilling, not only to ensure a reliable drilling operation but to control the tools in order to maximize the efficiency of the processes. In addition to the literature review, constant communication and assistance from experts in their respective fields were performed to ensure and aid with the project's success.

Data transfer will be a key element of the sensing system and its successful implementation on the micro-drilling device. The environment present during the drilling process represents an additional challenge to the method of transmission of data. The assessment of this challenge will be performed in future work.

CHAPTER 3. RESEARCH METHODOLOGY

3.1. Introduction

Current drilling devices and tools do not allow companies to maximize oil and gas extraction efficiently or effectively in depleted wells. For the development of these new drilling devices and the implementation of novel technologies, it is required to have reliable information from the BHA devices to the surface, information that robust and dependable sensing systems must gather.

For the successful development and implementation of this project, the methodology used was aimed to respond to the research questions presented in section 1.2.1 of Chapter 1. Also, it sought to achieve the proposed outcomes, which were designing and developing a smart sensing system prototype. The development of the prototype was based on a thorough review of the literature. The researcher identified success and failure cases to implement the more suitable technologies that helped obtain reliable measurements. The data from the sensors was gathered, processed, and sent using a communication protocol, and a cloud-based dashboard was developed to visualize the measurements.

3.2. Measuring variables

The oil and gas industry has two terms that are essential to understand how measurements are performed in conditions as harsh and extreme as in the process of oil extraction.

Logging while Drilling (LWD) is the process of making detailed records of the geological formation perforated by a drilling tool. The records can be either videos or physical measurements. Nowadays, an LWD system consists of sensors that make electrical, porosity, and lithology logs. LWD systems are implemented primarily in vertical drilling devices (Islam & Hossain, 2020).

Measurement while Drilling (MWD) is the system used for directional and horizontal drilling, and it focuses more on the measurements of the drilling device (e.g., inclination, azimuth, pressure, torque, force, temperature) (Islam & Hossain, 2020).

A system with characteristics similar to an MWD was designed considering its future implementation in a micro-drilling device. The sensing system will collect data on the critical variables for the prototype's operating and decision support. Inclination and azimuth measurements will be taken to determine the robot's Down-the-Hole (DTH) position and direction using the magnetic orientation of the earth as a reference. This information, along with data recorded with accelerometers and magnetometers, will be used to plan and correct the robot's direction and steering. Also, measurements of the drill bit's rotational speed, vibration DTH, DTH temperature, mudflow volume and pressure, and torque and weight on the bit will be sensed and recorded in real-time to provide information on the performance and technical operation of the robot. In Table 3.1, the different variables and their types are presented.

As shown in the table below, the design of the sensing system considered the future implementation in the micro-drilling device and its capability of handling both direct and indirect measurements. However, it is important to outline that the scope of this research project will contemplate only the variables that will be measured in the laboratory setting that was designed. The measurement of the variables critical for the micro-drilling device is part of future work.

A direct measurement is obtained with a measuring instrument that compares the variable to be measured with a standard. For example, to measure the wellbore temperature at a certain depth, a specific sensor can be used to gather the value.

To carry out a direct measurement is not always possible because there are variables that cannot be measured by direct comparison. An indirect measurement is one in which a quantity sought is estimated by measuring one or more different variables, and the value sought is calculated by estimation from the quantity or quantities directly measured. For example, to determine the drill bit's rotational speed and the ROP, first, it is necessary to measure other variables such as flow.

Table 3.1. Variables Relevant for the Research.

Variable	Type	Setting	Units of Measure
Vibration DTH	Direct	Micro-drilling device	Hz
DTH temperature	Direct	Micro-drilling device	[°F] or [°C]
Mudflow volume	Direct	Micro-drilling device	[gpm] or [L/min]
Weight on bit	Direct	Micro-drilling device	[lb] or [kg]
Inclination	Direct	Micro-drilling device	Angle [°] in X, Y, and Z axis
Magnetic direction	Direct	Micro-drilling device	Angle [°]
Mudflow's pressure	Direct	Micro-drilling device	[psi] or [bar]
Drill bit's rotational speed	Indirect	Micro-drilling device	[rpm]
Rate of Penetration (ROP)	Indirect	Micro-drilling device	[ft/hr] or [m/hr]
Torque	Indirect	Micro-drilling device	Nm
Hydraulic cylinder's piston position	Direct	Test bench / Micro-drilling device	[in] or [cm]
Hydraulic system's pressure	Direct	Test bench / Micro-drilling device	[psi] or [bar]
Hydraulic system's flow	Direct	Test bench / Micro-drilling device	[gpm] or [L/min]

3.3.Treatment and Instrumentation

The consistency and validity of the data are critical for developmental research. Thus, the researcher made sure that the measurements were consistent across the experiments under similar conditions. An inter-rater reliability plan was designed to guarantee that other researchers and operators can gather consistent data in similar operating conditions. The validity is a judgment based on evidence, and the researcher made sure that the results were consistent, and that correlation was present across the variables on the tests. The assessment of both reliability and validity was an ongoing process considered in the development of this research project.

3.4. Test Bench

A test bench was used as a case of study to implement and test the sensing system. The test bench consists of a variable displacement pump, reservoir, a pressure relief valve, a directional control valve, variable orifice valves, flow meters, pressure transducers, pressure gauges, and hydraulic actuators (Figure 3.1).

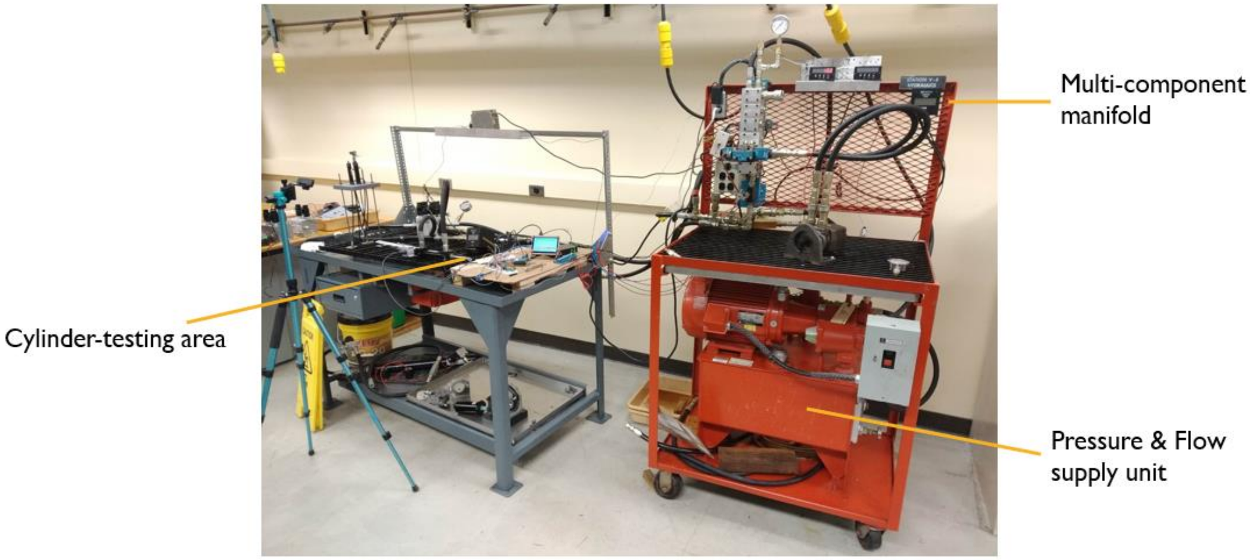

Figure 3.1. Hydraulic test bench.

Figure 3.2 shows the manifold used, one analog pressure transducer (upper left), and a flow meter display (middle right). Also, the arrangement of the string potentiometer attached to the end of the piston rod can be seen. The magnetic position transducer was placed at 3 mm of the other end of the piston rod.

The test bench features the actuation of a hydraulic motor and a hydraulic cylinder, critical components of a micro-drilling robot's drilling and steering mechanisms. The hydraulic motor rotation was controlled using a directional control valve while a variable displacement pump constantly delivered the flow.

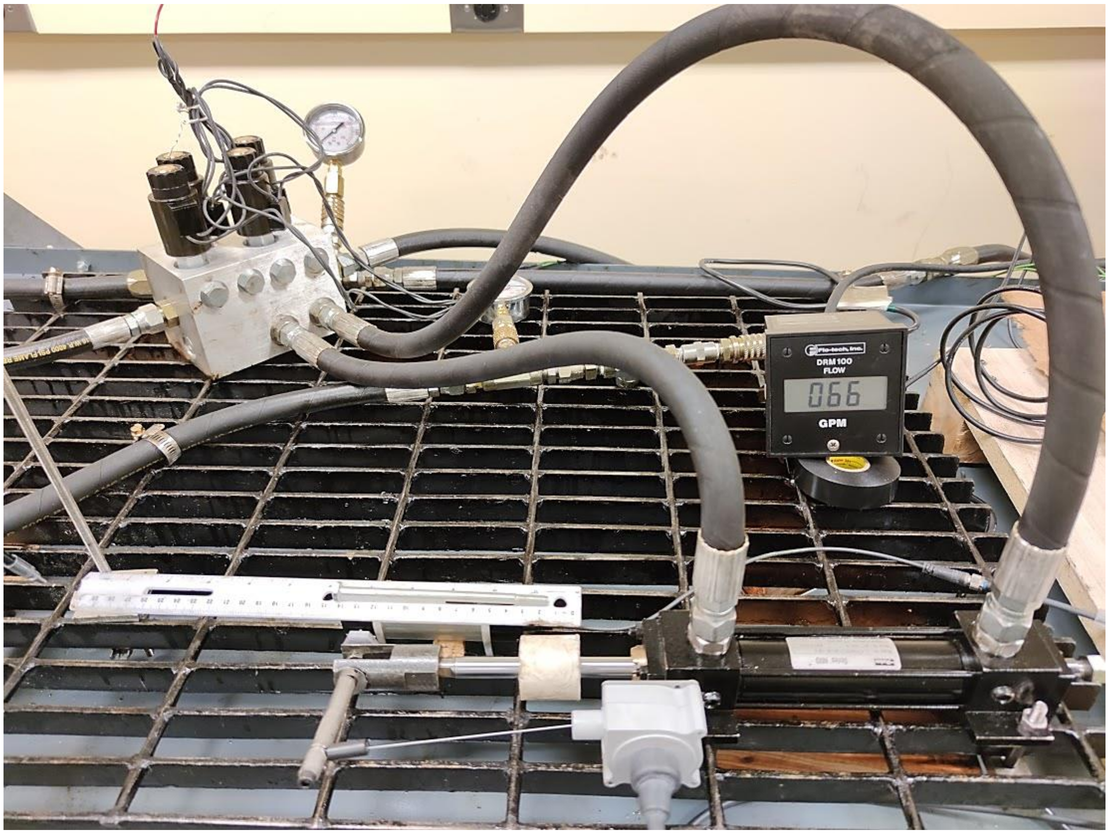

Figure 3.2. Cylinder and position transducers arrangement.

The extension and retraction of the hydraulic cylinder were controlled using a manifold with four 3-way valves. A position transducer (string potentiometer) was attached to the hydraulic cylinder to measure the rod's position. Similarly, an additional position transducer (magnetic) was placed at 3 mm on the rod's end to have a redundant measurement of one of the most relevant variables that is the piston rod's position. Such a method of actuation will be replicated in an additional pair of cylinders to conform a steering mechanism that will be integrated in the future in the drilling prototype. The details of the hydraulic test bench elements (Figure 3.3) are shown in Table 3.2.

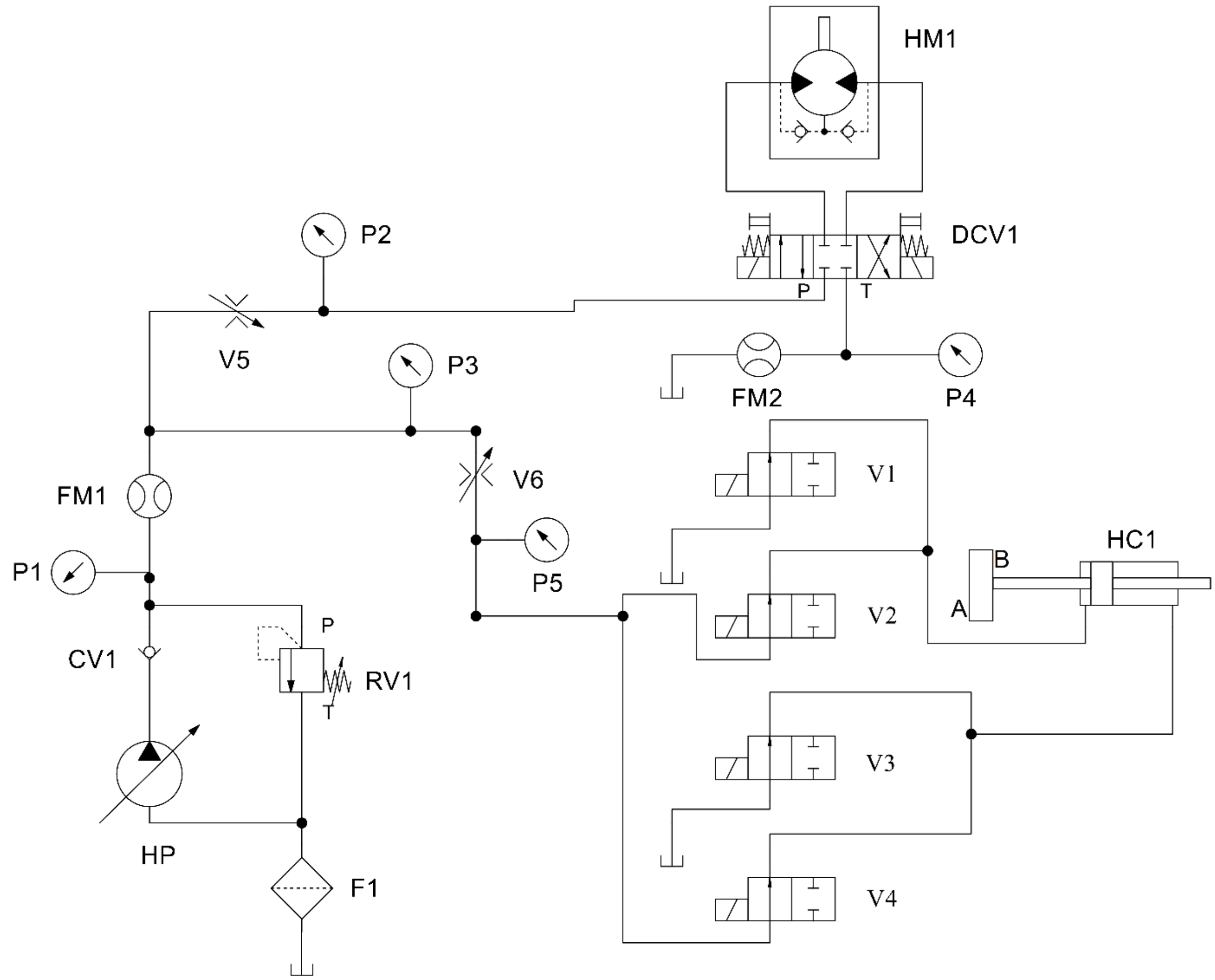

Figure 3.3. Test bench hydraulic circuit.

Table 3.2. Test bench elements.

ID	Description
HM1	Hydraulic Motor
DCV1	Directional Control Valve
HC1	Hydraulic Cylinder
RV1	Relief Valve
HP	Hydraulic Pump
CV1	Check Valve
F1	Filter
FM1, FM2	Flow Meter
A, B	Position Transducer
P1, P2, P3, P4, P5	Pressure Transducer
V1, V2, V3, V4	3-Way Valve
V5, V6	Variable Orifice

3.5. Model and Architecture

The sensing system was a critical element that needed to be designed for the test bench, and that includes characteristics that will make it easy to implement in the future on a micro-drilling device. This system will serve as the primary block that acquires the signals that can be later used for several purposes, like controlling the operation of the prototype's physical elements and providing information to the operator. Another example of a sensing system's importance in a drilling device is the robot's operating fluid pressure. This parameter must be maintained within specific ranges; otherwise, the fluid power systems can be damaged or create an accident. Therefore, by measuring the system's pressure and controlling it, the components' integrity and the robot's reliability can be ensured.

The sensing system's recorded data was sent to a microcontroller, where it was processed and then presented visually to the operator through a User Interface (UI) developed in a cloud-based dashboard. The data was filtered, processed, and sent to a controller that executed the desired commands and transmitted signals to the robot's various actuators.

The architecture of the system and its components are explained in detail in the following sections.

3.5.1. Sensors

The system's design integrates connections for several types of output signals from the selected sensors (i.e., PWM, digital 0-5V, analog 0-5V, analog 4-20 mA, and sine wave signals).

Table 3.3 shows the sensors that were implemented on the developed test bench. The table lists the sensors, along with the manufacturer and model of the sensor and the quantity required.

Table 3.3. Sensors required for the sensing system.

Sensor	Manufacturer	Model/Code	Qty	Accuracy	Range
Pressure Transducer	Omega	PX309-5KG5V	1	±0.25% Best Straight Line (BSL), max	0-5000 psi
Pressure Transducer	Honeywell	LM/2345-11	1	±0.5% of Full-Scale Range (FSR)	0-2000 psi
Flow Meter	Flo-Tech	FSC-375	2	±1% of FSR	0.53-4.29 gpm
Position Transducer	TE Connectivity	SP2-4	1	±0.25% of FSR	101.6-1270 mm
Position Transducer	SICK	MPA-107THTP0B01	1	±0.06% of FSR	0-107 mm

3.5.1.1. Pressure Transducer

A pressure transducer is an element that transforms the pressure into an analog electrical signal. This signal is proportional to the physical deformation of a diaphragm that induces a change to a strain gage inside the sensor.

A total of two digital pressure transducers were considered in the sensing system. The first sensor (Figure 3.4) was connected to the test bench's hydraulic system's low-pressure side. The second sensor (Figure 3.5) was mounted on the hydraulic line that is linked to one of the micro-hydraulic cylinders.

The pressure transducer PX309-5KG5V (Figure 3.4) has a stainless-steel construction. It can measure different pressures (i.e., gage, absolute, vacuum) and offers high stability and low drift in its measurements (Omega Engineering, n.d.). The pressure range goes from 0 to 5000 psi, and the output is a 0-5 V signal.

Figure 3.4. Pressure transducer PX309-5KG5V (Omega Engineering, n.d.).

The pressure transducer LM/2345-11 (Figure 3.5) has a rugged design that provides resistance to vibration and temperature variations (Honeywell, n.d.). The construction is also made with stainless steel, and the pressure range goes from 0 to 2,000 psi. The output for this sensor is an analog 4-20 mA signal.

Figure 3.5. Pressure transducer LM/2345-11 (Honeywell, n.d.).

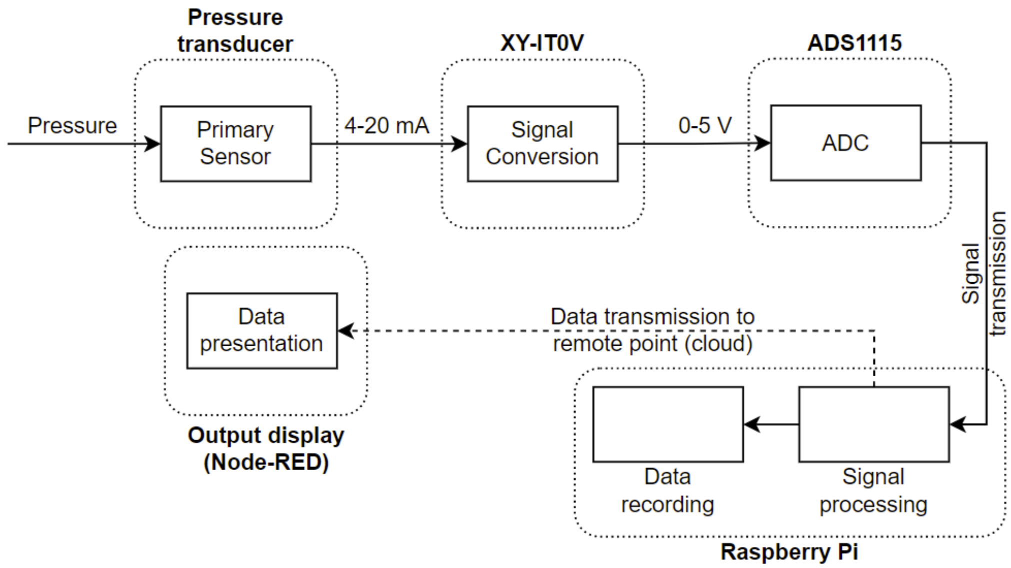

Figure 3.6. Pressure Sensor Architecture LM/2345-11.

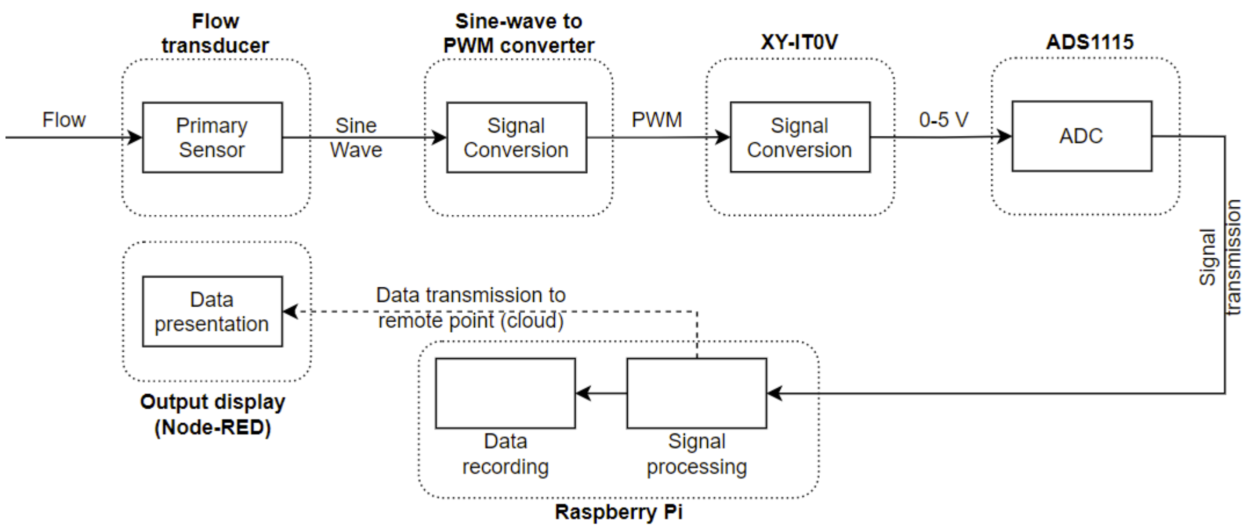

Figure 3.7. Pressure Sensor Architecture PX309-5KG5V.

3.5.1.2. Flow Meter

The FSC-375 (Figure 3.8) is a positive displacement flow meter that measures the flow rate on a given hydraulic line. This sensor was connected to the test bench to measure the output flow rate from the hydraulic motor. The FSC-375 sensing element is a turbine, and the output is a frequency signal (sine wave) that changes with respect to the flow rate that passes across the sensor. The sensor can handle pressures up to 6000 psi and temperatures up to 300 °F (Flo-Tech, 2019). The connections and processing required to read the sensor's output are shown in Figure 3.9.

Figure 3.8. Flow transducer FSC-375 (Flo-Tech, 2019).

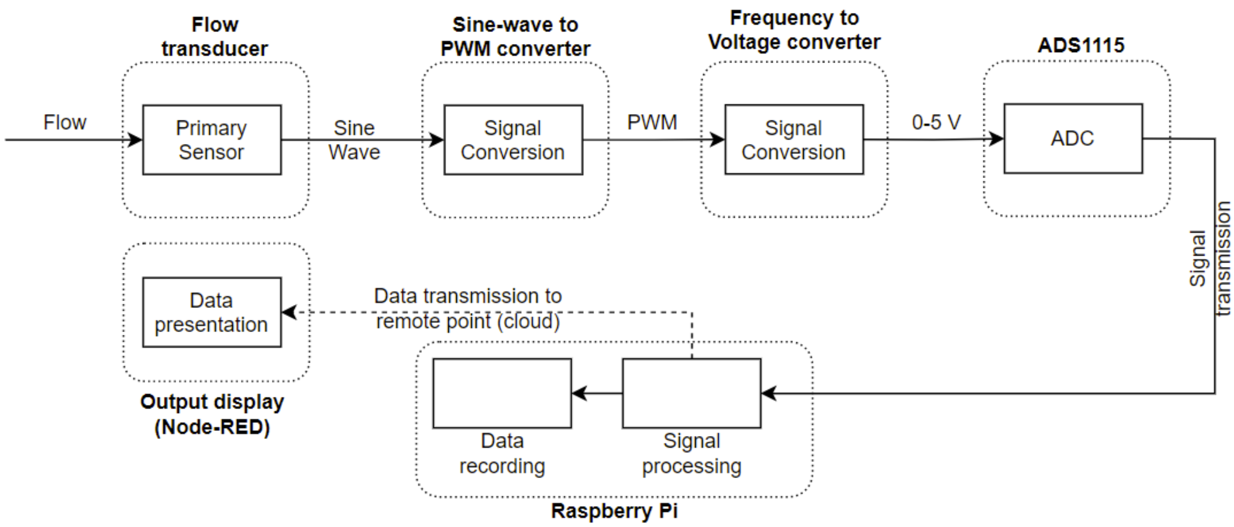

Figure 3.9. Flow Transducer Architecture FSC-375.

3.5.1.3.Position Transducer

There are different measuring methods to determine the position of the piston. The following are not only the most commonly used but also the ones that were found to be the most suitable for the expected application of the sensing system on the test bench.

The string-pot (draw-wire) sensor is a technology where a cable is attached to the object that will be measured (TE Connectivity, 2020). The cable is connected to an encoder that converts the cable's extension to a digital or analog signal proportional to the body's linear extension or velocity (Figure 3.10).

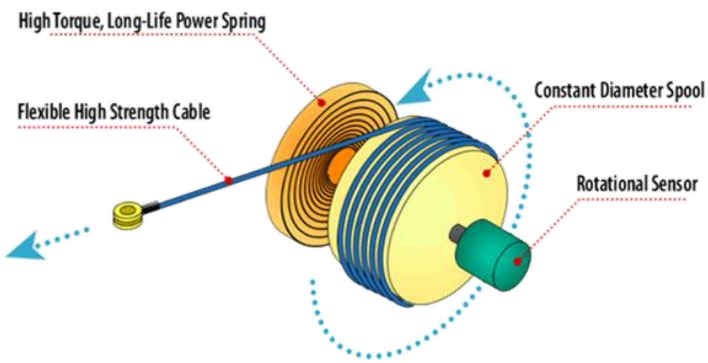

Figure 3.10. String pot sensor internal mechanism (TE Connectivity, 2020).

The magnetic field positioning sensor is a method where the sensor is directly mounted onto the cylinder (Figure 3.11), and an inner magnet determines the piston's position as it is extending or retracting. The internal magnet is attached to an element that varies its voltage or current in relation to the magnetic field. This is a sensor that detects a cylinder's piston position using a direct, non-contact method.

Figure 3.11. A magnetic sensor positioned in a pneumatic cylinder (SICK Sensor Intelligence, n.d.).

The laser sensor is a type of sensor that uses light triangulation to determine the speed and the distance at which the measured object moves from a reference point. This sensor can be threaded for mounting and can be found in very small sizes (Figure 3.12), but a drawback compared to the image-based laser sensor is that this can only measure a single point.

Figure 3.12. VSM-2 miniature self-contained sensor (Banner, n.d.).

The image-based laser sensor uses a combination of laser technology and image recognition to perform accurate measurements on areas or points on a surface (Figure 3.13). This sensor can also measure height, steps, maximum and minimum points, and width over an area. Also, it can check differences in height over an area which might be helpful to measure the tilt or inclination or a platform such as the one that is being implemented for the steering mechanism (Keyence, n.d.). This type of sensor might help characterize and calibrate the other sensors in the test bench. Still, its use on the final prototype is not feasible due to the environmental characteristics that the robot will face.

A summary of the advantages and disadvantages of the presented sensors can be seen in Table 3.4.

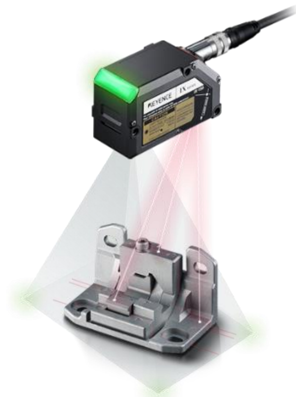

Figure 3.13. Model IX image-based laser sensor (Keyence, n.d.).

Table 3.4. Position sensor technologies summary.

Type	Advantages	Disadvantages
String Pot (Draw-wire) Sensor	• Low-maintenance and fast and easy installation • The measuring cable can be diverted over deflection pulleys • Reliable measurement in dirty environments	• Measurement can be affected by changes in cable (e.g., gravity, wind, fluid) over long distances • Measurement is sensible to temperature changes over long distances
Magnetic Field Positioning Sensor	• Easy adjustment of the sensor • Non-Contact measurement principle • Reliable and accurate measurements even in harsh environments	• Installation requires external mounting (more space)
Laser Sensor	• Non-Contact measurement principle • High output rate. • Measurements can be either moving or stationary • High accuracy and signal stability	• It is sensible to surface textures • Durability and longevity affected by the environment
Image-based Laser Sensor	• Image recognition allows for tracking targets throughout the scan area (no specific positioning) • Multiple measurements with one device (less mounting space, fewer connections) • Laser-based inspection is resistant to changes in lighting conditions and target contrast	• It requires a fixed mounting • Durability and longevity affected by the environment • It requires the software provided by the manufacturer to calibrate and operate

Based on the magnetic and string potentiometer sensor's operational characteristics, it was determined that these technologies were the best approach for the position measurement of the piston rod.

One of the selected sensors was the model MPA-107THTP0B01 by SICK (Figure 3.14). This sensor includes smart capabilities for the detection of moving parts within a specific range of its total length. Also, it uses an intelligent algorithm to adjust dynamically during operation, delivering an output signal that is highly linear and reproducible (SICK Sensor Intelligence, n.d.). The MPA-107THTP0B01 can deliver different signal outputs at once; a 4-20 mA, 0-10 V, and a digital IO-Link interface. This sensor can be submerged due to its high enclosure rate (IP67/IP68). The method does not require contact between the sensing element and the piston, which might be advantageous for future installation in the micro-drilling device.

Figure 3.14. MPA magnetic sensor (SICK Sensor Intelligence, n.d.).

As shown in Figure 3.15, the output of the sensor required an additional signal conversion step. The output that was used from this position transducer was the 0-10 V signal. Since the ADC can only read voltages between 0-5 V, a voltage divider circuit was integrated. The details of this circuit are shown in section 3.5.3.

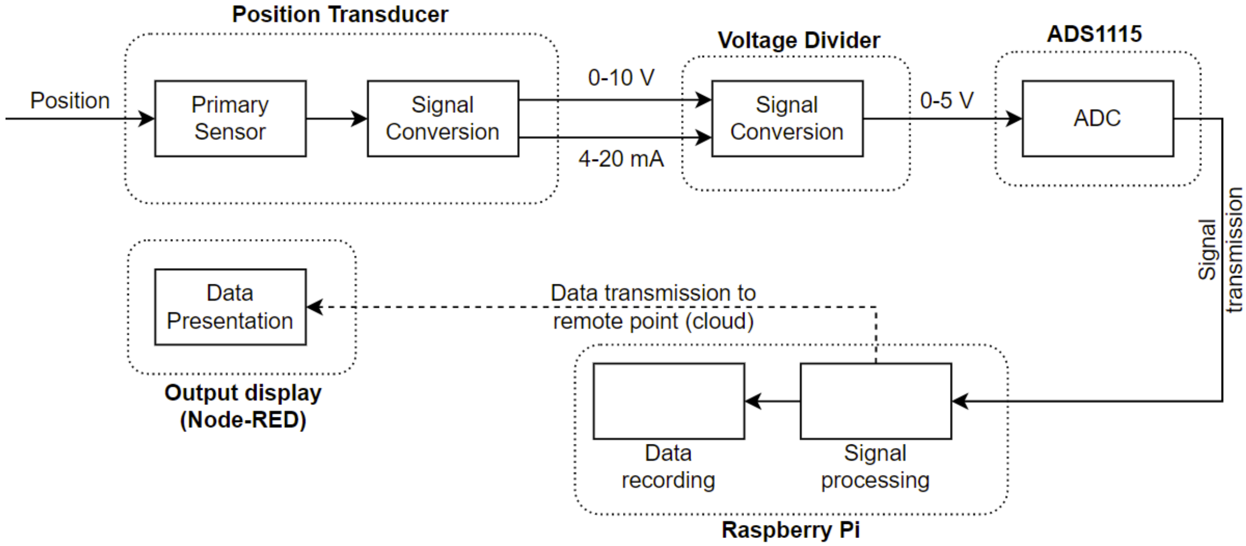

Figure 3.15. Position transducer architecture for MPA-107THTP0B01.

As the position of the rod is one of the critical measurements required for the micro-drilling device, a second position transducer was integrated to have redundant estimations. The other selected position transducer was a string potentiometer model SP2-4 (Figure 3.16).

Figure 3.16. Position transducer model SP2 (TE connectivity, n.d.).

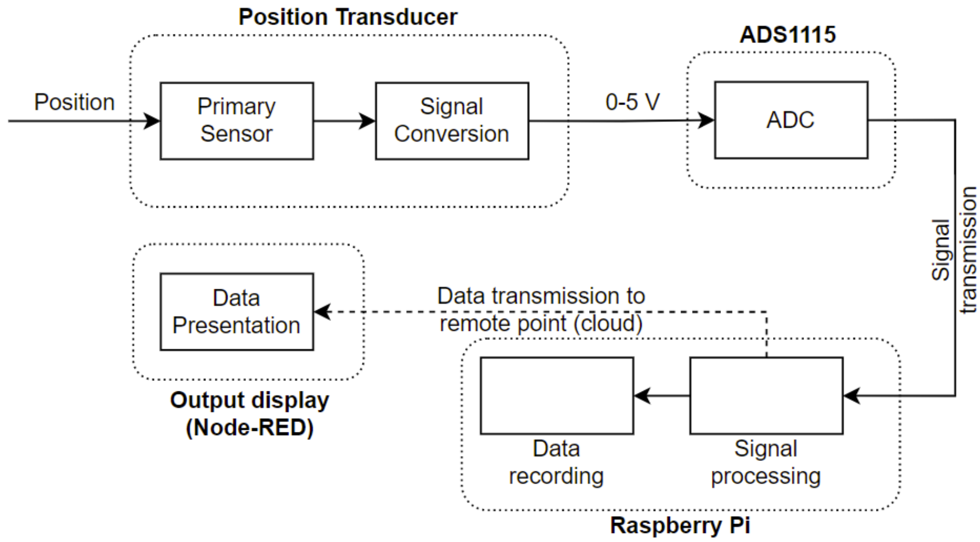

Figure 3.17. Position transducer architecture for SP2-4.

The position transducer model SP2-4 is a linear sensor that integrates a rugged polycarbonate enclosure (IP-50) with a compact design that provides high accuracy (see Table 3.3) and high repeatability (±0.05% of full stroke). Being an incremental sensor, it has an essentially infinite resolution (TE connectivity, n.d.), allowing continuous linear readings within the full stroke range. The output of this sensor does not require any additional signal conversion since it is proportional to the excitation level of the sensor. The SP2-4 excitation voltage can be a value between 3.3 and 10 V. For this project, the excitation voltage was set to 5 V, which is the voltage level that the ADC supports.

3.5.2. Sensor Communication Protocols

The Inter-Integrated Circuit (I^2C) serial communication protocol was used to connect the ADC modules and thus, the sensors, stressing the advantages it offers for the project, such as the use of only two wires to transmit information across the connected devices and a wide range of high-speed data transmission rates. The wires required to use this protocol are the clock signal (SCL) and the data signal (SDA) wires.

The I^2C communication protocol provides a synchronous connection, thus the use of an SCL wire. The I^2C protocol was designed to handle up to 127 devices and transmit information simultaneously; however, it can be easily upgraded using multiplexers. If no multiplexers are used, each device on the network must have a unique address (i.e., 0-0x7F hex).

For this protocol, messages or "packages" are broken up into four components:

a) Start condition: To initiate the address frame. This puts all secondary devices on notice that a transmission is about to start.
b) Address frame: Where the controller indicates the secondary devices to which the message is being sent.
c) Data frames: The data that will be transmitted.
d) Stop condition: Once all the data frames have been sent, the controller will generate a stop condition to notify that the information package was sent.

Even though this protocol allows for more than one master on the network, only one was required, being the Raspberry Pi the master node. Three data rates are commonly available for devices that operate with this protocol: fast mode (up to 1 MHz), high-speed mode (up to 3.4 MHz), and ultra-fast mode (up to 5 MHz). Given the data sample rate required for the project, the fast mode was used.

3.5.3. Signal Processing

The sensing system developed for this project was designed considering its future implementation on a robotic micro-drilling device. Therefore, the system was constructed contemplating the use of different industrial sensors and smart modules that operate at different voltages and that provide distinct output signals.

The signal processing part of a sensing system is critical for its correct functioning, operation, and reliability. Signal processing focuses on the reception, analysis, modification, and synthesis of the signals provided by the sensors. As seen in section 3.5.1, the sensors selected and described provide output signals of various types (e.g., analog 0-5 V, digital 0-5 V, 4-20 mA). These signals were processed and transformed into a signal that the ADC's and the central computer can read.

The Raspberry Pi 4 Model B (Figure 3.18) was selected as the main controller of the sensing system. Due to its processor quad-core ARM Cortex-A72 and its 4 GB of RAM, it is a powerful single-board computer that offers high processing capabilities (Raspberry Pi, n.d.). The Raspberry Pi also integrates 2.4 GHz and 5.0 GHz wireless communication, along with compatibility with Bluetooth 5.0 and BLE (Bluetooth Low Energy).

The Raspberry Pi can be used as a desktop computer running the Linux OS and also as a development board using its 40-pin two-track connector. This connector and its several GPIOs and serial communication ports were used to create the interface between the sensors and the Raspberry Pi. However, it is critical to highlight that the Raspberry Pi can only read signals of 3.3 V. An input voltage higher than 3.3 V can permanently damage the GPIO block. Thus, it was essential to process all the signals that are connected to these ports so the Raspberry Pi is protected and can function properly.

The Raspberry Pi has proven to be a reliable, low-cost, powerful microcontroller that can work in harsh environments for critical operations. John et al. (2017) used it to control and automate an 11 kV substation. Pasqual et al. (2017) created a data logger for motor activity detection in Artic environments based on a Raspberry Pi, where it was tested in real experimental conditions.

Figure 3.18. Raspberry Pi 4 Model B (Upton, 2019).

3.5.3.1. Data Acquisition

The Raspberry Pi does not have the capability to receive and process analog inputs. Therefore, it is crucial to use an Analog to Digital Converter (ADC) if it is required to read an analog signal. As shown in section 3.5.1, the sensing system included sensors whose output is not a digital signal.

The ADS1115 (Figure 3.19) is a module that includes a 16-bit ADC. The ADS1115 includes a programmable gain amplifier to aid in reading small single or differential signals. The ADC operates with digital voltages from 2 V to 5 V, both in power and logic. One advantage of this ADC over others in the market is that it offers an I^2C interface.

As commented in section 3.5.2, having this serial communication protocol allowed to have more than one device connected to a bus with only two wires. In the specific case of the ADS1115, the ADC offers four single-ended input channels that can also be used as two differential channels (Earl, n.d.). Also, the sample rate can be programmable between 8 to 860 samples per second.

The frequency of the ADCs was set to 2400 Hz to provide a sample rate of 20 running averaged readings per second. The averaged samples helped to reduce noise, smooth out the values, and decrease the number of outliers.

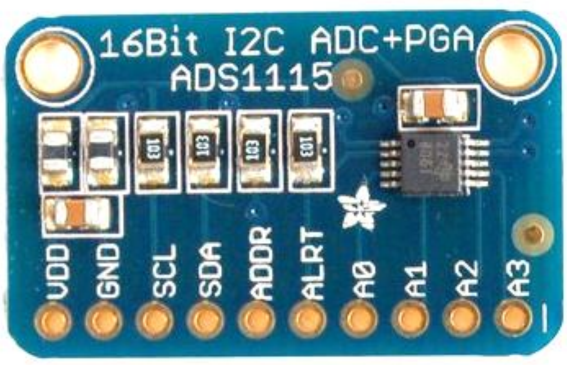

Figure 3.19. Analog to Digital Converter ADS1115 (Earl, n.d.).

The Raspberry Pi cannot directly receive current signals. For the case of the 4-20 mA signals, a converter module (Figure 3.20) was utilized to convert the current into a proportional analog voltage signal of 0-5 V.

Figure 3.20. XY-IT0V 4-20 mA to 0-5 V converter module (Amazon, n.d.).

The industrial-grade XY-IT0V module provides a high stability and good linearity measure. The current input supports 0-20 mA and 4-20 mA, and the output voltage supports 0-3.3 V, 0-5 V, and 0-10 V. In this project, for the pressure transducer in Figure 3.5, the required conversion was from 4-20 mA to a 0-5 V output that the ADC (Figure 3.19) will read.

For the magnetic position transducer (Figure 3.4), a circuit divider was required to step down the voltage from 0-10 to 0-5 V. The voltage divider consisted of an array of two resistors R_1 and R_2 connected in series form. The input voltage is passed through these resistors, where they act as potential dividers. Given the maximum output of the position transducer (10 V) across this circuit, the desired output voltage of 5 V can be obtained by using $R_1 = R_2 = 1\ k\Omega$:

$$V_{out} = \frac{R_1}{R_1 + R_2} * V_{out} = \frac{1\ k\Omega}{1\ k\Omega + 1\ k\Omega} * 10\ V = 5\ V$$

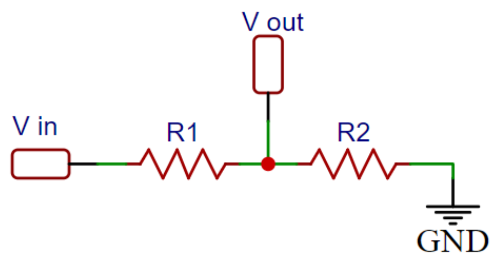

Figure 3.21. Voltage divider circuit.

The flow sensor (Figure 3.8) provided a waveform output. Thus, a processing section was implemented before sending the signal to the microcontroller or data acquisition module. The analog output was translated into a digital signal that the GPIOs can support in the microcontroller. For this, a sine wave to PWM converter circuit (Figure 3.22) was used to transform the sensor's wave output into a signal proportional to the input, and that can be read by either the Raspberry Pi or an external module.

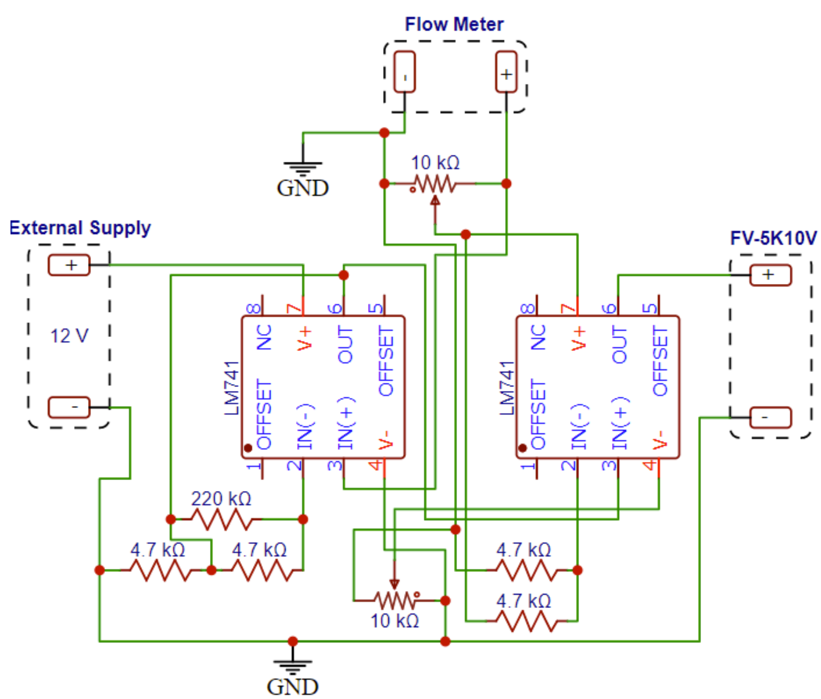

Figure 3.22. Sine wave to PWM converter circuit.

The converter's output was sent to the PWM to voltage module (Figure 3.23), where the frequency of the PWM signal was transformed into an analog signal from 0-5 V or 0-10 V that was then sent to the ADC.

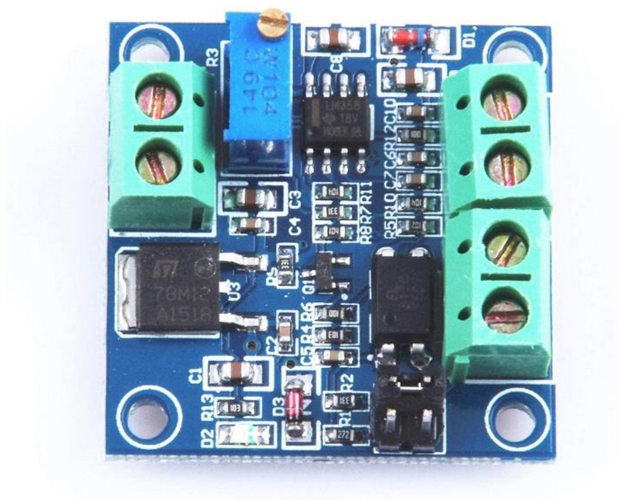

Figure 3.23. FV-5K10 PWM to voltage module (Amazon, n.d.).

3.5.3.2.Telemetry

Based on the table presented by Mwachaka et al. (2018), an evaluation of different telemetry technologies' features was performed. The original table shows the most used telemetry technologies in the oil and gas industry and provides an analysis of their critical features. These features were then ordered based on the expected relevance for the micro drilling robot into which the smart sensing system will be implemented (Table 3.5). A feature in the first position implies that it is crucial for the project, representing the biggest challenge. On the other hand, the feature in the sixth position is less critical, and the effort can be focused on the different challenges.

Table 3.5. Ranking Parameters Table.

Features	Telemetry Technology				Relevance for prototype
	Electromagnetic (Radiofrequency)	Acoustics	Mud Pulses	Wired drill pipe	
Signal interference	High	Medium	Medium	Low	1
Signal attenuation	High	High	Medium	N/A	2
Data quantity	Medium	Low	Medium	Very high	3
Max. transmission data rate (bps)	10	20	20	57,600	4
Installation and other cost	Medium	Medium	Low	High	5
Maximum depth (meters)	5500	3700	12,200	Unlimited	6

For the project's purposes, the telemetry system choose was wired since the sensing system was implemented on a test bench located in a controlled environment. Thus, it was possible to have the advantages of wired telemetry (e.g., low signal interference, high data transmission rates) without the disadvantages that are commonly faced in a drilling operation (e.g., installation and other costs).

However, in section 5.1, it is described how telemetry will be a critical factor for the successful prototype implementation in the future. In this section, based on the current challenges and considering the constraints that a micro-drilling robotic device might face in a drilling operation, a telemetry technology was selected and proposed to be implemented as part of future work.

The telemetry technologies are explained in more detail along with their characteristics in subsection 2.7 of this document.

3.6. Cloud-based Dashboard

The test bench can be controlled virtually based on Point-to-Point (P2P) communication from an electronic device such as a computer or a smartphone to the Raspberry Pi that controls and monitors the sensing system. A virtual dashboard was developed, including controls, buttons, and some of the most critical measurements to aid the operator in the device's decision-making process. It is important to note that full cloud-based control was not considered because of the uncertainty of having a reliable bandwidth and internet availability in the field, situations representing a challenge and risk (e.g., losing the connection with a robot DTH would be dangerous). In addition, as mentioned in section 2.8, data integrity and security are a challenge faced by IIoT devices.

Based on the literature review conducted, it was identified that there are two main frameworks to develop virtual dashboards.

a) Sinatra is a web application framework for Ruby, which is an object-oriented programming language. Sinatra was specifically developed to work and be easily implemented for IoT applications. Most Sinatra-based platforms are free since several companies allow integration for developing and prototyping projects (Flatiron School, n.d.).
b) Express is a web application framework for Node.js that is a cross-platform, back-end environment. Even though Express was created inspired by Sinatra, Express is written in JavaScript, making it lightweight and improving its growth capability in complex projects (Yaapa, 2013).

Node-RED was selected to develop the dashboard. It is an Express-based programming tool to connect the smart sensing system's hardware and software. Node-RED uses the Express application framework, and it allows the integration of several online services and the real-time deployment of "flows" or instructions (Mardan, 2014). This framework was chosen because it allows for connecting different platforms, making it easier to communicate the JavaScript flows with the Linux codes from the Raspberry Pi. Node-RED also integrates several collaborative libraries, templates, and pre-arrange flows that can be modified and adapted for different functions.

CHAPTER 4. RESULTS

4.1. Dashboard

Figure 4.1 shows the dashboard created in Node-RED where the user can read operational information (e.g., processor, memory and disk usage, temperature) from the Raspberry Pi used as the host of the service and send commands for the reboot or shutdown of the computer.

The programming and development of the dashboard were made through function blocks. The flows created for the design of the cloud-based dashboard can be seen in APPENDIX A.

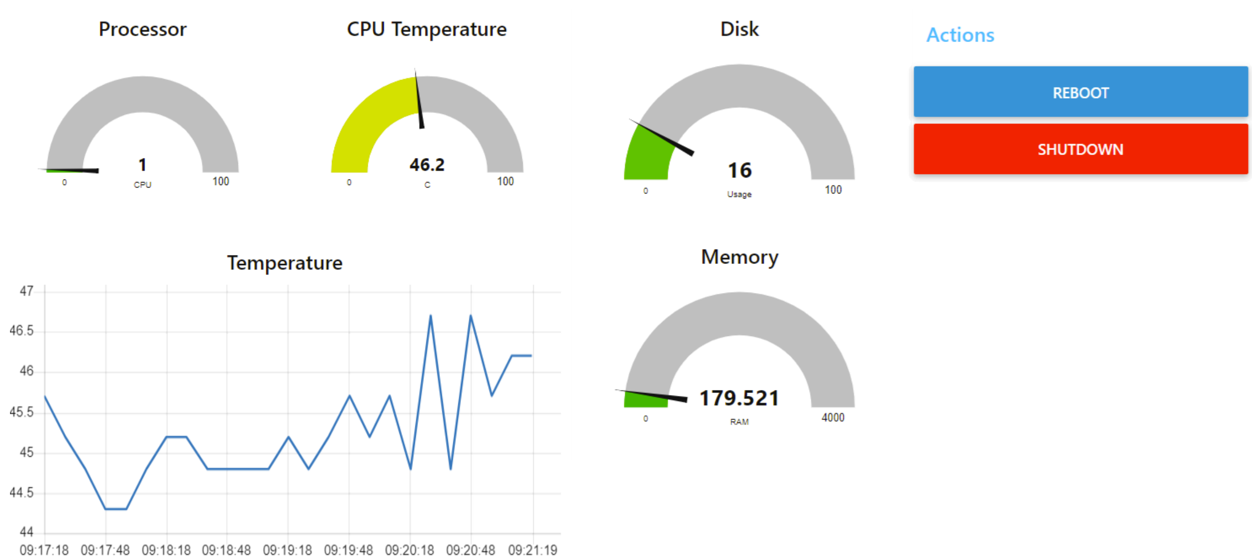

Figure 4.1. Raspberry Pi monitoring and control.

Viewing Figure 4.2, it can be seen that information from five signals was being read in real-time. The cylinder control could be performed in three ways. The first one was manually through the "RETRACTION," "EXTENSION," and "STOP" buttons.

The second method to control the cylinder was through the setting of a goal distance. The position transducer constantly provided the readings of the rod's position. Independently of the starting point of the cylinder, when the user inputs a desired distance, the comparison and control blocks (Appendix A. Figure A. 4) determined if the current position was different than the goal position. After processing the information, the control system determined if the output signal for the cylinder was for extension or retraction.

Two relays of an eight-channel relay shield module were used to control the manifold valves (Appendix B. Figure B. 1). The relay module integrates optocouplers to protect the microcontroller GPIOs from overcurrent and overvoltage from the 12 V circuit that feds the valves (Amazon, n.d.). One of the two relays was activated to extend and the other one to retract the rod in order to move the piston rod until it reached the goal position and then stopped.

The third method to control the piston's rod position was by providing the control system with a signal with the desired operation. Section 4.3, it is shown how the cylinder was operated following a waveform input signal.

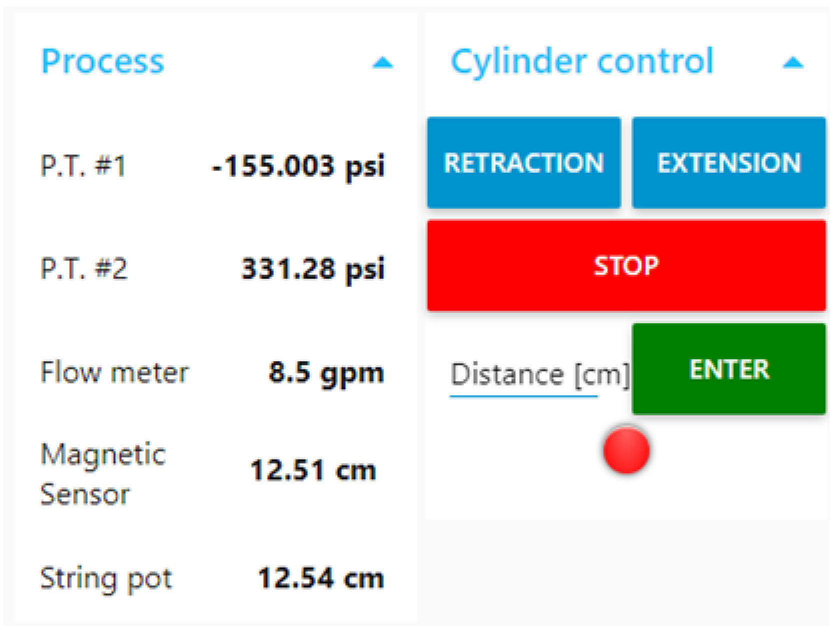

Figure 4.2. Test bench monitoring and control.

Finally, the virtual dashboard also had the capability to plot the variable almost in real-time. However, this process was performed on the cloud with Node-RED's servers, making the plotting process somewhat slow and not reliable enough for the control system. For this reason, and as shown in the architecture diagrams of section 3.5, the data logging was performed directly in the Raspberry Pi.

The data storing for post-processing and analysis from all the sensors was a task performed in parallel with the operation in Node-Red, and it was executed in real-time. An example of the plots generated in the dashboard is shown in Figure 4.3, where some of the voltage readings from the ADCs were plotted over time.

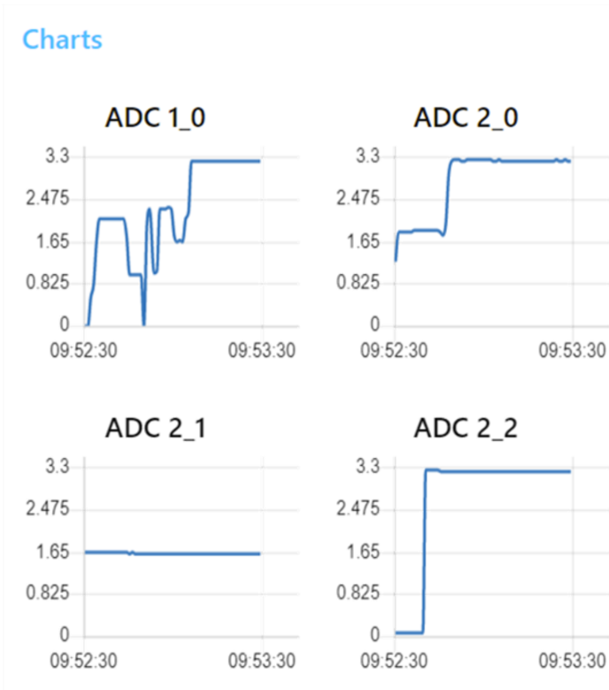

Figure 4.3. Example of plots generated for the ADC readings (time vs. voltage).

4.2.Printed Circuit Board (PCB)

The integration of all the electronic and electric components required the design of a reliable and robust circuit board that could incorporate all the elements needed for the signal processing, data acquisition, and control of the test bench.

A Printed Circuit Board (PCB) prototype (Figure 4.4) was developed following the appropriate design considerations for the correct operation of the electronics, the sensors, and the central computer. The PCB was designed based on Surface Mount Technology (SMT) components (Figure 4.5). This allowed the creation of a smaller and more compact version of the board compared to Through-Hole components. The electronics schematic is shown in Appendix B (Figure B. 1). The detailed description of the PCB elements is shown in Appendix D. As shown in Table D.1, the PCB design included the connections required for the sensors proposed in this project. Additionally, it has three open connections for other sensors in case that the sensing system requires the integration of more sensors.

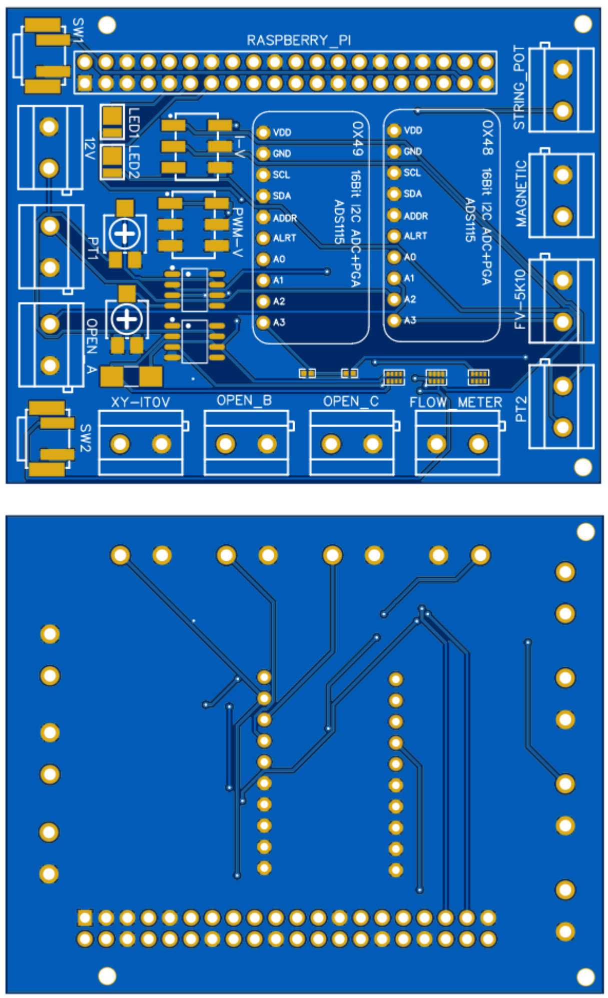

Figure 4.4. Top and bottom view of the PCB for the test bench (57x72 mm).

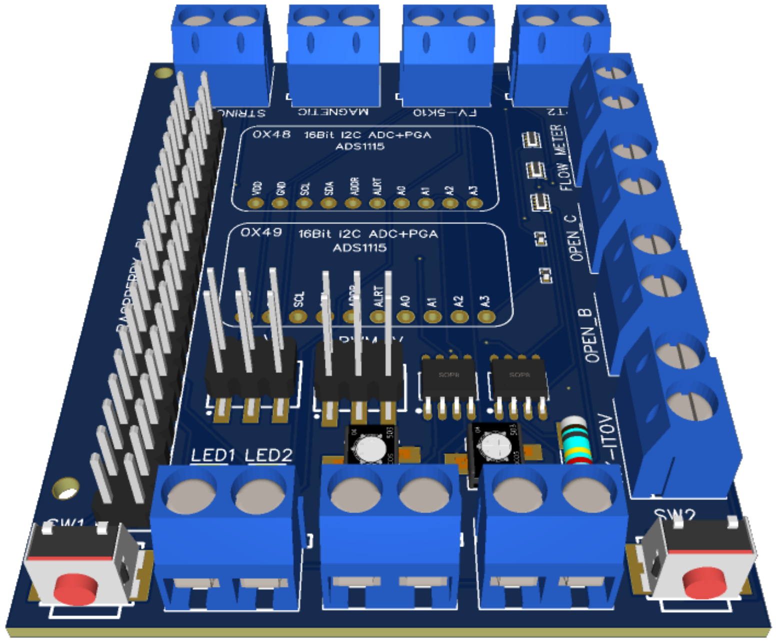

Figure 4.5. 3-D view of the PCB for the test bench (57x72 mm).

4.3.Experimental Tests

Based on the test bench described in section 3.4 and after the sensor's characterization, a set of three experiments was designed to test how accurate and reliable the sensing system is. For all three sets of experiments, a total of three runs were made for each one of them (Table 4.1).

The first test was the extension from the "zero" position of the cylinder (5.1 cm) to 95% of the full stroke (12.5 cm). The cylinder started from the zero position and automatically extended until it reached the desired extension of 12.5 cm. The goal was to get to the final position and immediately stop.

The second test was the extension from the "zero" position of the cylinder to 75% of the full stroke (10 cm). The methodology for this set of experiments was the same as for the previous set.

The third test was to follow a waveform to test the dynamic response from the system. In this case, the cylinder started from the "zero" position, then it was extended until it reached 100% of the full stroke, and then it retracted back to the initial position. This process was repeated for three full cycles.

Table 4.1. Set of experiments.

	Experiment		
	Stop at 12.5 cm	Stop at 10 cm	Waveform cycle
# of test	1	4	7
	2	5	8
	3	6	9

In all cases, the measurement of the operational variables was performed. The variables measured were:

- Experiment/group
- Number of reading
- Time
- String potentiometer voltage and conversion to centimeters
- Magnetic potentiometer voltage and conversion to centimeters
- Pressure transducer (1) voltage and conversion to psi
- Pressure transducer (2) voltage and conversion to psi
- Flow transducer in gpm

All the readings were obtained as a single string of data that was interpreted and processed in real-time by the cloud-based dashboard. At the same time, the data was logged by the central computer (Raspberry Pi).

4.4. Analysis of Results

The analysis of variance technique (ANOVA) is a tool for studying the effect of one or more factors (each with two or more levels) on the mean of a continuous variable. Therefore, it is the statistical test to use when comparing the means of two or more groups. This technique can also be generalized to study the possible effects of factors on the variance of a variable.

To investigate if the sensing and control systems are working effectively and reliably, it is required to determine if the piston rod is being extended and stopped at the desired distance (first and second experiments). For the third experiment, it is expected that the piston will follow the input cycle of extensions and retractions. This section covers the ANOVA results and their interpretation.

The null hypothesis from which the different types of ANOVA start is that the mean of the variable studied is the same in the different groups, in contrast to the alternative hypothesis that at least two means differ significantly. ANOVA allows comparing multiple means, but it does so by studying the variances.

The essential operation of an ANOVA consists of calculating the mean of each of the groups and then comparing the variance of these means (inter-variability) against the average variance within the groups (intra-variability). Under the null hypothesis that the observations of the different groups all come from the same population (they have the same mean and variance), the weighted variance between groups will be the same as the average variance within the groups. As the group means are further apart, the variance between means will increase and will no longer be equal to the average variance within the groups.

The statistical value studied in the ANOVA is the F-ratio. This is the ratio between the variance of the group means and the average of the variance within the groups. This statistic follows a distribution known as the F-Fisher.

If the null hypothesis is fulfilled, the F-statistic acquires the value of one since the inter-variance will be equal to the intra-variance. The more the group means differ, the greater the variance between means compared to the mean of the variance within the groups. This results in obtaining F-values greater than one and, therefore, less likely that the distribution will acquire such extreme values (less than the p-value).

Before performing the ANOVA tests, it is critical to validate the model assumptions:

- Normality
- Constant variance
- Independence
- Outliers

To ensure that the ANOVA test will be robust enough, it is first necessary to check the assumption of normality in the data from the experiments (Table 4.1). First, among the tests of the first experiment (stop at 99% of full stroke), then for the second experiment (stop at 75% of full stroke), and finally for the third experiment (cycle of extensions and retractions).

The normality plot can be used to check the normality assumption graphically. As can be seen in Figure 4.6, Figure 4.7, and Figure 4.8, the data among the experiments and for each test fell near the lines. Additionally, most of the points fell within the 25th and 75th percentiles, which indicate a normal distribution. Thus, the normality assumption was validated.

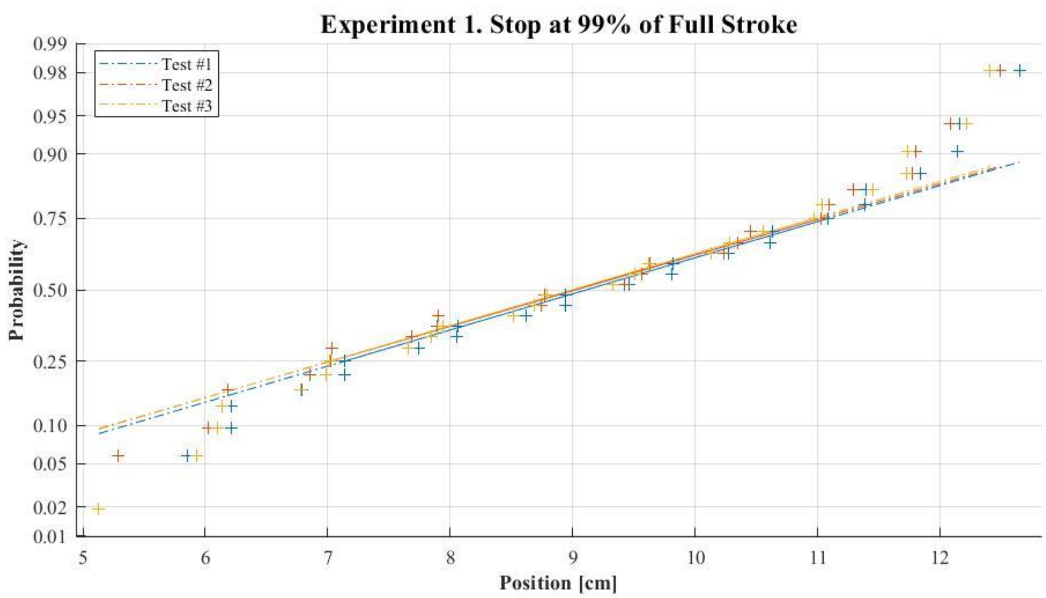

Figure 4.6. Normality plot for Experiment 1.

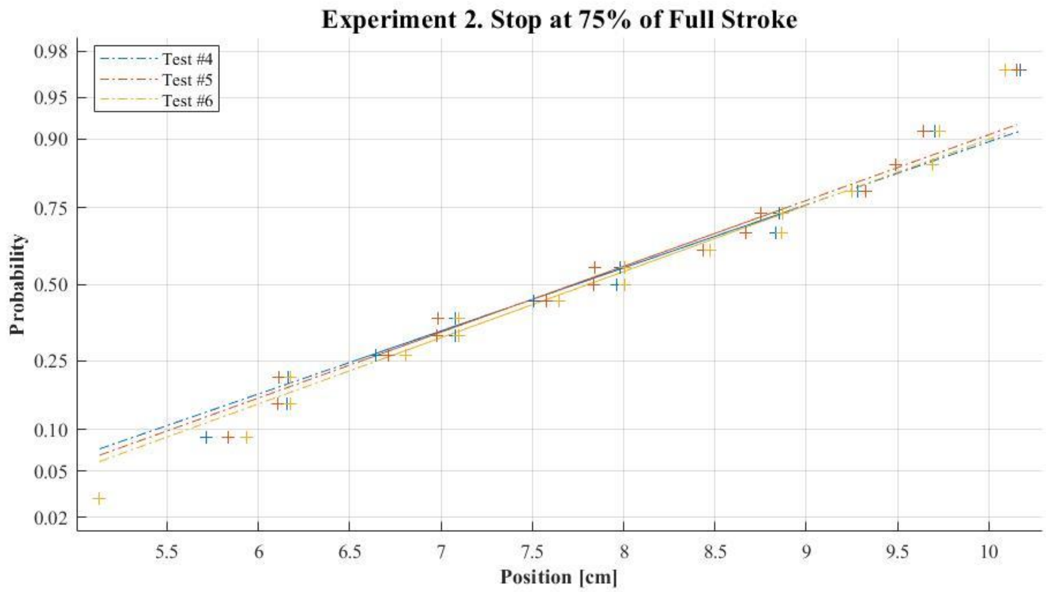

Figure 4.7. Normality plot for Experiment 2.

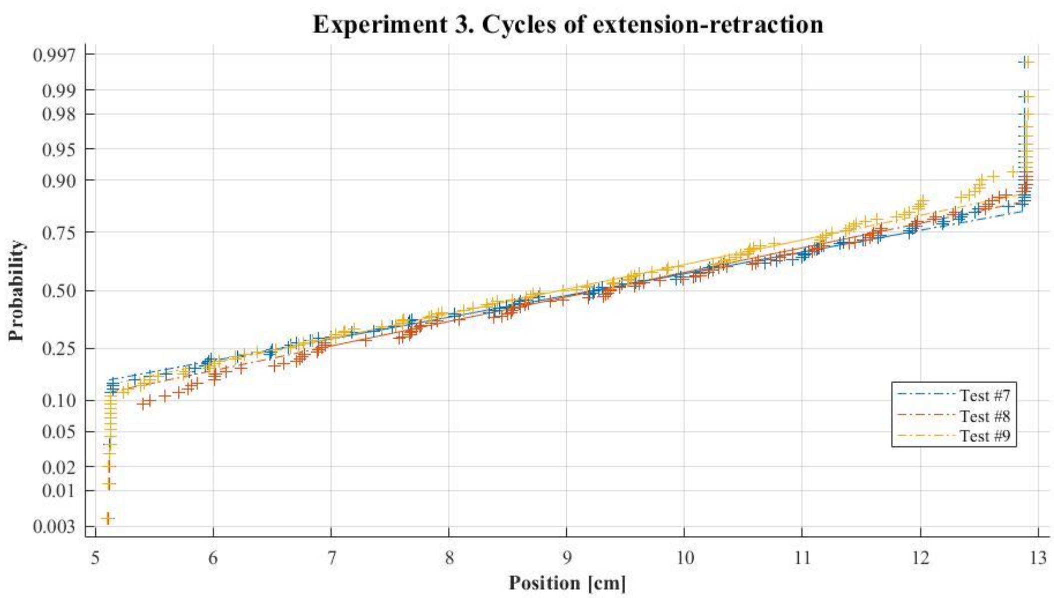

Figure 4.8. Normality plot for Experiment 3.

In addition to the graphical validation of the normality assumption, a formal Anderson-Darling test was performed for the first and second experiments. As shown in Table 4.2, at a significance level of 0.05, the result is that the test fails to reject the null hypothesis in all the cases (Test result = 0). Thus, it can be concluded that the data comes from a population with a normal distribution.

Table 4.2. Anderson-Darling test results.

		Output			
	# of test	Test result	P-value	Test statistic	Critical value
Experiment 1	1	0	0.5633	0.3077	0.7283
	2	0	0.3354	0.4046	0.7283
	3	0	0.5579	0.3026	0.7283
Experiment 2	4	0	0.8378	0.2124	0.7149
	5	0	0.8336	0.2139	0.7149
	6	0	0.7825	0.2313	0.7149

The assumption of variance and independence can be confirmed graphically by analyzing the residuals. By checking the histogram of residuals and the symmetry plots of residuals for each test (Figure 4.9, Figure 4.10, and Figure 4.11), we can observe that there are not patterns in the data. Additionally, it can be seen that the distribution of each test does not depend on the others. Hence, it can be concluded that the assumptions of variance and independence are valid.

Outlier data can completely invalidate the conclusions of an ANOVA. If extreme residuals are observed, it is necessary to study in detail which observations they belong to, being advisable to recalculate the ANOVA without them and compare the results obtained. The data shows no extreme outliers that could affect the hypothesis testing or that might bias the Type I or Type II errors.

Given that all the assumptions were validated, it can be concluded that the models are appropriate. Therefore, the ANOVA can be performed with certainty.

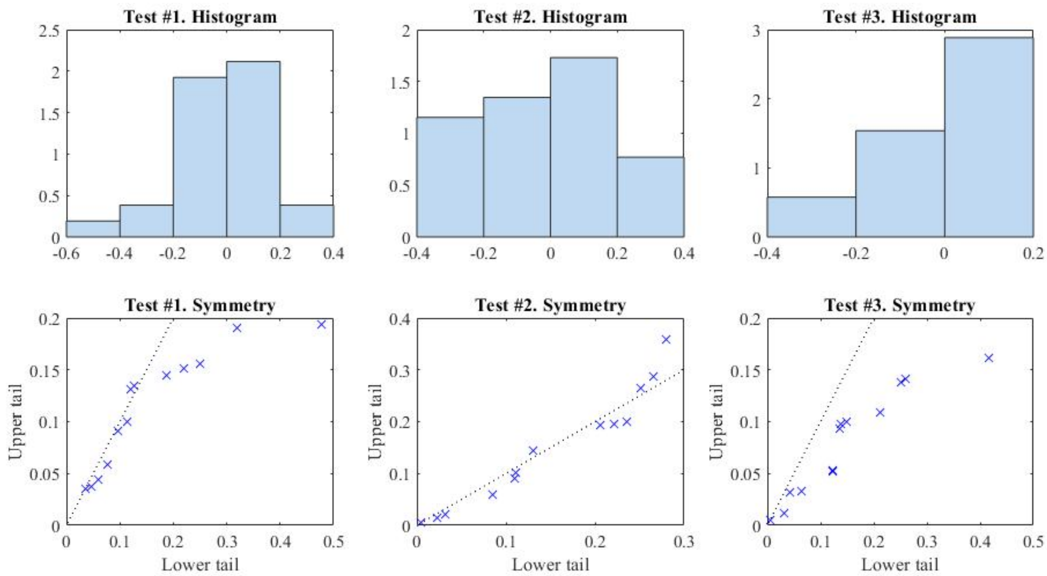

Figure 4.9. Residuals plots for Experiment 1.

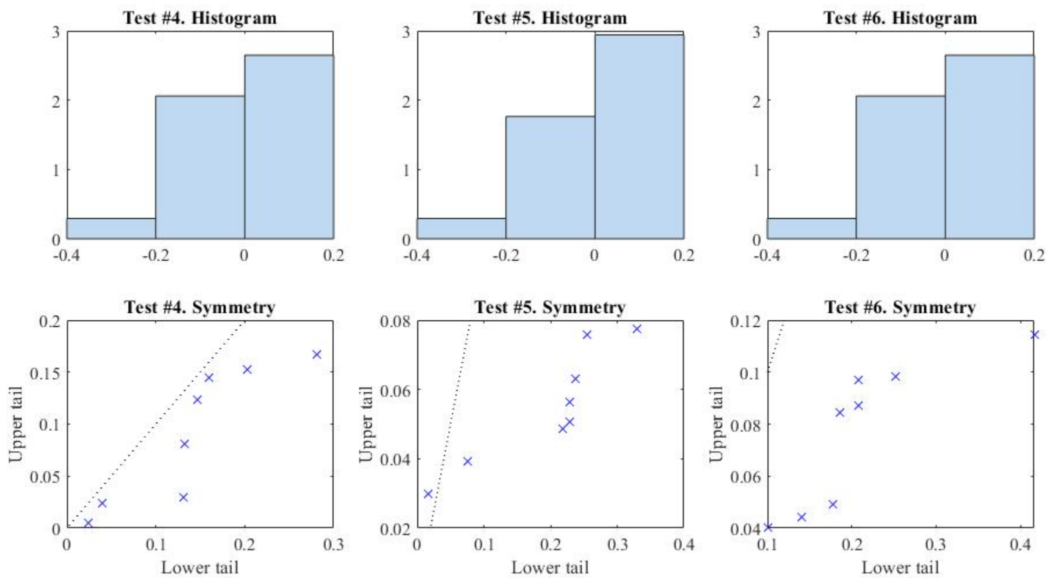

Figure 4.10. Residuals plots for Experiment 2.

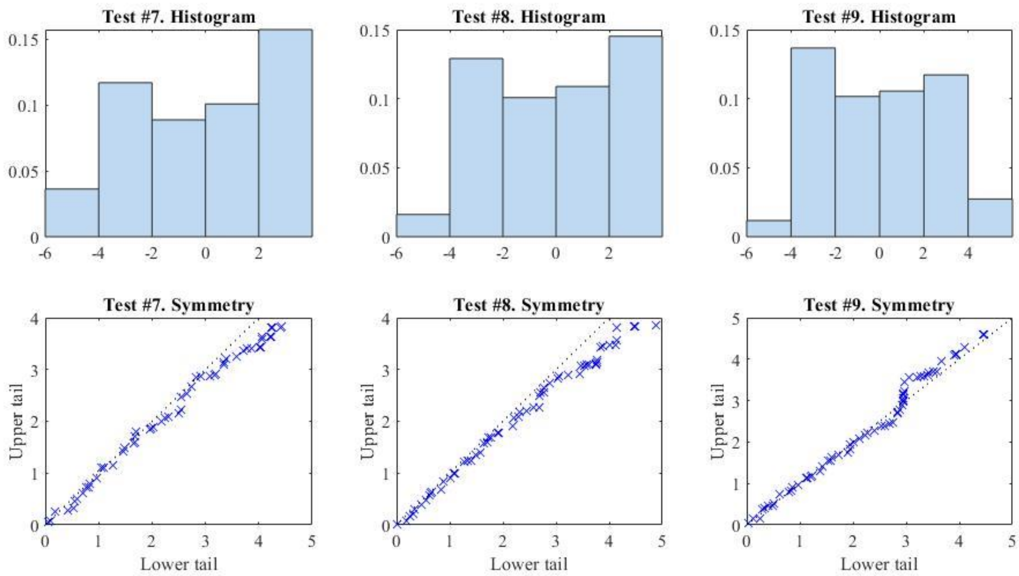

Figure 4.11. Residuals plots for Experiment 3.

4.4.1. ANOVA

4.4.1.1. Model

The statistical model for the ANOVA to be performed on the data gathered by the sensing system is:

$$y_{ij} = \mu + \tau_i + \epsilon_{ij}$$

Where:

$$i = 1,2, \dots, a$$

$$j = 1,2, \dots, n_i$$

$$\mu \rightarrow grand\ mean$$

$$\tau_i \rightarrow i_{th}\ treatment\ effect$$

$$\epsilon_{ij} \sim N(0, \sigma^2) \rightarrow error$$

The constraint is:

$$\sum_{i=1}^{a} n_i \tau_i = 0$$

The hypotheses are:

$$H_0: \tau_1 = \tau_2 = \cdots = \tau_a = 0 \; vs. H_1: \tau_i \neq 0$$

For at least one i.

The test statistic is:

$$F_0 = \frac{\frac{SS_{treatments}}{a-1}}{\frac{SS_E}{N-a}} = \frac{MS_{treatments}}{MS_E}$$

The decision rule is, if:

$$F_0 > F_{\alpha,a-1,N-a}$$

Then H_0 is rejected.

4.4.1.2. Results

Viewing Appendix C, the ANOVA tables are shown. Table C.1 shows the ANOVA results for experiment one. As it can be seen, the p-value is equal to 0.9323, which is significant. This indicates that the measured position within the tests of the first experiment is highly similar. Additionally, with an F-statistic = 0.0695 and at a significance level of 0.05, it can be concluded that the test fails to reject the null hypothesis. Therefore, it can be inferred that the mean values across the tests are equal to each other.

As a complementary test, a multiple comparison test was conducted to determine if the tests are different from each other within every experiment. Table C.2 shows that the p-value of all the comparisons (>0.9) indicates that the data across the tests were consistent. This supports the previous conclusions.

Table C.3 shows the ANOVA results for experiment two. As it can be seen, the p-value is equal to 0.9861, which is significant. This indicates that the measured position within the tests of the second experiment is highly similar. Additionally, with an F-statistic = 0.0140 and at a significance level of 0.05, it can be concluded that the test fails to reject the null hypothesis. Therefore, it can be inferred that the mean values across the tests are equal to each other. Table C.4 shows that the p-value of all the comparisons (>0.9) indicates that the data across the tests were consistent. This supports the previous conclusions.

Finally, Table C.5 shows the ANOVA results for experiment three. This indicates that the measured position within the tests of the third experiment is similar, and it can be inferred that the mean values across the tests are equal to each other. As it can be seen, the p-value is equal to 0.5784, which is not as significant as the one obtained for experiments one and two. However, by validating with an F-statistic = 0.5484 and at a significance level of 0.05, it can be concluded that the test fails to reject the null hypothesis. Table C.6 shows that the p-value of the three tests indicates that the data across the tests were consistent. By calculating Tukey's critical distance, it can be corroborated that no tests groups have means significantly different. This supports the previous conclusions.

The box plots show the distribution of the data in each experiment around their respective medians. These plots provide a visual aid to perform graphical hypothesis testing by making a comparison of the medians for each test in the experiments. As can be seen in Figure 4.12, Figure 4.13, and Figure 4.14, the plots indicate a failure to reject the null hypothesis. The medians within each experiment appear to be similar. Thus, it can be inferred that the tests were reliable (with a 95% of confidence) across each experiment. This conclusion is consistent with the results from the ANOVA.

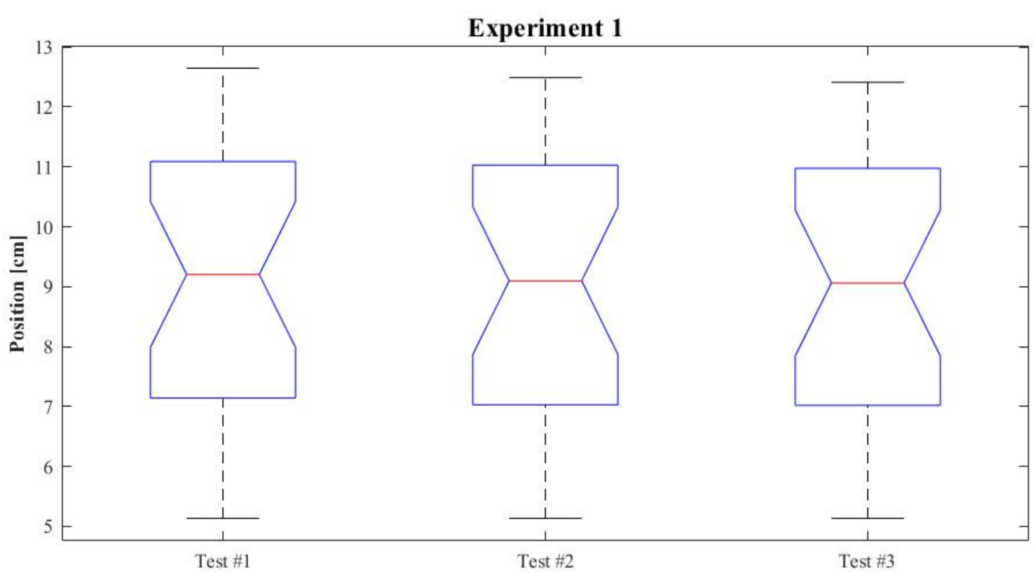

Figure 4.12. Box plots for Experiment 1.

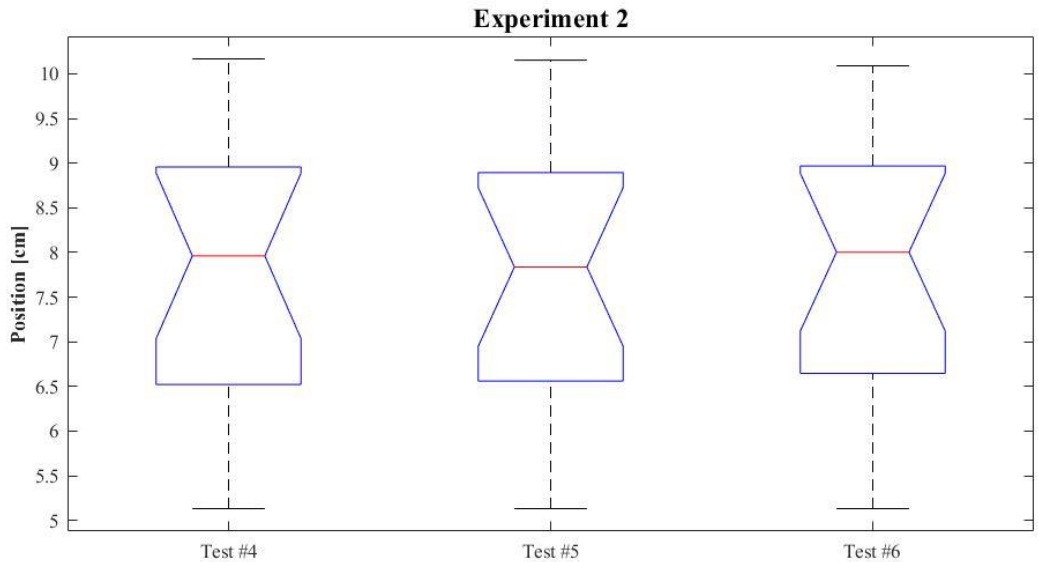

Figure 4.13. Box plots for Experiment 2.

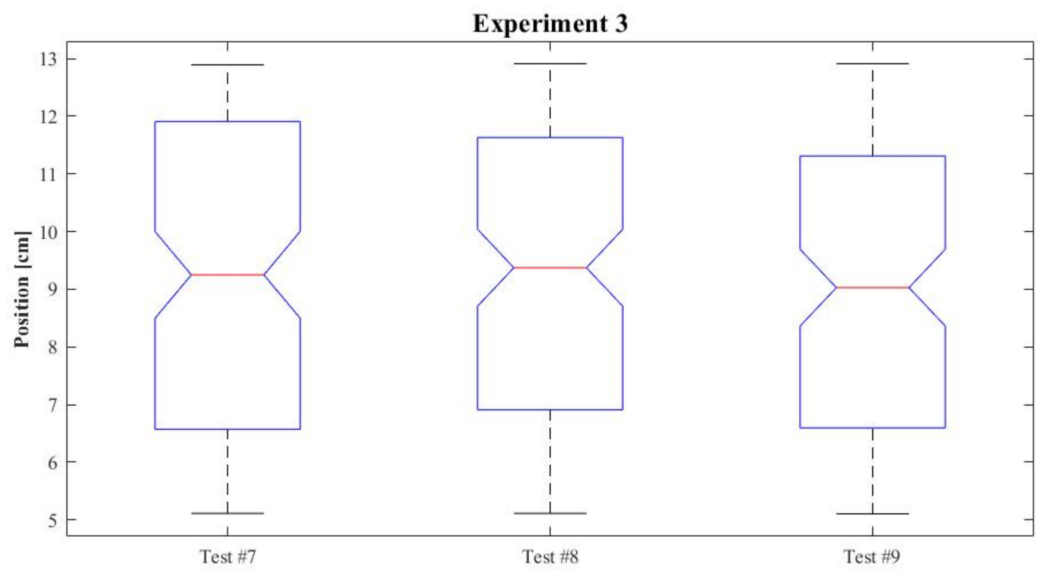

Figure 4.14. Box plots for Experiment 3.

4.4.1.3. Conclusions

Based on the results obtained in section 4.4.1.2, it can be concluded that the sensing system provided reliable measurements with a confidence level of 0.05. The ANOVA results showed that the data taken with the sensing system were consistent across the experiments for all the tests.

In the case of the first experiment (from zero to 95% of full stroke), the system accurately measured the position of the piston rod, and it precisely fed the control system. The piston rod was extended at the same speed across tests, which indicates that the hydraulic system was stable. However, as shown in Figure 4.15, the extension of the piston rod is not entirely linear. This is a consequence of the sizing of the hydraulic components like the pump and the valves, which are rated to supply higher flows than those required by the hydraulic cylinder. Thus, the pump's output was manually regulated to a flow rate that can keep up the system's pressure and allow the piston rod to be moved.

The pattern described above can also be seen in the extension plots for experiments two and three. The box plots shown above confirmed that the stopping times and the measurements along the piston stroke were steady in the tests for the first experiment.

For the second experiment (from zero to 75% of full stroke), the results were consistent with experiment one. The ANOVA results showed that the sensing system accurately acquired the position signals from the test bench. The control system achieved the goal position with a constant extension speed, and the estimation tells that it will follow this trend over 98% of the time.

As shown in Figure 4.16, the extension of the piston rod was similar for the three tests. The extension pattern was consistent, and the desired distance was achieved.

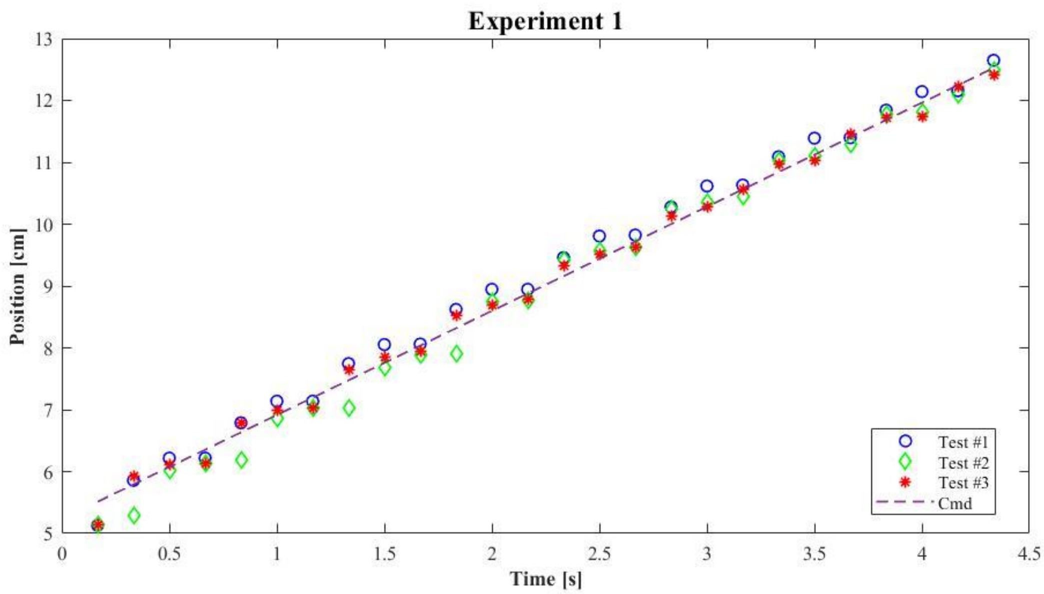

Figure 4.15. Piston rod extension for Experiment 1.

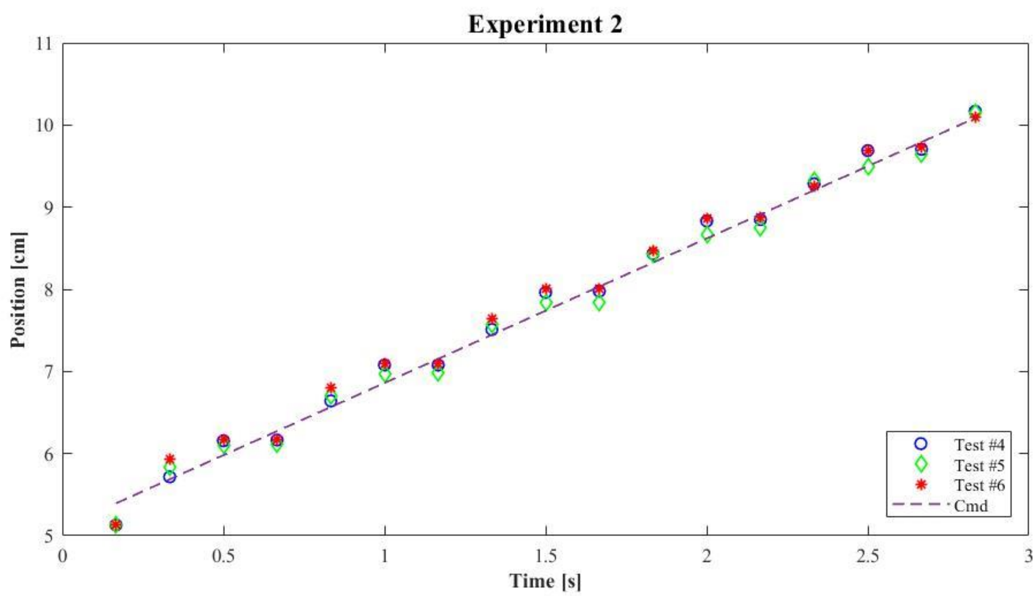

Figure 4.16. Piston rod extension for Experiment 2.

The third experiment, which consisted of following a cycle of extensions and retractions (waveform), had results that were not as solid in the ANOVA even though they were consistent with experiments one and two. This can be attributed to the subtle differences in the starting and finishing times for each cycle, as shown in Figure 4.17.

Nevertheless, the ANOVA supported the conclusion that the measurements across the tests correspond to a similar pattern. This conclusion was supported by the multiple comparison test and the box plots.

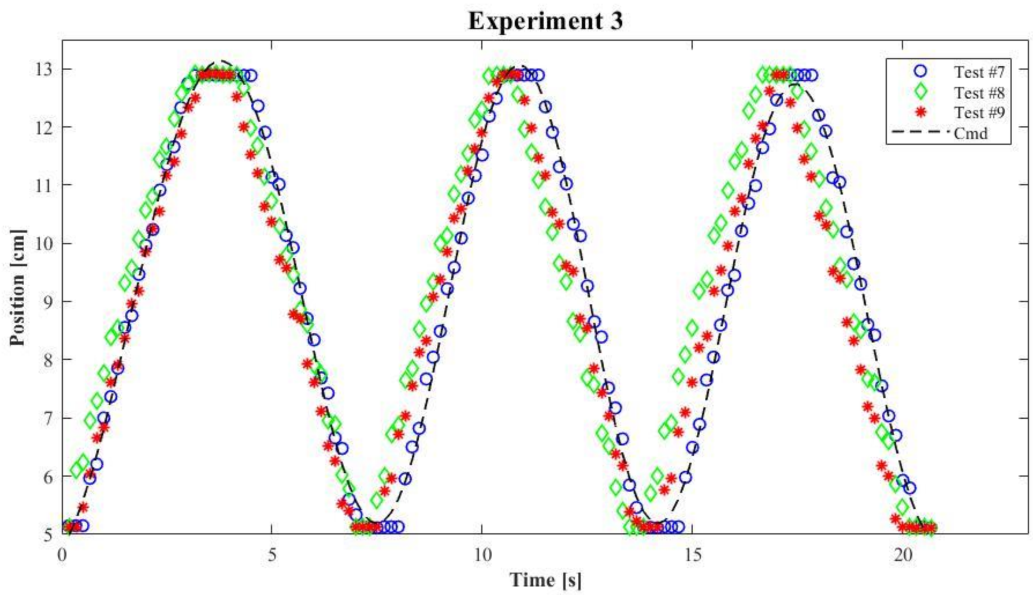

Figure 4.17. Piston rod extension and retraction cycles for Experiment 3.

CHAPTER 5. SUMMARY, CONCLUSIONS, AND RECOMMENDATIONS

5.1. Future Work and Conclusions

5.1.1. Conclusions

The first part of this study consisted of a thorough literature review that was performed to identify the problems that the oil and gas industry faces regarding oil extraction optimization. It was found that there is a lack of efficient machinery that allows the companies to cost-effectively extract all the oil from the reserves, even using Horizontal Directional Drilling (HDD) techniques. The development of efficient tools that allow increasing the payout of a well requires drilling robots that can create small diameter branches in the wells, and that can steer faster and more reliable than current HDD devices. One of the critical steps to create such devices is developing trustworthy and robust sensing systems that can provide accurate operational measurements to the operator.

The purpose of this study was to develop a prototype of a smart sensing system that could be implemented in the future in a micro-drilling device. For this, flexibility, scalability, and reliability were critical components of the design. The outcome of this project was a reliable sensing system capable of acquiring, synthesizing, and filtering the data from the different sensors present in a test bench used as a case study. The gathered data was processed and prepared to be sent to other systems to be visualized, logged, or evaluated to perform an action by a control system.

A prototype of a printed circuit board was developed based on the requirements of the implemented sensing system. The board included the connectors and data processing elements to integrate the test bench's sensors and communicate with the chosen microcontroller. The electrical schematics and drawings of the board were presented, and the board can be created and integrated for future work. Additionally, the PCB included three open connectors for the future integration of more sensors to the test bench.

A cloud-based dashboard was created as part of the sensing system. The dashboard was developed in Node-RED, a cloud framework that allows the user to control some of the actions of the test bench. Furthermore, it enables the user to read in real-time the data from the sensors easily.

One open control loop was created to determine the extension of a hydraulic cylinder. Based on the sensing system data and with a microcontroller, the piston rod position was determined, and an action of extension or retraction was executed based on the desired position. The system was evaluated with different experiments moving to a desired piston rod stroke position and following a wave form signal.

Finally, the sensing system data was tested using several statistical methods and tools, and it was proven to be reliable and robust. The system performed according to the expectations in all of the tests and provided accurate measurements at a significance level of 0.05.

5.1.2. Micro Drilling Robot Implementation

Even though the wired telemetry used to integrate all the elements from the smart sensing system and the test bench provided a reliable connection and fast data rate transmissions, this might not be possible in an oil field.

Based on the literature review and given the project’s constraints, electromagnetic or radiofrequency telemetry was identified as the best possible solution for a micro-drilling device such as this. Radiofrequency telemetry provides data rates at speeds that can give the reliability and sturdiness required by a more robust control system. In addition, given that the signals sent from the DTH device to the main computer on the surface are primarily measurements from the sensors, the bandwidth is sufficient. The micro-drilling prototype is expected to work in depths of around 200 to 2000 m.

For future work, an appropriate approach to take regarding telemetry would be to install an antenna and a receiver to send data along 200 to 400 m. After that, the use of signal extenders and repeaters will be required because the geology and the noise derived from the robot's operation will attenuate the signal. Techniques of convolution and signal compression will be needed once the project reaches this point.

On the other hand, Table 5.1 shows the sensors that are recommended to be implemented on the micro-drilling device. The table lists the sensors, along with the manufacturer and model of the sensor and the expected quantity required. It is important to highlight that these sensors are compatible with the sensing system developed for this thesis work.

Table 5.1. Additional devices recommended to implement on the micro-drilling device.

Element	**Type**	**Manufacturer**	**Model/Code**	**Qty**
Hydraulic cylinder	Actuator	Bansbach	HZ16	3
Current and voltage sensor	Sensor	Adafruit	INA169	1
Inertial Measurement Unit	Sensor	Adafruit	BNO055	3
Position transducer	Sensor	SICK	MPA-107THTP0B01	2

For the sensing system, the selected Inertial Measurement Unit (IMU) was the BNO055 (Figure 5.1), which is a 9-axis orientation module developed by BOSCH. This IMU integrates an ARM Cortex-MO microprocessor that filters and processes the sensors' data and delivers it to the user in a single chain of characters.

The BNO055 output is a digital signal that is connected to the Raspberry Pi using the I^2C communication protocol (Figure 5.2). This module provides the following measurements:

- Absolute Orientation
- Angular Velocity Vector
- Acceleration Vector
- Magnetic Field Strength Vector
- Linear Acceleration Vector
- Gravity Vector
- Temperature

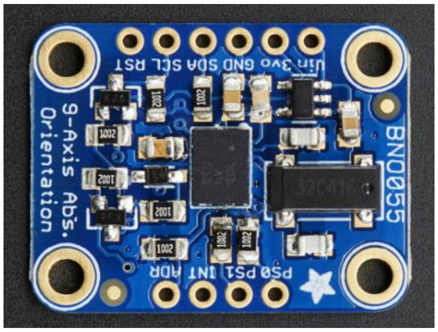

Figure 5.1. Inertial Measurement Unit (IMU) BNO055 (Townsend, n.d.).

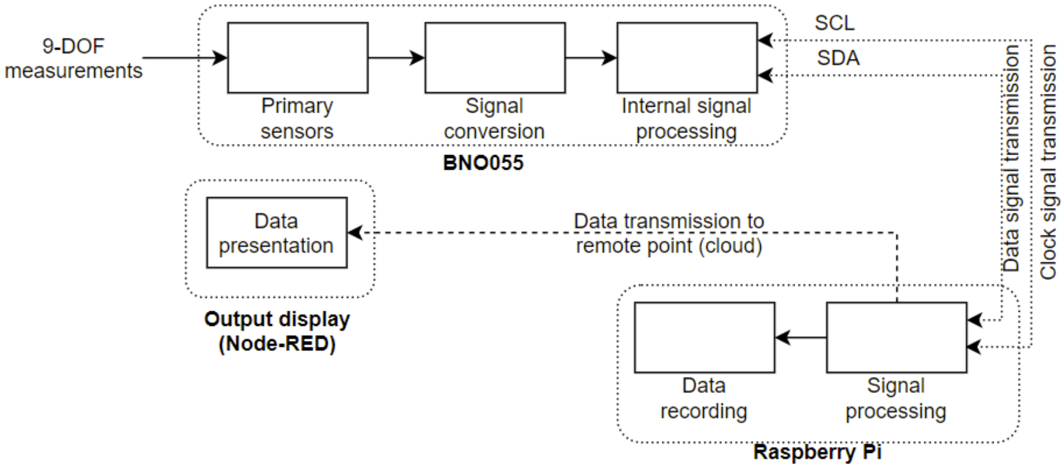

Figure 5.2. Inertial Measurement Unit Architecture.

The BNO055 will be used to determine the relative position of the platform that will be connected to the micro-hydraulic cylinders and determine its orientation and tilt. This module will provide the user with information regarding the acceleration and spatial orientation of the device. It is expected to use at least three of these modules, one that will be placed near the drill bit, the second one on the steering mechanism, and the third one on the first section of the robot.

Most of the electronics are powered by a 12 V battery. Therefore, measuring the variables related to the system's power source is critical for the operation. The percentage of charge and the current and power delivered by the battery must be measured. The module INA169 (Figure 5.3) integrates the sensors to measure the voltage and current drawn on an electric circuit. The output of this module is an analog 0-5 V signal that is proportional to the values being read. This module can measure voltage values from 0 to 60 V DC and up to 5 A.

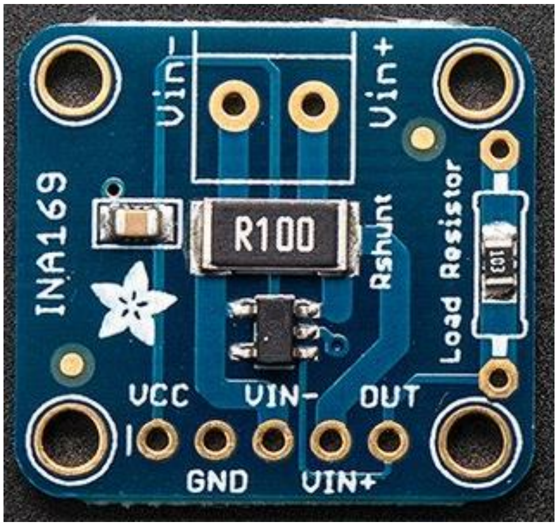

Figure 5.3. Module INA169 (Adafruit Industries, n.d.).

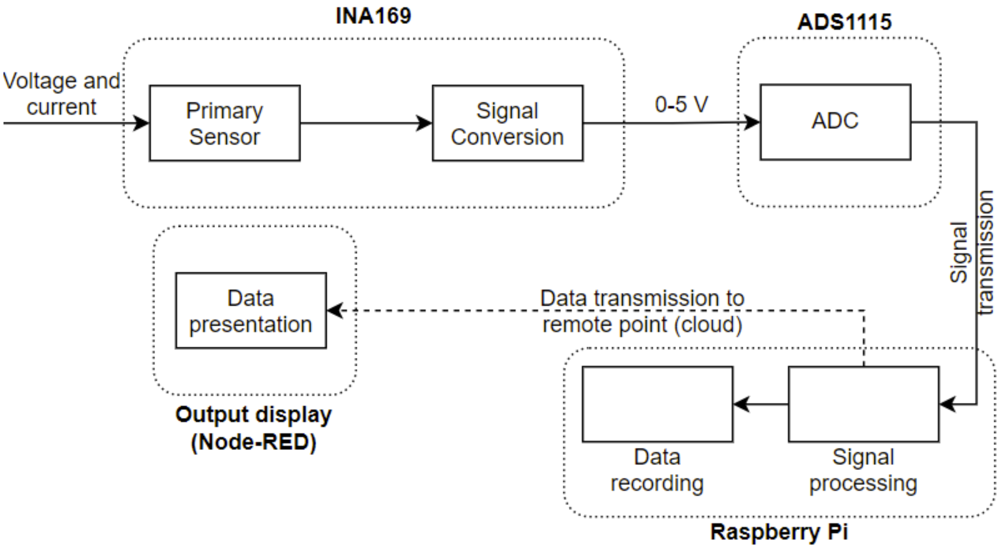

Figure 5.4. Voltage and Current Transducer Architecture.

For the robot, an arrangement based on three micro-hydraulic cylinders (Figure 5.5) can be designed to simulate what will be a steering and propulsion subsystem on the micro-drilling device. The double-acting cylinders have a 16 mm (0.63") piston diameter, an 8 mm (0.315") rod diameter, and a stroke of 40 mm (1.58"). The cylinders have two ports connecting each hydraulic chamber, and connectors and adapters can be used to direct the flow either through a hose or with tubing.

Figure 5.5. Hydraulic cylinder HZ16 (Bansbach Easy Lift, 2020).

Each cylinder rod end is attached to a spherical rolling joint and connected to a plate that provides the desired degrees of freedom by creating a moving platform. This moving platform will help ensure the parallelism between the cylinders. A drilling subsystem will be attached to the base that will be moved and steered based on the micro-hydraulic cylinders’ extension and retraction.

Regarding the control on the cloud-based dashboard, it will be required first to control the motor's rotation and then move forward and develop a control for speed. As a starting point, an essential three-commands control can be implemented (Figure 5.6). In Figure A. 2, the proposed operational block flow is shown.

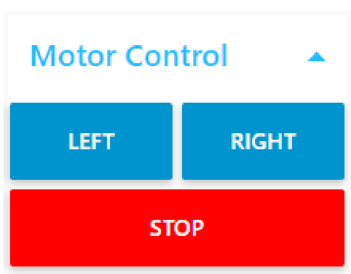

Figure 5.6. Proposed control for the rotation of a motor.

LIST OF REFERENCES

Abughaban, M. (2017). *Extending the reach of drilling: Better wellbore trajectory and torque & drag models* (Order No. 10604706). Available from ProQuest Dissertations & Theses Global. (1975373827). https://search.proquest.com/docview/1975373827?accountid=13360

Adafruit Industries. (n.d.). *INA169 Analog DC Current Sensor Breakout - 60V 5A Max*. Adafruit Industries Blog RSS. https://www.adafruit.com/product/1164.

Afsarimanesh, N., Zia, A. I., Mukhopadhyay, S. C., Kruger, M., Yu, P., Kosel, J., & Kovacs, Z. (2016). Smart Sensing System for the Prognostic Monitoring of Bone Health. *Sensors, 16*(7), 976. http://dx.doi.org/10.3390/s16070976

Alarie, A. P., & Petteruti, A. J. (1968). Acoustic Telemetry and Control System. *The Journal of the Acoustical Society of America*, *44*(6), 1748-1750.

Alavi, A., Hasni, H., Lajnef, N., & Chatti, K. (2016). Continuous health monitoring of pavement systems using smart sensing technology. *Construction & Building Materials, 114*, 719-736.

Allaby, M. (2020). *A Dictionary of Geology and Earth Sciences* (5th ed.). Oxford University Press. *American/Caribbean Petroleum Engineering Conference.* Buenos Aires, Argentina, April 27-29.

Amazon (n.d.). *KNACRO PWM to Voltage Module 0% -100% PWM Converted to 0-10V Voltage Suitable for Signal Interface Switching for PLC or Other Industrial Control(PWM-to-Voltage 0-10V).* https://www.amazon.com/KNACRO-voltage-converted-voltage-Voltage/dp/B06XCVY3GM?th=1

Amazon (n.d.). *SunFounder 5V 8 Channel Relay Shield Module for Arduino R3 2560 1280 ARM PIC AVR STM32 Raspberry Pi 3, 2 Model B & B+*. https://www.amazon.com/SunFounder-Channel-Shield-Raspberry-Arduino/dp/B00DR9SE4A

Amazon. (n.d.). *Ximimark 3Pcs Current to Voltage Converter Module 0/4-20mA to 0-3.3V 0-5V 0-10V Voltage Transmitter Signal Conversion Conditioning Board*. https://www.amazon.com/Ximimark-Converter-Transmitter-Conversion-Conditioning/dp/B07MYXVDDX.

Arps, J. J., & Arps, J. L. (1964). The subsurface telemetry problem-A practical solution. *Journal of Petroleum Technology*, *16*(05), 487-493.

Atashnezhad, A., Wood, D., Fereidounpour, A., & Khosravanian, R. (2014). Designing and optimizing deviated wellbore trajectories using novel particle swarm algorithms. *Journal of Natural Gas Science and Engineering, 21*(3), 1184-1204.

Azar, J., & Samuel, G. (2007). *Drilling Engineering*. Tulsa: PennWell Books.

Baig, M. M. (2015). *Control and optimization of directional drilling* (Order No. 10688912). Available from ProQuest Dissertations & Theses Global. (2357399376). https://search.proquest.com/docview/2357399376?accountid=13360

Banner. (n.d.). *VSM-2 series MICRO SENSOR*. https://www.bannerengineering.com/us/en/products/sensors/photoelectric-sensors/vsm-2.html?sort=4#all

Bansbach Easy Lift. (2020). Micro-hydraulic cylinders. https://www.bansbach.com/index.php/en/products/micro-hydraulics

Beattie, A. (2020). The Cost of Shale Oil vs. Conventional Oil. https://www.investopedia.com/articles/active-trading/051215/cost-shale-oil-versus-conventional-oil.asp

Berro, M. J., & Reich, M. (2019). Laboratory investigations of a hybrid mud pulse telemetry (HMPT)–A new approach for speeding up the transmitting of MWD/LWD data in deep boreholes. *Journal of Petroleum Science and Engineering*, *183*, 106374.

Bingham, M.G., 1964. A new approach to interpreting Rock Drillability. *Oil Gas J.* 94-101.

Bommer, P. (2008). *A primer of oilwell drilling* (7th Edition). Austin, TX: The University of Texas.

Britannica, T. Editors of Encyclopaedia (2017, December 7). *Petroleum trap*. Encyclopedia Britannica. https://www.britannica.com/science/petroleum-trap

Chang, Xin, Zhou, Jun, Guo, Yintong, He, Shiming, Wang, Lei, Chen, Yulin, Jian, Rui. (2018). Heat Transfer Behaviors in Horizontal Wells Considering the Effects of Drill Pipe Rotation, and Hydraulic and Mechanical Frictions during Drilling Procedures. *Energies (Basel), 11*(9), 2414.

Chin, W. C. (2018). *Measurement While Drilling*. Newark: John Wiley & Sons, Incorporated.

Çıkım, T., Gözüaçık, D., & Koşar, A. (2014). Power reclamation efficiency of a miniature energy-harvesting device using external fluid flows. *International Journal of Energy Research, 38*(10), 1318-1330.

Dai, H., Zhang, P., & Lueth, T. C. (2015). Quantitative assessment of parkinsonian tremor based on an inertial measurement unit. *Sensors*, *15*(10), 25055-25071.

Dareing, D. W. (2019). *Oilwell Drilling Engineering*. New York, N.Y: The American Society of Mechanical Engineers.

Dissanayake, G., Sukkarieh, S., Nebot, E., & Durrant-Whyte, H. (2001). The aiding of a low-cost strapdown inertial measurement unit using vehicle model constraints for land vehicle applications. *IEEE transactions on robotics and automation*, *17*(5), 731-747.

Drumheller, D S. (1992). *An overview of acoustic telemetry*. United States.

Du, J., Liu, B., & Xia, B. (2008). The control scheme for three-pad static bias device of push-the-bit rotary steerable system. *Oil Drilling & Production Technology*, *30*(6), 5-10.

Earl, B. (n.d.). *Adafruit 4-Channel ADC Breakouts*. Adafruit Learning System. https://learn.adafruit.com/adafruit-4-channel-adc-breakouts.

ElGizawy, M. L. (2009). *Continuous measurement-while-drilling surveying system utilizing MEMS inertial sensors* (Order No. NR51182). Available from ProQuest Dissertations & Theses Global. (304844507). https://search.proquest.com/docview/304844507?accountid=13360

Emmerich, W., Akimov, O., Brahim, I. B., & Greten, A. (2015). Reliable high-speed mud pulse telemetry. In *SPE/IADC Drilling Conference and Exhibition*. Society of Petroleum Engineers.

Fang, D., Shang, J., Luo, Z., Feng, Y., & Chen, F. (2018). Research on Hydraulic Performance of Downhole Traction Robot in Oil Field. *IOP Conference Series: Earth and Environmental Science*, *108*(3), 1-5.

Flatiron School. (n.d.). *What Is Sinatra*. Learn. https://learn.co/lessons/what-is-sinatra.

Flo-tech. (2019). *Turbine Flow Sensors: User manual*. Badger Meter.

Franconi, N., Bunger, A., Sejdić, E., & Mickle, M. (2014). Wireless Communication in Oil and Gas Wells. *Energy Technology (Weinheim, Germany)*, *2*(12), 996-1005.
Freudenrich, C., & Strickland, J. (2018). *How Oil Drilling Works*. https://science.howstuffworks.com/environmental/energy/oil-drilling.htm/printable

Gardner, W. R., Hyden, R. E., Linyaev, E. J., Gao, L., Robbins, C., & Moore, J. (2006). Acoustic telemetry delivers more real-time downhole data in underbalanced drilling operations. In *IADC/SPE Drilling Conference*. Society of Petroleum Engineers.

Gomaa, M. A. K. (2016). *Online control and optimization of directional drilling* (Order No. 10746905). Available from ProQuest Dissertations & Theses Global. (2363032319). https://search.proquest.com/docview/2363032319?accountid=13360

Gravdal, A. E., Lorentzen, R. J., & Time, R. W. (2010). Wired drill pipe telemetry enables real-time evaluation of kick during managed pressure drilling. In *SPE Asia pacific oil and gas conference and exhibition*. Society of Petroleum Engineers.

Hadavand, Z. (2015). *Reduction of wellbore positional uncertainty during directional drilling* (Order No. 1605647). Available from ProQuest Dissertations & Theses Global. (1756714492). https://search.proquest.com/docview/1756714492?accountid=13360

Hareland, G., Rampersad, P.R. (1994). Drag-bit model including wear. *In: III Latin*

Harper, G., Almanza, E., Fosså, A., Finley, D., & Strang, G. (2003, January). Implementation of advanced acoustic telemetry system adds value and efficiency to well testing operations. In *SPE Asia Pacific Oil and Gas Conference and Exhibition*. Society of Petroleum Engineers.

Hawthorn, A., & Aguilar, S. (2017, October). New wireless acoustic telemetry system allows real-time downhole data transmission through regular drillpipe. In *SPE Annual Technical Conference and Exhibition*. Society of Petroleum Engineers.

Honeywell. (n.d.). *Model LM.* Gage Pressure Transducer. https://sensing.honeywell.com/honeywell-test-and-measurement-model-lm-pressure-transducer-datasheet-008702-1-en.pdf.

Hossain, M. E., & Al-Majed, A. A. (2015). *Fundamentals of Sustainable Drilling Engineering*. Wiley.

Hu, F., & Hao, Q. (2013). *Intelligent sensor networks : The integration of sensor networks, signal processing and machine learning*. Boca Raton, FL: CRC Press.

Hunter, G., Stetter, J., Hesketh, P, & Liu, C. (2010). Smart Sensor Systems. *The Electrochemical Society Interface, 19*(4), 29-34.

Industrimigas. (2013). *Drilling and Casing the Wellbore*. IndustriMigas. http://www.industrimigas.com/2013/06/drilling-and-casing-wellbore.html

Islam, M. Rafiqul, & Hossain, M. Enamul. (2020). *Drilling Engineering*. San Diego: Elsevier Science & Technology.

Jagannathan, S., & Priyatharshini, R. (2015, July). Smart farming system using sensors for agricultural task automation. In *2015 IEEE Technological Innovation in ICT for Agriculture and Rural Development (TIAR)* (pp. 49-53). IEEE.

Jia, L. J. (2011). *Applications of seismic while drilling in shear-velocity measurement* (Order No. 10567499). Available from ProQuest Dissertations & Theses Global. (1874860351). https://search.proquest.com/docview/1874860351?accountid=13360

Jian, X., Wang, Y., & Yang, P. (2012). Schematic Design and Research on Steering Mechanism of Drilling Robot. *Applied Mechanics and Materials*, *189*(7), 321-325.

John, A., Varghese, R., Krishnan, S. S., Thomas, S., Swayambu, T. A., & Thasneem, P. (2017). Automation of 11 kv substation using raspberry pi. *In 2017 International Conference on Circuit, Power and Computing Technologies (ICCPCT)* (pp. 1-5). IEEE.

Jongheon, K., & Hyun, M. (2017). Development of a Novel Hybrid-Type Rotary Steerable System for Directional Drilling. *IEEE Access*, *5*(10), 24678-24687.

Jr., I., Antunes, P., Gonzalez, F., Yamachita, R., Nascimento, A. and Goncalves, J. (2015) A Review of Telemetry Data Transmission in Unconventional Petroleum Environments Focused on Information Density and Reliability. *Journal of Software Engineering and Applications, 8*, 455-462. doi: 10.4236/jsea.2015.89043.

Kendig, C. E. (2016). What is proof of concept research and how does it generate epistemic and ethical categories for future scientific practice?. *Science and Engineering Ethics*, *22*(3), 735-753.

Keyence. (n.d.). Image-Based Laser Sensor IX Series. KEYENCE. https://www.keyence.com/ss/products/measure/ix-h/.

Khanna, A., & Kaur, S. (2020). Internet of Things (IoT), Applications and Challenges: A Comprehensive Review. *Wireless Personal Communications*, *114*, 1687-1762.

Kim, J., Jung, S, Choi, S., & Myung, H. (2015). Reaction torque minimization method for keeping drilling direction of the hybrid rotary steerable system. *2015 12th International Conference on Ubiquitous Robots and Ambient Intelligence (URAI),* Goyag, South Korea, 146-147.

Kimmes, N. (2016). *Planning for monitoring of probe hole drilling and pre-excavation grouting with measurement while drilling (MWD), vibration monitoring, and ground penetrating radar (GPR)* (Order No. 10134993). Available from ProQuest Dissertations & Theses Global; Technology Collection. (1802532505). https://search.proquest.com/docview/1802532505?accountid=13360http://www.purdue.edu/gradschool/research/thesis/index.html

Kurdi, A. (2010). *Regulation and political costs in the oil and gas industry: An investigation of discretion in reporting earnings and oil and gas reserves estimates* (Order No. 3436535). Available from ProQuest Dissertations & Theses Global. (818469101). https://search.proquest.com/docview/818469101?accountid=13360

Lee, J. (2017, September 27). *NEW! Know Your Valves.* https://www.valvemagazine.com/magazine/sections/new-know-your-valves/8736-christmas-tree-or-wellhead.html

Li, X., Gao, D., Zhou, Y., Zhang, H., & Yang, Y. (2017). Study on the prediction model of the open-hole extended-reach limit in horizontal drilling considering the effects of cuttings. *Journal of Natural Gas Science and Engineering*, *40*(5), 159-167.

Liu, Q., Zhao, J., Zhu, H., Wang, G., & Mclennan, J. (2019). Review, classification and structural analysis of downhole robots: Core technology and prospects for application. *Robotics and Autonomous Systems*, *115*(5), 104-120.

Liu, S. (2020, June 15). *Internet of Things (IoT) - Statistics & Facts*. https://www.statista.com/topics/2637/internet-of-things/

Lowson, B., & Beckman, J. (1997). Horizontal, extended reach drilling *Offshore, 57*(2), 49-50, 64.

Ma, T., Chen, P., & Zhao, J. (2016). Overview on vertical and directional drilling technologies for the exploration and exploitation of deep petroleum resources. *Geomechanics and Geophysics for Geo-Energy and Geo-Resources*, *2*(4), 365-395. doi: https://doi.org/s40948-016-0038-y

Mahmood, N., Marchenko, N., Gidlund, M., & Popovski, P. (2021). *Wireless Networks and Industrial IoT Applications, Challenges and Enablers* (1st ed. 2021. ed.).

Managi, S. (2002). *Technological change, depletion and environmental policy in the offshore oil and gas industry* (Order No. 3063774). Available from ProQuest Dissertations & Theses Global. (251800187). https://search.proquest.com/docview/251800187?accountid=13360

Mardan, A. (2014). *Express. js Guide: The Comprehensive Book on Express. js*.

McDowell, B. (2006, May). *AGA Financial Forum*. https://www.slideshare.net/BPfanpage/natural-gas-101-an-introduction-to-the-natural-gas-industry

Miller, S. A. (2017). *Developmental research methods*. Sage publications.

Moreno, J. C., de Lima, E. R., Ruíz, A. F., Brunetti, F. J., & Pons, J. L. (2006). Design and implementation of an inertial measurement unit for control of artificial limbs: application on leg orthoses. *Sensors and Actuators B: Chemical*, *118*(1-2), 333-337.

Motahhari, H.R., Hareland, G., James, J.A. (2010). Improved drilling efficiency technique using integrated PDM and PDC bit parameters. J. Can. *Petrol. Technol. 49 (10)*, 45-52.

Mucci, S. A. (2015*). Managing political and investment risk in the international oil and gas industry* (Order No. 3705191). Available from ProQuest Dissertations & Theses Global. (1690904434). https://search.proquest.com/docview/1690904434?accountid=13360

Mwachaka, S.M., Wu, A. & Fu, Q. (2018). A review of mud pulse telemetry signal impairments modeling and suppression methods. *Journal of Petroleum Exploration and Production Technology*, *9*(1), 779–792. https://doi.org/10.1007/s13202-018-0483-y

Oak Ridge National Laboratory. Office of Energy Efficiency Renewable Energy. (2012). *Estimating the Impact (Energy, Emissions and Economics) of the US Fluid Power Industry*. Washington, DC: Oak Ridge, TN: United States. Dept. of Energy. Office of Energy Efficiency and Renewable Energy.

Office of Oil Gas. The United States. Energy Information Administration. (1997). *Natural gas monthly*, July 1997 (DOE Technical report; DOE/EIA--0130(97/07)). Washington, DC: Oak Ridge, Tenn.: United States. Energy Information Administration.

Omega Engineering. (n.d.). *General Purpose, Stainless Steel Pressure Trasnducers*. https://www.omega.com/en-us/pressure-measurement/pressure-transducers/p/PX309.

Panno, Sam, & Kelly, W. (2018). *PRI researchers gain new insights into how groundwater flows within the Illinois Basin*. http://isgs.illinois.edu/achievements/september/pri-researchers-gain-new-insights-how-groundwater-flows-within-illinois-basin

Park, B., Kim, J., Park, J., Shin, J., & Myung, H. (2013). Hybrid 4-pad rotary steerable system for directional drilling of unconventional resources. *2013 10th International Conference on Ubiquitous Robots and Ambient Intelligence (URAI)*, Jeju, South Korea, 659-660.

Pasquali, V., D'Alessandro, G., Gualtieri, R., & Leccese, F. (2017). A new data logger based on Raspberry-Pi for Arctic Notostraca locomotion investigations. *Measurement*, *110*, 249-256.

Raspberry Pi. (n.d.). *Raspberry Pi 4*. https://www.raspberrypi.org/products/raspberry-pi-4-model-b/.

Ray, P. P. (2018). A survey on Internet of Things architectures. *Journal of King Saud University-Computer and Information Sciences*, *30*(3), 291-319.

Rockhold, M., Zhang, F., White, S., Bonneville, A., & Gilmore, T. (2014). Estimation of rock mechanical, hydraulic, and thermal properties using wire-line log and core data from the FutureGen2.0 Site, well No. 1, Morgan County, Illinois. *Society of Exploration Geophysicists International Exposition and 84th Annual Meeting SEG 2014*, (1), 4903–4907. https://doi.org/10.1190/SEG-2014-1380.pdf

Sampaio, J. (2006). Planning 3D well trajectories using cubic functions. *Journal of Energy Resources Technology*, *128*(4), 257-267.

Sampaio, J. (2017). Designing Three-Dimensional Directional Well Trajectories Using Bezier Curves. *Journal of Energy Resources Technology-Transactions of the Asme, 139*(3): 032901.

Schwarz, P. (2013). *The impact the price of oil has on a product manufacturer in the oil and gas industry* (Order No. 1541656). Available from ProQuest Dissertations & Theses Global. (1418751217). https://search.proquest.com/docview/1418751217?accountid=13360

Sehrawat, D., & Gill, N. S. (2019). Smart Sensors: Analysis of Different Types of IoT Sensors. *2019 3rd International Conference on Trends in Electronics and Informatics (ICOEI)*, 523-528.

Sheehan, C. (2014). A wonderful life. (Economic benefits of horizontal drilling and hydraulic fracturing) (On the Money) (Column). *Oil and Gas Investor*, *34*(4), 15.

SICK Sensor Intelligence. (n.d.). Position sensors MPA. SICK. https://www.sick.com/us/en/magnetic-cylinder-sensors/position-sensors/mpa/c/g270351

Sisinni, E., Saifullah, A., Han, S., Jennehag, U., & Gidlund, M. (2018). Industrial internet of things: Challenges, opportunities, and directions. *IEEE Transactions on Industrial Informatics*, *14*(11), 4724-4734.

Soares, C., Daigle, H., & Gray, K. (2016). Evaluation of PDC bit ROP models and the effect of rock strength on model coefficients. *Journal of Natural Gas Science and Engineering, 34*, 1225-1236.

Spinnler, R. F., & Stone, F. A. (1978). *Mud pulse logging while drilling telemetry system: design, development, and demonstrations* (No. BERC/TPR-78/4). Teleco Oilfield Services, Inc., Middletown, CT (USA).

Squire, W. D., & Whitehouse, H. J. (1979). A new approach to drill-string acoustic telemetry. In *SPE Annual Technical Conference and Exhibition*. Society of Petroleum Engineers.

Stephenson, M. (2015). *Shale gas and fracking*. Elsevier. doi: https://doi.org/10.1016/C2014-0-00197-9

Sun, L. (2010). *Research on pressure measurement while drilling* (Order No. 10537962). Available from ProQuest Dissertations & Theses Global. (1870394122). https://search.proquest.com/docview/1870394122?accountid=13360

TE connectivity (n.d.). *SP2 Compact String Pot – Incremental*. https://www.te.com/usa-en/product-SP2-4.html

TE Connectivity. (2020, August 14). What is a String Pot? What is a string pot? https://www.te.com/usa-en/products/sensors/position-sensors/potentiometric-sensors/cable-actuated-position-sensors/what-is-a-string-pot.html

Townsend, K. (n.d.). *Adafruit BNO055 Absolute Orientation Sensor*. https://learn.adafruit.com/adafruit-bno055-absolute-orientation-sensor

Upton, E. (2019, July 24). *Raspberry Pi 4 on sale now from $35*. Raspberry Pi Blog. https://www.raspberrypi.org/blog/8gb-raspberry-pi-4-on-sale-now-at-75/.

Vacca, A. (2018). Energy Efficiency and Controllability of Fluid Power Systems. *Energies*, *11*(5), 1169.

Vestavik, O., Syse, H., Hole, J., & Aleksandersen, J. (2011). New approach to extend horizontal-drilling reach. *JPT, Journal of Petroleum Technology*, *63*(5), 92-95.

Vong, P. K., Rodger, D., & Marshall, A. (2005). Modeling an electromagnetic telemetry system for signal transmission in oil fields. *IEEE transactions on magnetics*, *41*(5), 2008-2011.

Wang, H., Yu-cai, S., Wei-qing, C., Guo-shan, Z., Jian-yun, W., & Cao, G. (2019). Dynamic behavior analysis of push-the-bit rotary steerable bottom hole assembly. *Journal of Mechanical Science and Technology*, *33*(4), 1-11.

Wang, Q., Gao, H., Jiang, B., Yang, J., & Lv, Z. (2018). Relationship model for the drilling parameters from a digital drilling rig versus the rock mechanical parameters and its application. *Arabian Journal of Geosciences*, *11*(13). https://doi.org/10.1007/s12517-018-3715-z

Wang, R., Xue, Q., Han, L., Sun, F., & Yue, W. (2014). Torsional vibration analysis of push-the-bit rotary steerable drilling system. *Meccanica*, *49*(7), 1601-1615.

Wang, Y. (2010). *Research on inertial instrument for oil or gas well measurement while drilling based on fiber optic gyroscope* (Order No. 10342096). Available from ProQuest Dissertations & Theses Global. (1870377737). https://search.proquest.com/docview/1870377737?accountid=13360

Wen, H. (2019). *Toward Inertial-Navigation-On-Chip* (Springer Theses). Cham: Springer International Publishing AG.

Wilson, J. K. (2017). *Non-linear drillstring modeling with applications to induced vibrations in unconventional horizontal wells* (Order No. 10662630). Available from ProQuest Dissertations & Theses Global. (1964384556). https://search.proquest.com/docview/1964384556?accountid=13360

Wolfe, C. A., Morris, S. A., & Baule, A. (2009). Enhanced real-time wellbore stability monitoring using high definition imaging with wired-pipe telemetry. In *SPE/IADC Drilling Conference and Exhibition*. Society of Petroleum Engineers.

Xie, H. (2017). The research of the drilling pipe's small-scale mode used in acoustic telemetry while drilling. *Functional Materials, 23*(4), 117-121.

Yaapa, H. (2013). *Express web application development*. Packt Publishing Ltd.

Yang, W. J. (2011). *Design of the control system for a rotary steerable tool engineering prototype* (Order No. 10515470). Available from ProQuest Dissertations & Theses Global. (1873879344). https://search.proquest.com/docview/1873879344?accountid=13360

Yi, J., Wang, H., Zhang, J., Song, D., Jayasuriya, S., & Liu, J. (2009). Kinematic modeling and analysis of skid-steered mobile robots with applications to low-cost inertial-measurement-unit-based motion estimation. *IEEE transactions on robotics*, *25*(5), 1087-1097.

Yun, C. B., & Min, J. (2011). Smart sensing, monitoring, and damage detection for civil infrastructures. *KSCE Journal of Civil Engineering*, *15*(1), 1-14.

Zaghari, B., Weddell, A., Esmaeili, K., Bashir, I., Harvey, T., White, N., Wang, L. (2020). High-Temperature Self-Powered Sensing System for a Smart Bearing in an Aircraft Jet Engine. *IEEE Transactions on Instrumentation and Measurement*, *69*(9), 6165-6174.

Zhang, D. C., Yu, P., Beard, S., Qing, P., Kumar, A., & Chang, F. K. (2007, April). A new SMART sensing system for aerospace structures. In *Unmanned Systems Technology IX* (Vol. 6561, p. 656107). International Society for Optics and Photonics.

Zhang, L., Liu, G., & Li, W. (2018). Analysis and optimization of control algorithms for RSSTSP for horizontal well drilling. *Journal of Petroleum Exploration and Production Technology*, *8*(4), 1069-1078.

Zhang, Z. K., Cho, M. C. Y., Wang, C. W., Hsu, C. W., Chen, C. K., & Shieh, S. (2014, November). IoT security: ongoing challenges and research opportunities. In *2014 IEEE 7th international conference on service-oriented computing and applications* (pp. 230-234). IEEE.

APPENDIX A. NODE-RED OPERATIONAL BLOCK FLOWS

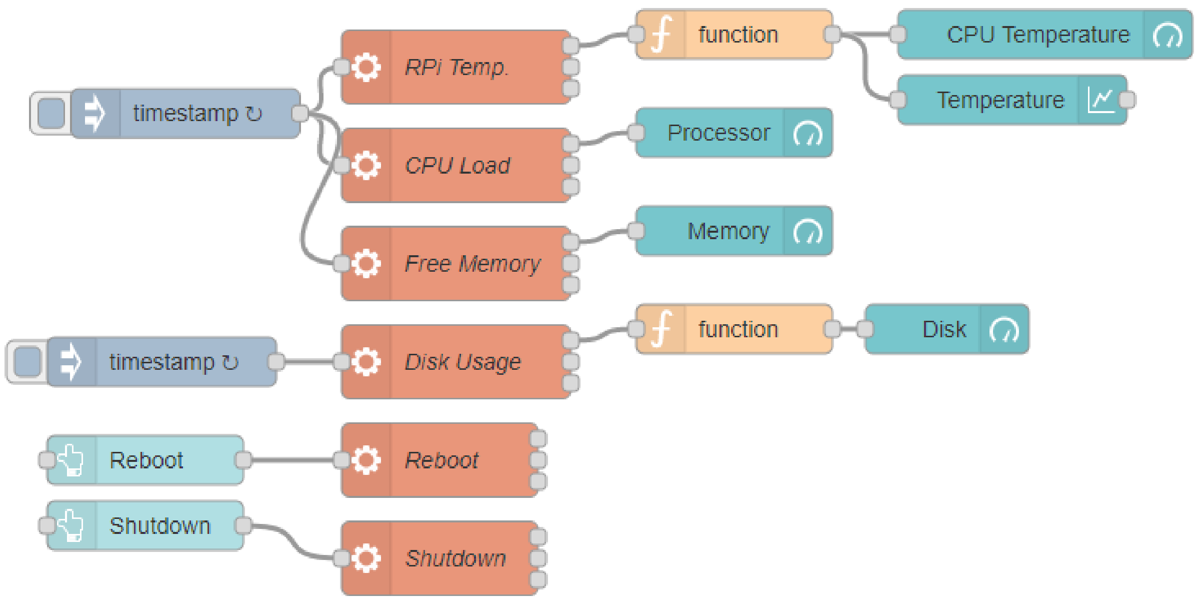

Figure A. 1. Raspberry Pi monitoring.

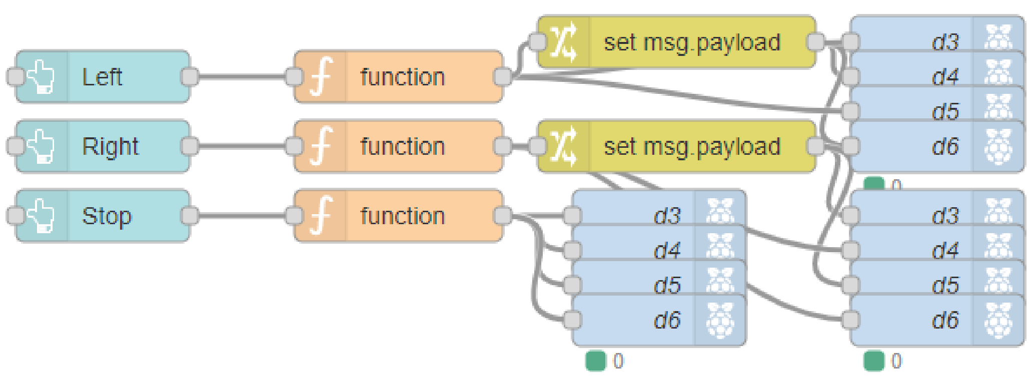

Figure A. 2. Motor control.

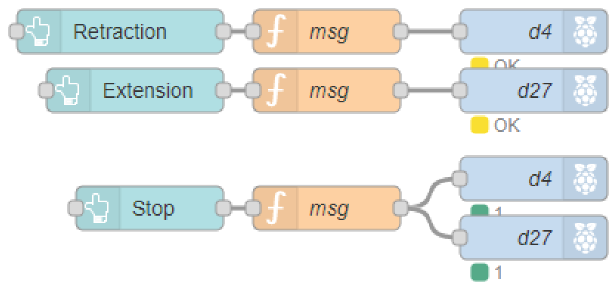

Figure A. 3. Manual cylinder control.

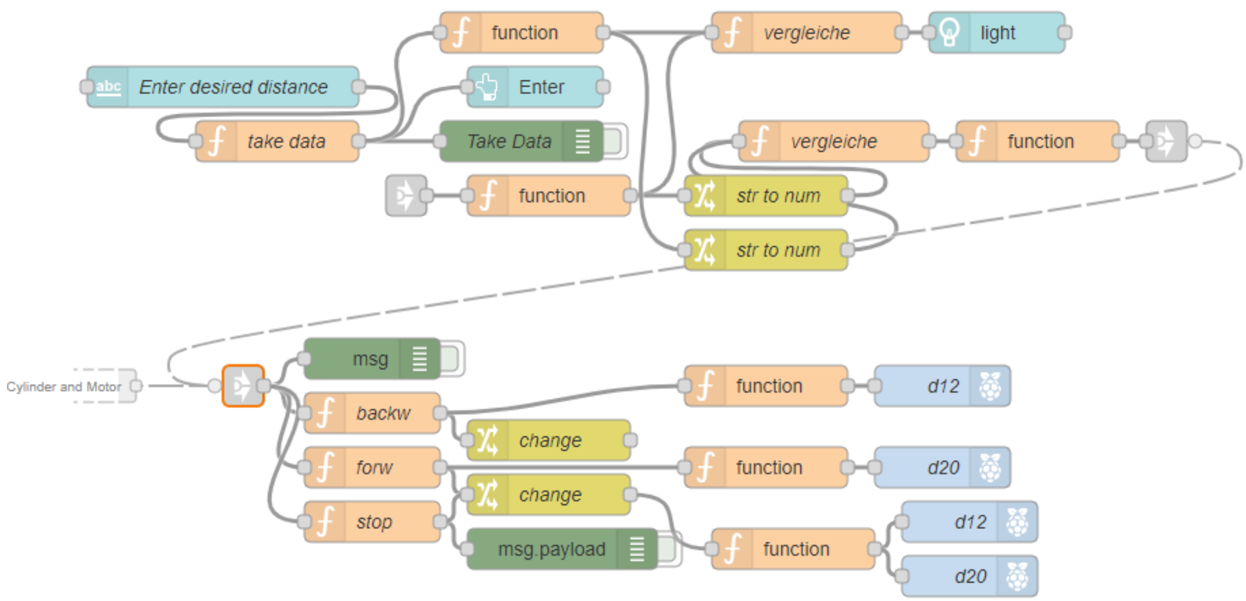

Figure A. 4. Desired distance acquisition and control

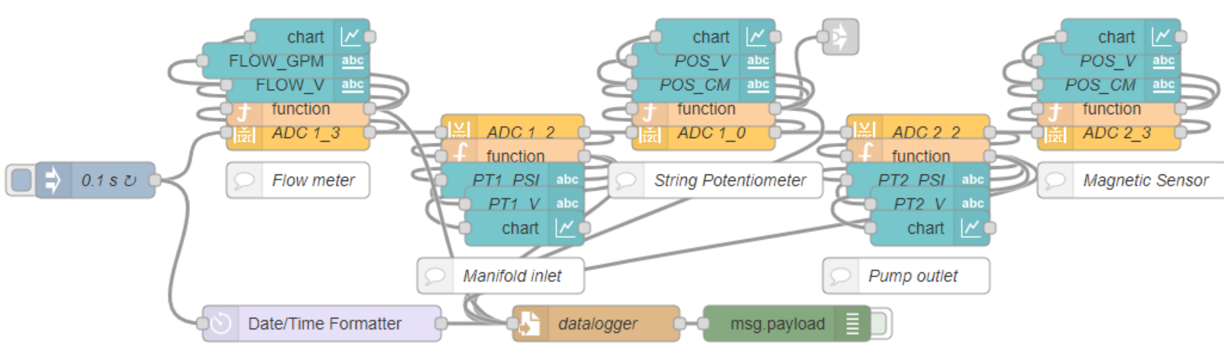

Figure A. 5. Data acquisition, processing, and plotting.

APPENDIX B. ELECTRONIC SCHEMATIC

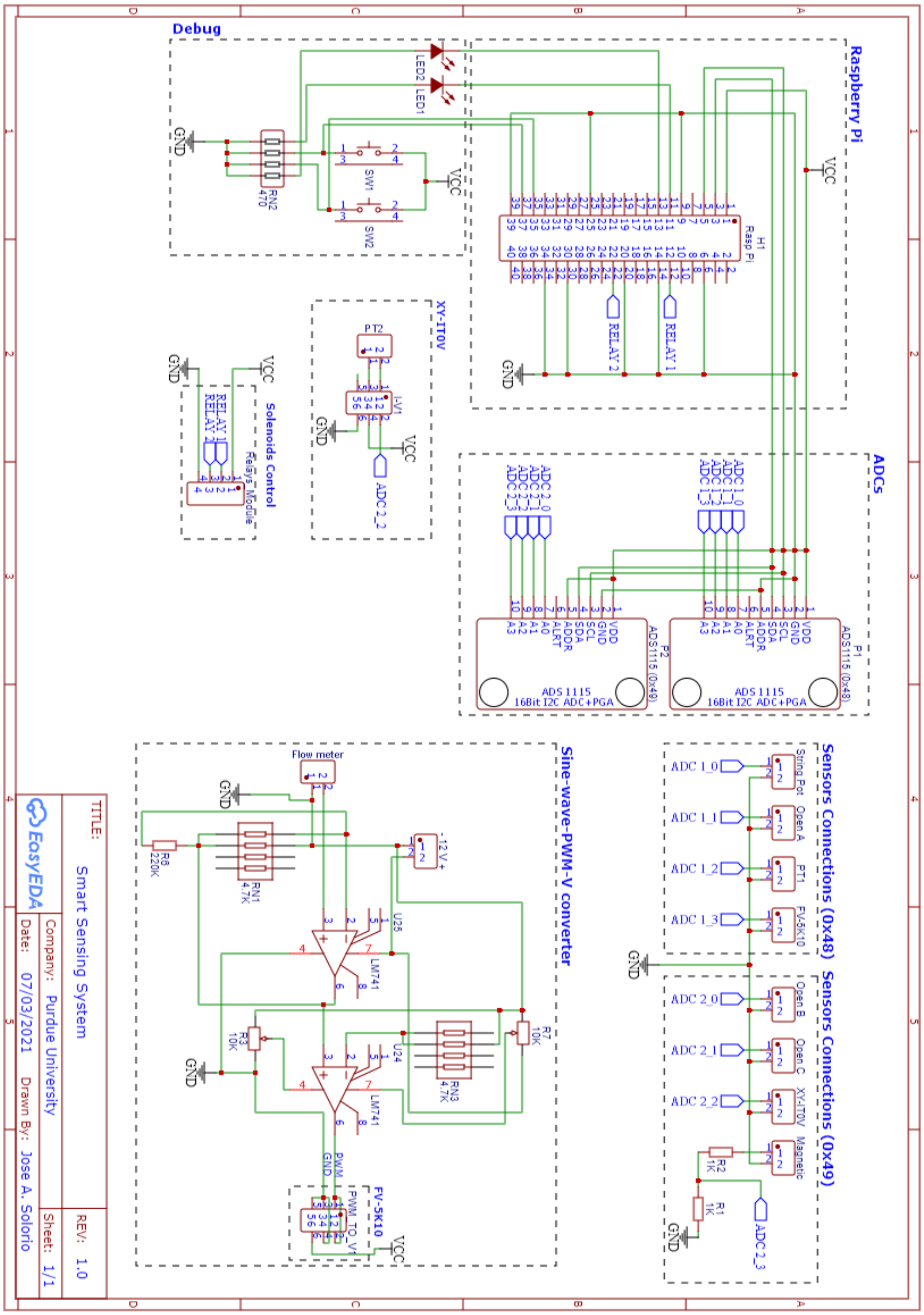

Figure B. 1. Smart sensing system general schematic.

APPENDIX C. ANOVA TABLES

Table C.1. ANOVA table for Experiment 1.

Source	SS	df	MS	F	Prob>F
Columns	0.7264	2	0.3632	0.0695	0.9329
Error	407.7273	78	5.2273		
Total	408.4537	80			

Table C.2. Multiple comparison test results for Experiment 1.

Comparison		
Test	**Test**	**p-value**
1	2	0.9270
1	3	0.9742
2	3	0.9871

Table C.3. ANOVA table for Experiment 2.

Source	SS	df	MS	F	Prob>F
Columns	0.0629	2	0.0315	0.0140	0.9861
Error	107.7061	48	2.2439		
Total	107.7690	50			

Table C.4. Multiple comparison test results for Experiment 2.

Comparison		
Test	**Test**	**p-value**
1	2	0.99953
1	3	0.9969
2	3	0.9847

Table C.5. ANOVA table for Experiment 3.

Source	SS	df	MS	F	Prob>F
Columns	7.8809	2	3.9405	0.5484	0.5784
Error	2.6515e+03	369	7.1856		
Total	2.6594e+03	371			

Table C.6. Multiple comparison test results for Experiment 3.

Comparison		
Test	**Test**	**p-value**
1	2	0.9039
1	3	0.8127
2	3	0.5505

APPENDIX D. PCB

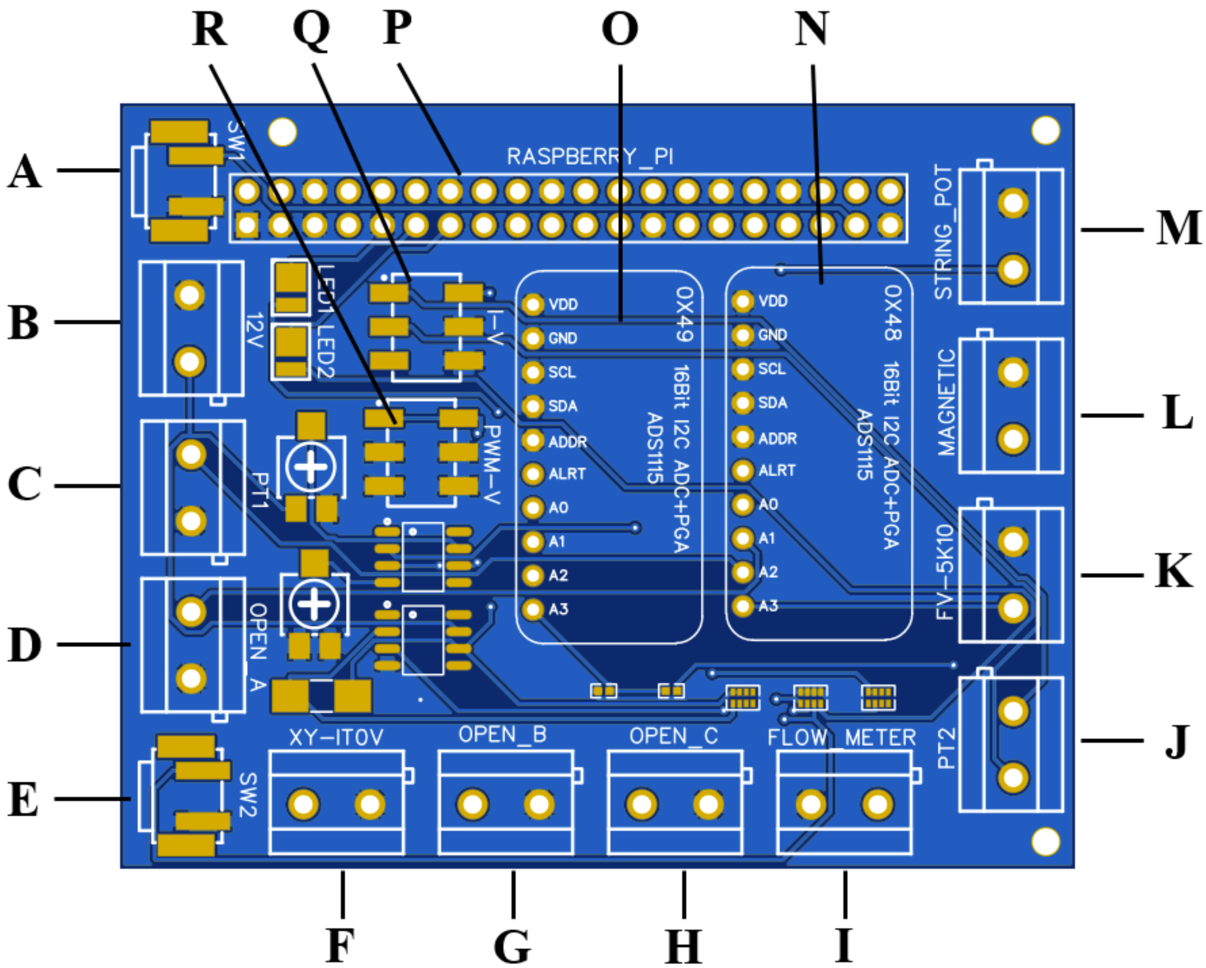

Figure D. 1. PCB detailed schematic.

Table D.1. Description of PCB elements.

ID	Element
A	Push button 1
B	12 V external supply
C	Connection for pressure transducer 1
D	Open connection for sensor
E	Push button 2
F	Connection for output of current to voltage converter (XY-IT0V)
G	Open connection for sensor
H	Open connection for sensor
I	Connection for flow meter
J	Connection for pressure transducer 2
K	Connection for output of PWM to voltage converter (FV-5K10)
L	Connection for position transducer (Magnetic)
M	Connection for position transducer (String potentiometer)
N	ADC 1 (ADS1115)
O	ADC 2 (ADS1115)
P	Headers for connection to Raspberry Pi GPIOs
Q	Headers for connection to current to voltage converter
R	Headers for connection to PWM to voltage converter